



**Calhoun: The NPS Institutional Archive**  
**DSpace Repository**

---

Theses and Dissertations

1. Thesis and Dissertation Collection, all items

---

1968

# Investigation of subharmonic ripple in a forced limit-cycling regulator.

Hyde, Wilton Hubert, Jr.

Monterey, California. U.S. Naval Postgraduate School

---

<http://hdl.handle.net/10945/12485>

---

This publication is a work of the U.S. Government as defined in Title 17, United States Code, Section 101. Copyright protection is not available for this work in the United States.

*Downloaded from NPS Archive: Calhoun*



Calhoun is the Naval Postgraduate School's public access digital repository for research materials and institutional publications created by the NPS community. Calhoun is named for Professor of Mathematics Guy K. Calhoun, NPS's first appointed -- and published -- scholarly author.

**Dudley Knox Library / Naval Postgraduate School**  
**411 Dyer Road / 1 University Circle**  
**Monterey, California USA 93943**

<http://www.nps.edu/library>

NPS ARCHIVE  
1968  
HYDE, W.

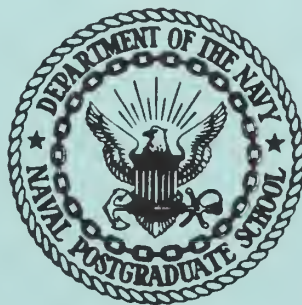
INVESTIGATION OF SUBHARMONIC RIPPLE  
IN A FORCED LIMIT-CYCLING REGULATOR

by

Wilton Hubert Hyde



# UNITED STATES NAVAL POSTGRADUATE SCHOOL



## THESIS

INVESTIGATION OF SUBHARMONIC RIPPLE  
IN A FORCED LIMIT-CYCLING REGULATOR

by

Wilton Hubert Hyde, Jr.

December 1968

*This document has been approved for public release and sale; its distribution is unlimited.*

LIBRARY  
NAVAL POSTGRADUATE SCHOOL  
MONTEREY, CALIF. 93940

INVESTIGATION OF SUBHARMONIC  
RIPPLE IN A FORCED LIMIT-CYCLING  
REGULATOR

by

Wilton Hubert Hyde, Jr.  
Major, United States Marine Corps  
B.S., Naval Academy, 1961

Submitted in partial fulfillment of the  
requirements for the degree of  
MASTER OF SCIENCE IN ELECTRICAL ENGINEERING

from the

NAVAL POSTGRADUATE SCHOOL  
December 1968

## ABSTRACT

Some Nonlinear Feedback Control Systems under high gain conditions exhibit the phenomenon of subharmonic instability, or contain subharmonics of the fundamental output frequency. A general discussion of subharmonics in nonlinear systems is followed by an investigation of ripple instability in a forced limit-cycling voltage regulator containing a thyristor or SCR bridge utilizing an ON-OFF switching scheme.

A digital computer program is used to simulate the dynamic response of the system under different loading conditions and for different reference voltage levels.

---

# TABLE OF CONTENTS

Section		Page
1.	Introduction . . . . .	9
2.	A general study of subharmonics in a nonlinear system . . . . .	10
3.	Description of the system . . . . .	38
4.	Synthesis of the forced limit-cycling regulator . . . . .	51
5.	Conclusions . . . . .	75
6.	Recommended areas for further study . . . . .	76
Appendix		
1.	Computer program and numerical data for simulation of system . . . . .	79





# LIST OF ILLUSTRATIONS

Figure		Page
2-1	Region in which 1/3-harmonic oscillation is sustained. Magnetization curve by the equation $f(v) = c_1 v + c_3 v^3$	15
2-2	Region in which 1/3-harmonic oscillation is sustained. Magnetization curve by the equation $f(v) = c_1 v + c_3 v^3 + c_5 v^5 + c_7 v^7 \dots$	16
2-3	Computer block diagram for Equation (2-10)	18
2-4	Region in which the 1/2-harmonic is sustained; nonlinearity by cubic function (analog-computer analysis).	19
2-5	Region in which the 1/2-harmonic is sustained; nonlinearity by symmetrically quadratic function (analog-computer analysis).	20
2-6	Region in which the 1/2-harmonic is sustained (calculated).	21
2-7	Oscillatory circuit containing reactor with direct current superposed.	22
2-8	Region in which the 1/2-harmonic is sustained (experimental).	24
2-9	General control loop	25
2-10	Waveforms of 2-phase power supply, stable operation	26
2-11	Waveforms of 2-phase power supply, presence of ripple instability	27
2-12	Generalized arrangement of m-phase amplifier	29
2-13	Output waveforms of m-phase amplifier, resistive or diode-clamped load	29
2-14	Unbalanced operation of a thyristor amplifier	30
2-15	Describing function for thyristor amplifiers with subharmonic input signals of order 1/2	37

Figure		Page
2-16	Use of describing function to test for ripple instability	37
3-1	Block diagram for Regulated Thyristor Power Supply	38
3-2	Simplified block diagram	39
3-3	Three-phase, full-wave, forced limit-cycle, regulator	41
3-4	Firing sequence of thyristor bridge	42
3-5	Cut-off sequence of thyristor bridge	43
3-6	Thyristor bridge output pulse	44
3-7	Untitled	46
3-8	Graph of pulse width versus pulse	47
4-1	Filter and load	52
4-2	Signal flow graph for linear system	52
4-3	The dead zone characteristics of the feedback system	54
4-4	$V_{out}$ vs. Time, $V_{ref} = 60.0$ volts	56
4-5	$V_{in}$ vs. Time, $V_{ref} = 60.0$ volts	57
4-6	$V_{out}$ vs. Time, $V_{ref} = 58.0$ volts, $60.0$ volts	59
4-7	$V_{in}$ vs. Time, $V_{ref} = 58.0$ volts, $60.0$ volts	60
4-8	$V_{out}$ vs. Time, $V_{ref}$ decreasing	62
4-9	$V_{out}$ vs. Time, $V_{ref}$ decreasing	63
4-10	$V_{out}$ vs. Time, $V_{ref}$ decreasing	64
4-11	$V_{out}$ vs. Time, $\alpha = 0.5$ and $0.0$	65
4-12	$V_{in}$ vs. Time, $\alpha = 0.5$	66
4-13	$V_{out}$ vs. Time, $\alpha = 0.0$ and $2.0$	67

Figure		Page
4-14	$V_{out}$ vs. Time, $V_{source} = 130.0$ volts	68
4-15	$V_{in}$ vs. Time, $V_{source} = 130.0$ volts	69
4-16	Response of linear filter, gain versus frequency	73



## 1. Introduction

There are many physical applications where a very stable direct current power supply is desirable. This is usually accomplished by taking a multiphase alternating current signal, full wave rectifying it and then passing it through what is essentially a low pass filter. The output then is some DC level on which rides a small value of "ripple". The ripple frequency is some multiple of the source input signal and is due to the filter's being non-ideal.

For most applications the amplitude of the ripple voltage is not so great that the power supply cannot be used and considered to be a stable DC source.

However, with the advent of the computer and switches that need only millivolts of fluctuations to switch, it is desirable to have power supplies that are more tightly regulated and effect a fast recovery from fluctuations in source supply and noise perturbations. This scheme is usually accomplished with higher loop gain.

When the loop gain increases to higher values, however, it has been witnessed that the amplitude of the ripple increases and contains components of frequencies that are lower than those witnessed under lower gain conditions.

Power supplies that employ silicon controlled rectifiers (thyristors) which are of the phase-control type are known to contain these subharmonics under high gain conditions.<sup>11</sup>

The nature of this paper is to investigate and verify the occurrence of subharmonics in a forced limit-cycling regulator employing silicon controlled rectifiers that are not phase fired. While verifying the fact that they do exist, an investigation is

made in an attempt to determine how these subharmonics are caused, what frequencies are present, and under what conditions they occur.

The ultimate goal of such investigation, of course, would be to discover means to predict the occurrence of subharmonics, their frequencies and amplitudes, with hopes of designing means to compensate the system so that these subharmonics do not present too great of a degrading effect on the output of the regulated power supply.

## 2. A general study of subharmonics in a nonlinear system.

If a linear system is forced by a sinusoidal input, the resulting steady-state output is also a sinusoid. However, a nonlinear system driven by a sinusoid does not produce a sinusoidal output, but the output contains harmonics which are frequencies that are integral multiples of the driving frequency.

In some cases the output may contain one or more frequencies that are lower than the forcing frequency. These frequencies are characteristically integral submultiples of the driving function and are called subharmonics. The subharmonics may be small in amplitude when compared to the driving frequency or may be so great in comparison that the forcing frequency may be neglected.

Unfortunately, there are no general rules available by which one may ascertain whether the occurrence of subharmonic oscillations is possible. Many references on the subject suggest that the question of predicting subharmonics can be answered by considering whether or not a sinusoidally forced differential equation of the form

$$\ddot{v} + k \dot{v} + f(v) = B \cos \nu \tau \quad (2-1)$$

can have a solution at a frequency of  $\omega/N$ , where  $N$  is an integer.

Equation (2-1) is a classical equation of the theory of nonlinear systems and is known as Duffing's Equation.

It has been found from experimentation that the occurrence of subharmonic oscillations in physical systems is strongly dependent on the starting conditions. The amplitude and frequency of the driving force must fall within certain definite limits. Because of this strong dependency on initial conditions it would appear that sub-harmonics would only be a transient problem. However, in a nonlinear system the oscillation is non-sinusoidal and contains harmonics of the fundamental frequency. It is possible to maintain the oscillation in a steady-state, under some conditions, by supplying energy to the system at any of these harmonic frequencies. Hence, the driving force is a harmonic of the fundamental frequency, or the fundamental frequency is an integral submultiple of the forcing frequency. This then is a condition for subharmonic generation.

## 2.1 Duffing's equation

Perhaps the most exhaustive study of the subharmonic phenomenon has been accredited to Hayashi.<sup>6</sup> The following examples of subharmonic oscillation applying Duffing's Equation have been taken from his work.

Consider the fundamental equation

$$\frac{d^2v}{dt^2} + 2\delta \frac{dv}{dt} + f(v) = B \cos \omega t, \quad (\omega = 2, 3, 4, \dots) \quad (2-2)$$

in which  $2\delta$  is a constant damping coefficient and  $f(v)$  is a term representing the nonlinear restoring force.



The period of the forcing function is  $2\pi/\nu$ , and the subharmonic  $1/\nu$  has a period  $2\pi$  and may be expressed by a linear combination of  $\sin \tau$  and  $\cos \tau$ .

What follows is an investigation of the relationship between the nonlinear characteristic expressed by the term  $f(v)$  and the order  $1/\nu$  of the subharmonic oscillations.

Consider the restoring force to be the polynomial

$$f(v) = \sum_{k=1}^n c_k v^k = c_1 v + c_2 v^2 + c_3 v^3 + \dots \quad (2-3)$$

where  $c_1, c_2, c_3, \dots$  are constants which are determined by the nonlinear characteristics. These constants are subject to the constraint that

$$c_1 + c_2 + c_3 + c_4 + \dots = 1 \quad (2-4)$$

In steady state one may assume that the solution of equation (2-2) has the form

$$v_0 = z + x \sin \tau + y \cos \tau + w \cos \nu \tau \quad (2-5)$$

The approximation for  $w$  is given by

$$w = \frac{1}{1 - \nu^2} B \quad (2-6)$$

which is legitimate as long as the nonlinearity is small.

By substituting (2-5) into (2-2) and equating the coefficients of the  $\sin \tau$  and  $\cos \tau$  terms separately to zero, the following results are obtained according to the form of the nonlinear characteristics found in (2-3).

Case 1.  $f(v) = c_1 v + c_3 v^3.$

The nonlinearity is symmetrical, or  $f(v)$  is an odd function, and in this case the constant term  $z$  can usually be disregarded.

Then for  $n = 2, 4, 5, \dots$ , substitution as mentioned above yields

$$\begin{aligned} [1 - 3/4 (\chi^2 + \eta^2) - 3/2 \omega^2] \chi + k \eta &= 0 \\ [1 - 3/4 (\chi^2 + \eta^2) - 3/2 \omega^2] \chi - k \eta &= 0 \end{aligned} \quad (2-7)$$

where  $k = 2\delta/c_3$ . By simultaneous solution one obtains that

$$k(\chi^2 + \eta^2) = 0 \quad (2-8)$$

Equation (2-8) implies that the amplitude of subharmonic oscillations is zero as long as  $k \neq 0$ , or damping is present. Hence subharmonics of order  $1/2, 1/4, 1/5, \dots$  cannot occur in this case. But real roots of  $\chi$  and  $\eta$  which do not simultaneously go to zero may be obtained for  $\nu = 3$ . Thereby, one may conclude that subharmonics of order  $1/3$  may occur when the nonlinear term  $c_3 v^3$  is present.

Case 2.  $f(v) = c_1 v + c_2 v^2 + c_3 v^3.$

Since the nonlinearity is unsymmetrical the constant term  $z$  in (2-5) must be considered. It is found under rigorous solution that subharmonics of the order  $1/2$  may exist in this case.

Case 3.  $f(v) = c_1 v + c_5 v^5.$

Although the cubic term  $c_3 v^3$  does not appear in the nonlinearity, detailed investigation reveals that subharmonics of order  $1/3$  still occur, along with those of order  $1/5$ .

After establishing theoretically the possible occurrence of subharmonic solutions to Duffing's Equation, Hayashi presents the results of several experimental investigations, a synopsis of which follows.

#### 2.1.1 Experimental investigation of subharmonic of order 1/3.

The experimental data was obtained using an electric oscillatory circuit containing a saturable-core inductor and a capacitor in series. The circuit equation takes the form of Equation (2-2) when a 60 cps a.c. voltage is applied to the circuit. If an initial condition is prescribed appropriately, a subharmonic oscillation of 20 cps may be started in the circuit. If one theoretically used a transformer core whose characteristic is expressed as

$$f(v) = c_1 v + c_3 v^3$$

the graph of Figure 2-2 is obtained. However, the nonlinear characteristic of the ordinary transformer core is not truncated with the cubic term and is expressed by

$$f(v) = c_1 v + c_3 v^3 + c_5 v^5 + c_7 v^7 + \dots$$

and the region in which 1/3-harmonic oscillation is sustained appears in Figure 2-1.

By connecting a number of inductance coils in series and adjusting the length of the air gap which is interposed in each core a fairly good approximation of the characteristic

$$f(v) = c_1 v + c_3 v^3$$

is obtained.

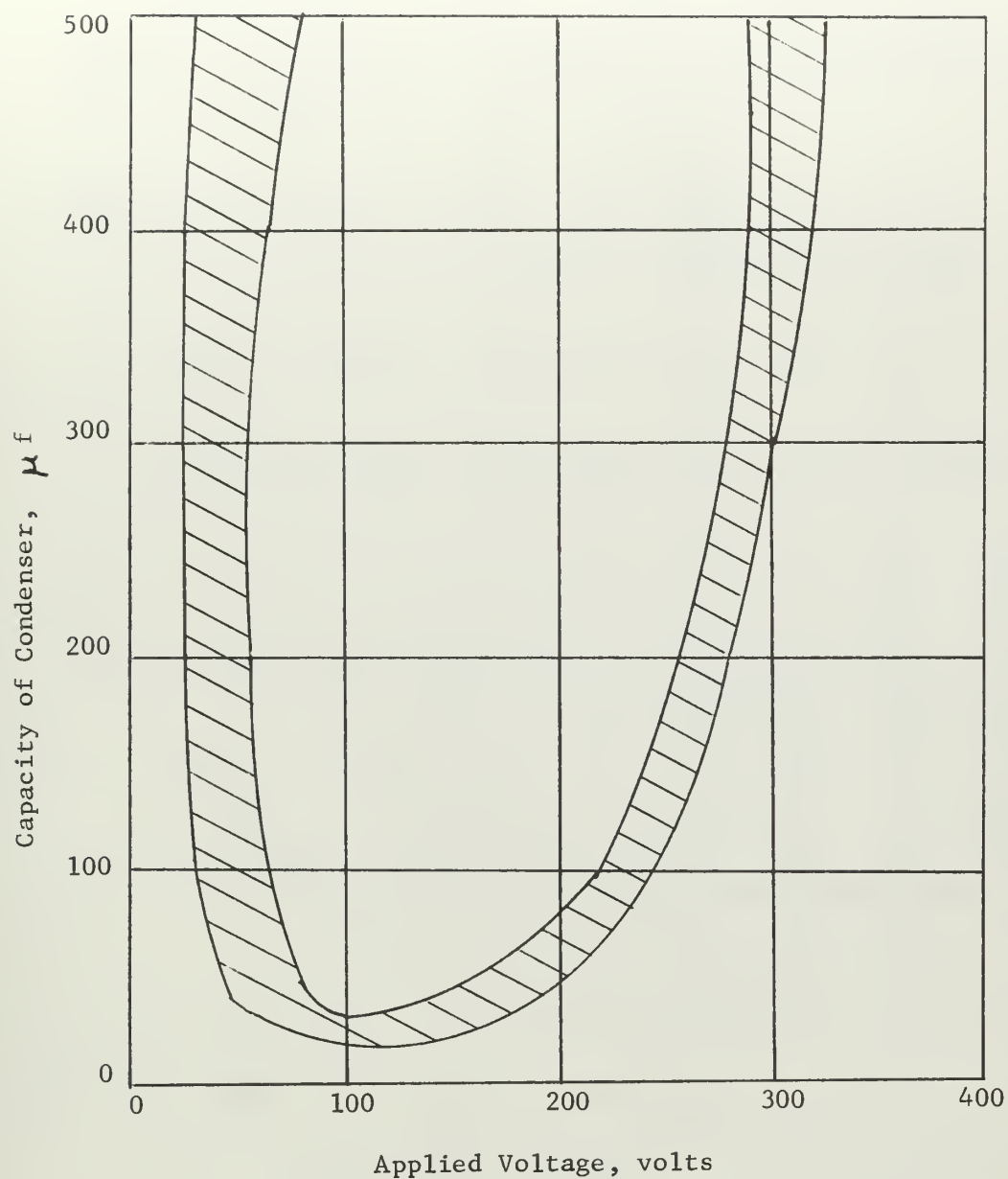


Figure 2-1. Region in which 1/3-harmonic oscillation is sustained. Magnetization curve by the equation

$$f(v) = c_1 v + c_3 v^3.$$

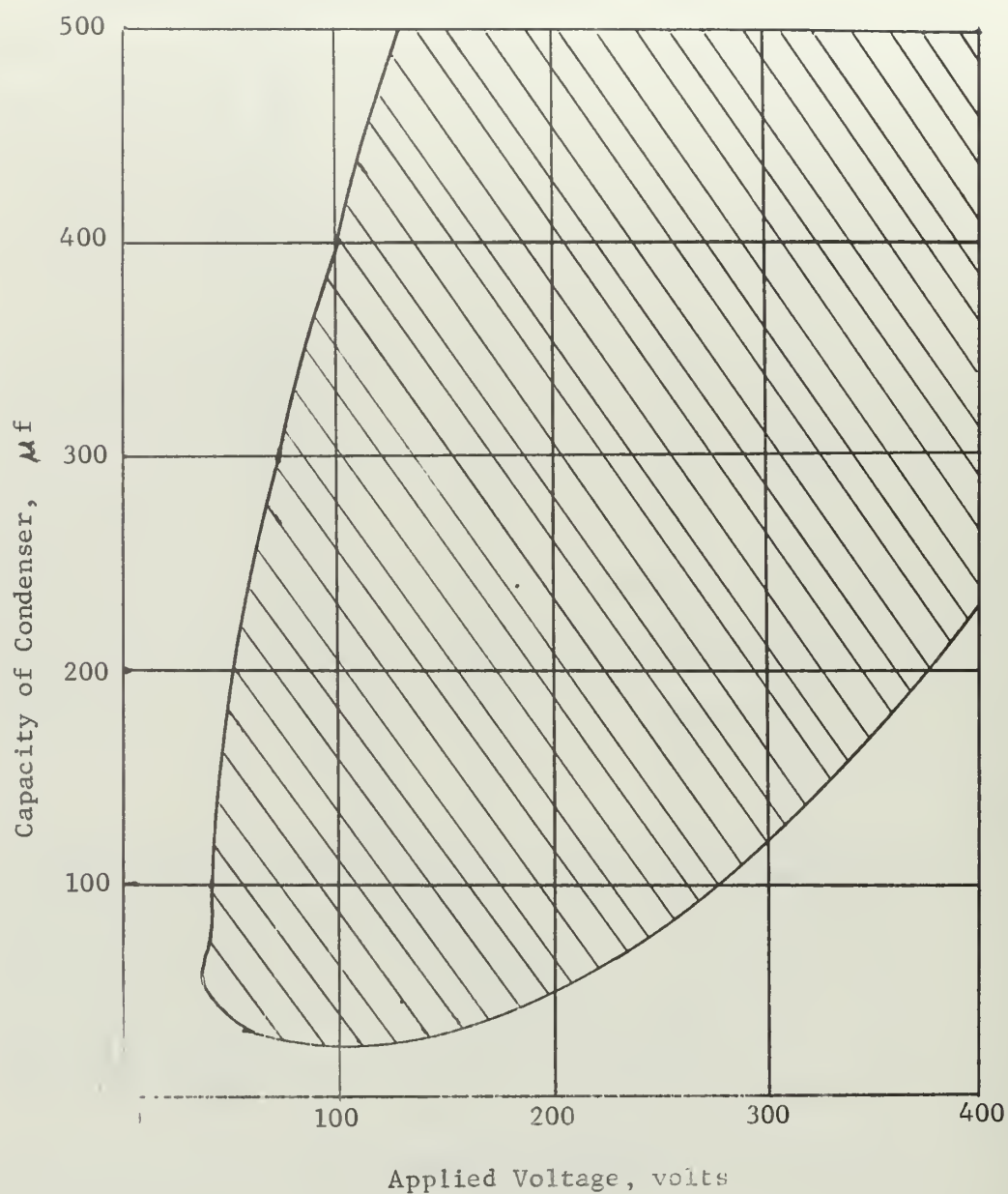


Figure 2-2. Region in which 1/3-harmonic oscillation is sustained. Magnetization curve by equation

$$f(v) = c_1 v + c_3 v^3 + c_5 v^5 + c_7 v^7 + \dots$$

When two cores are used, one with an air gap and the other without, the experimental verification to the analytical analysis is quite satisfactory.

### 2.1.2 Experimental investigation of subharmonics of order 1/2.

Investigations of systems described by the equations

$$\frac{d^2v}{dt^2} + 2\delta \frac{dv}{dt} + v^3 = B \cos 2\omega t + B_0 \quad (2-9)$$

$$\frac{d^2v}{dt^2} + 2\delta \frac{dv}{dt} + |v|v = B \cos 2\omega t + B_0 \quad (2-10)$$

can be done using an analog computer. Figure 2-3 shows the block diagram of an analog computer set up of Equation (2-10). To obtain a set up of Equation (2-9) one needs to replace the servomultiplier by an ordinary multiplier which gives a cubic nonlinearity.

If the initial conditions of  $v(0)$  and  $\dot{v}(0)$  are chosen appropriately one may start 1/2-harmonic oscillations. Slowly varying the values of  $B$  and  $B_0$  produces the regions in which 1/2-harmonics are sustained and Figures 2-4 and 2-5 show the experimental results for Equations (2-9) and (2-10) respectively.

Figure 2-6 is a graph of the region in which 1/2-harmonic oscillations are sustained using theoretical calculations.

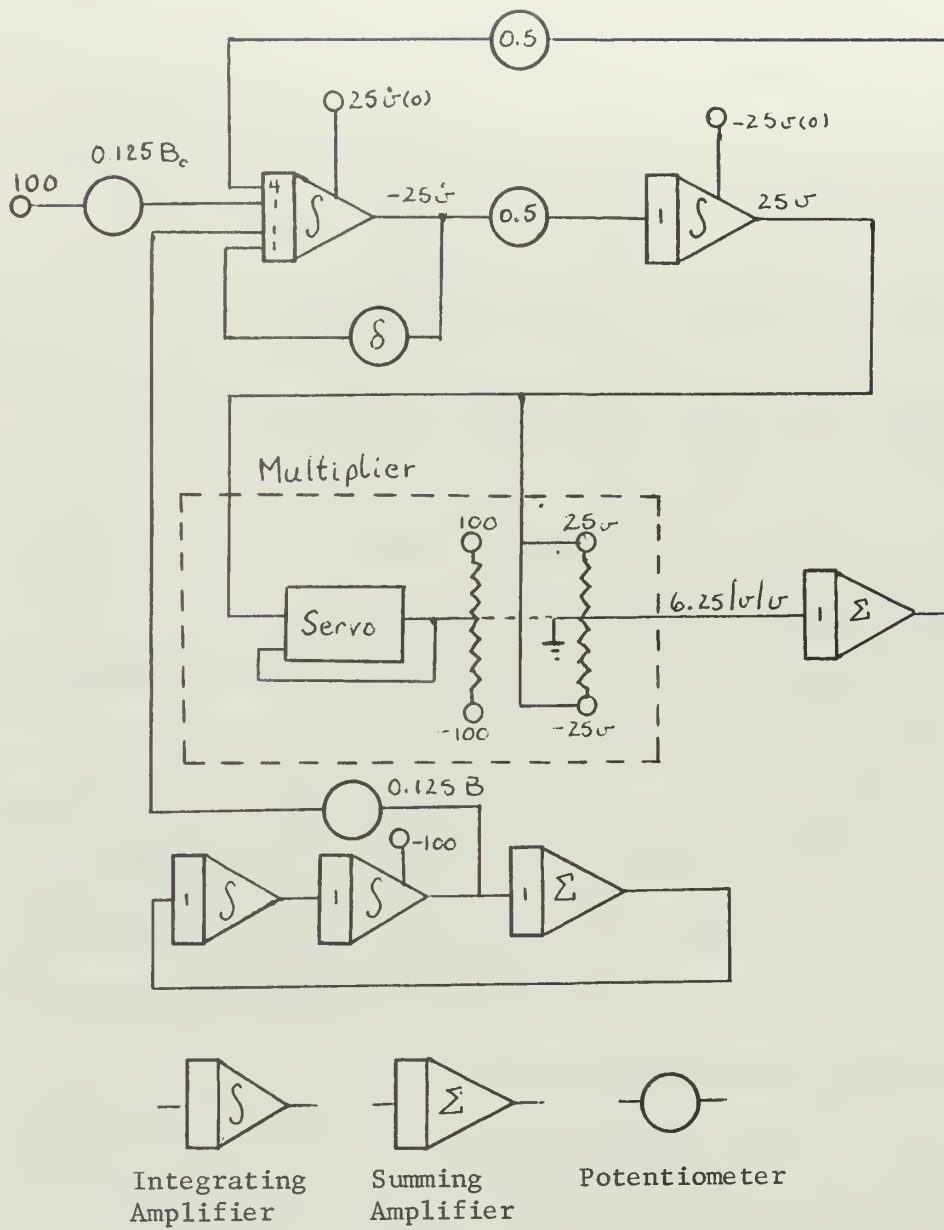


Figure 2-3. Computer block diagram for Equation (2-10).



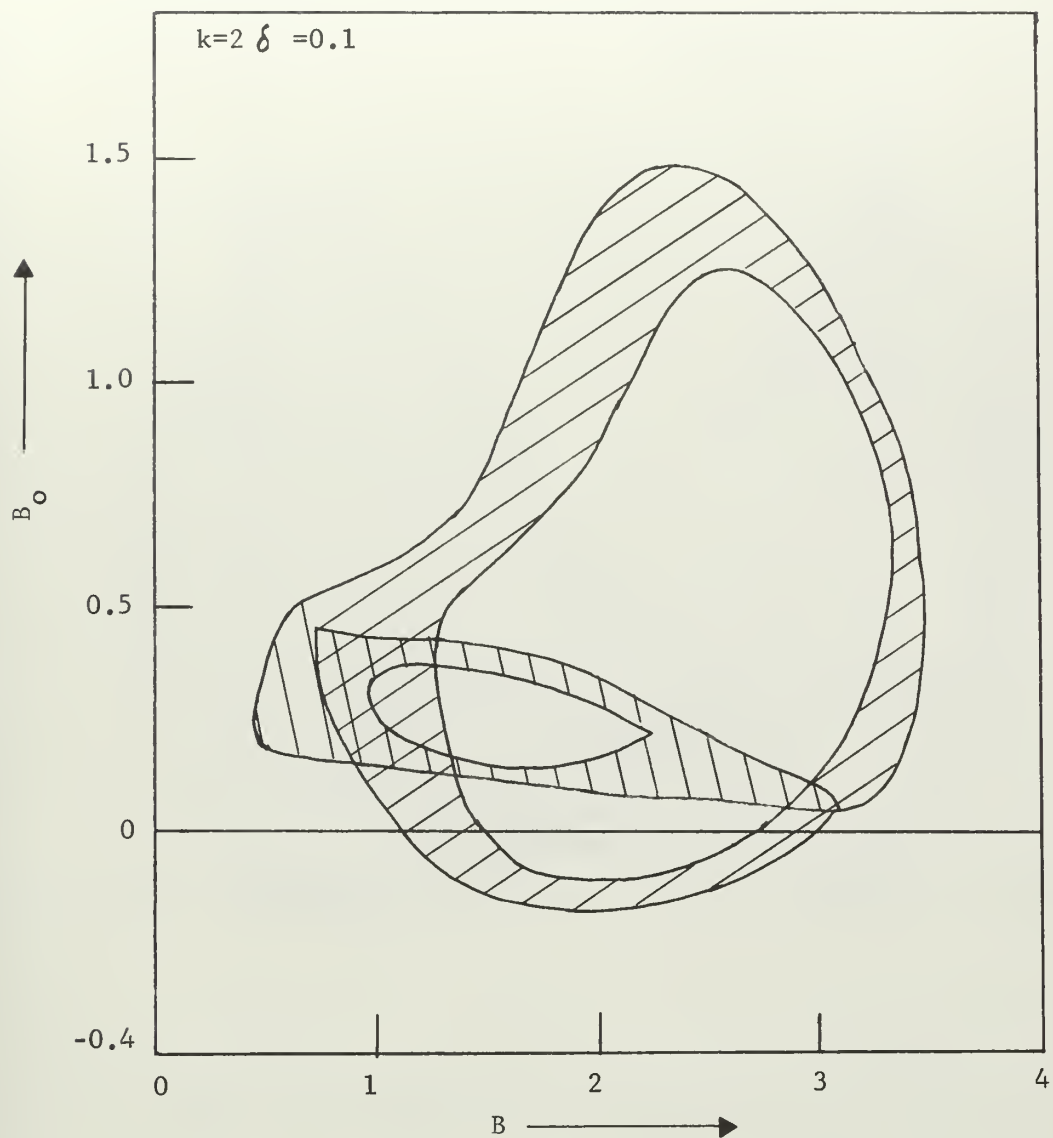


Figure 2-4. Region in which the 1/2-harmonic is sustained; nonlinearity by cubic function (analog-computer analysis).



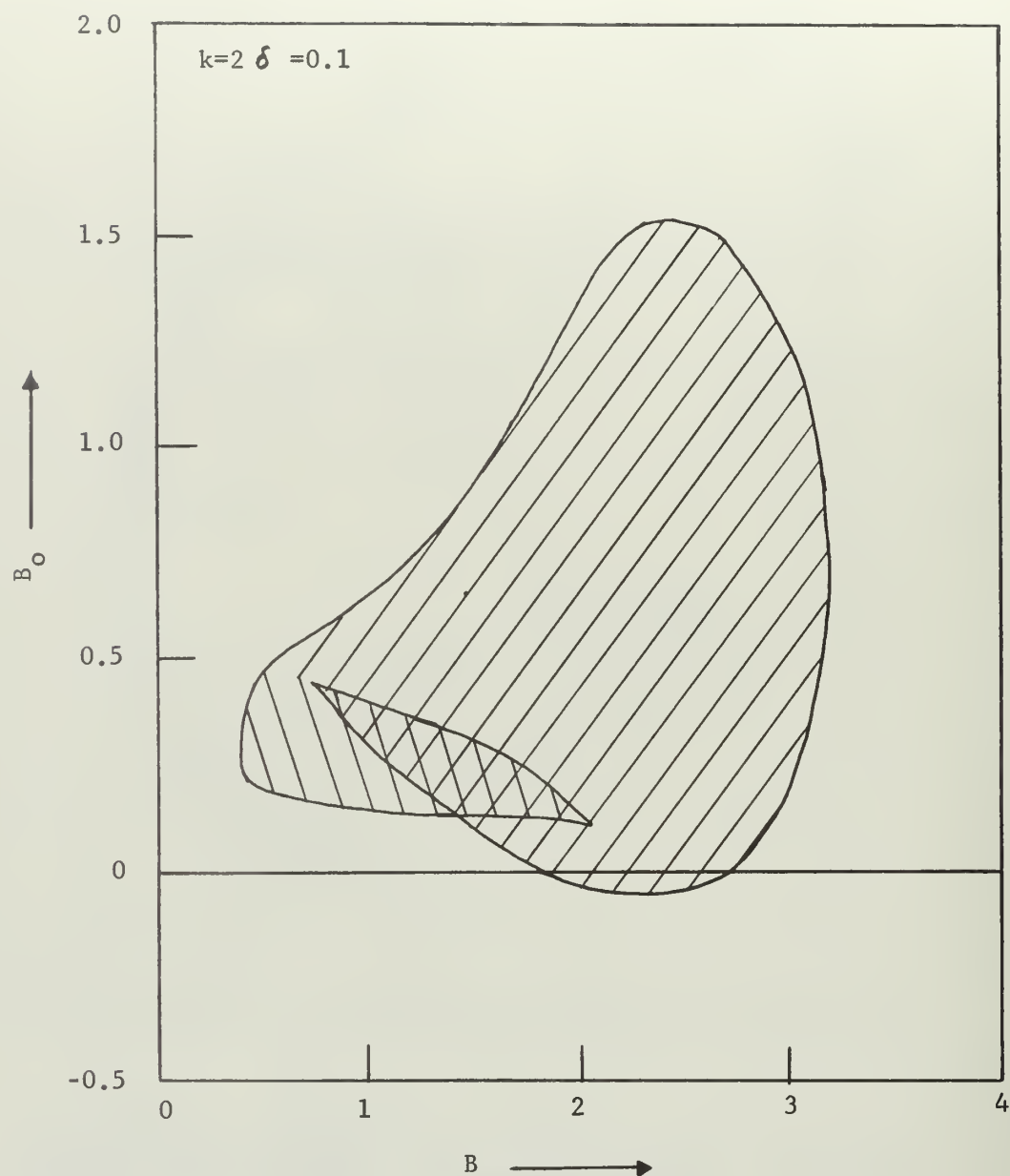


Figure 2-5. Region in which the 1/2-harmonic oscillation is sustained; nonlinearity by symmetrically quadratic function (analog-computer analysis).

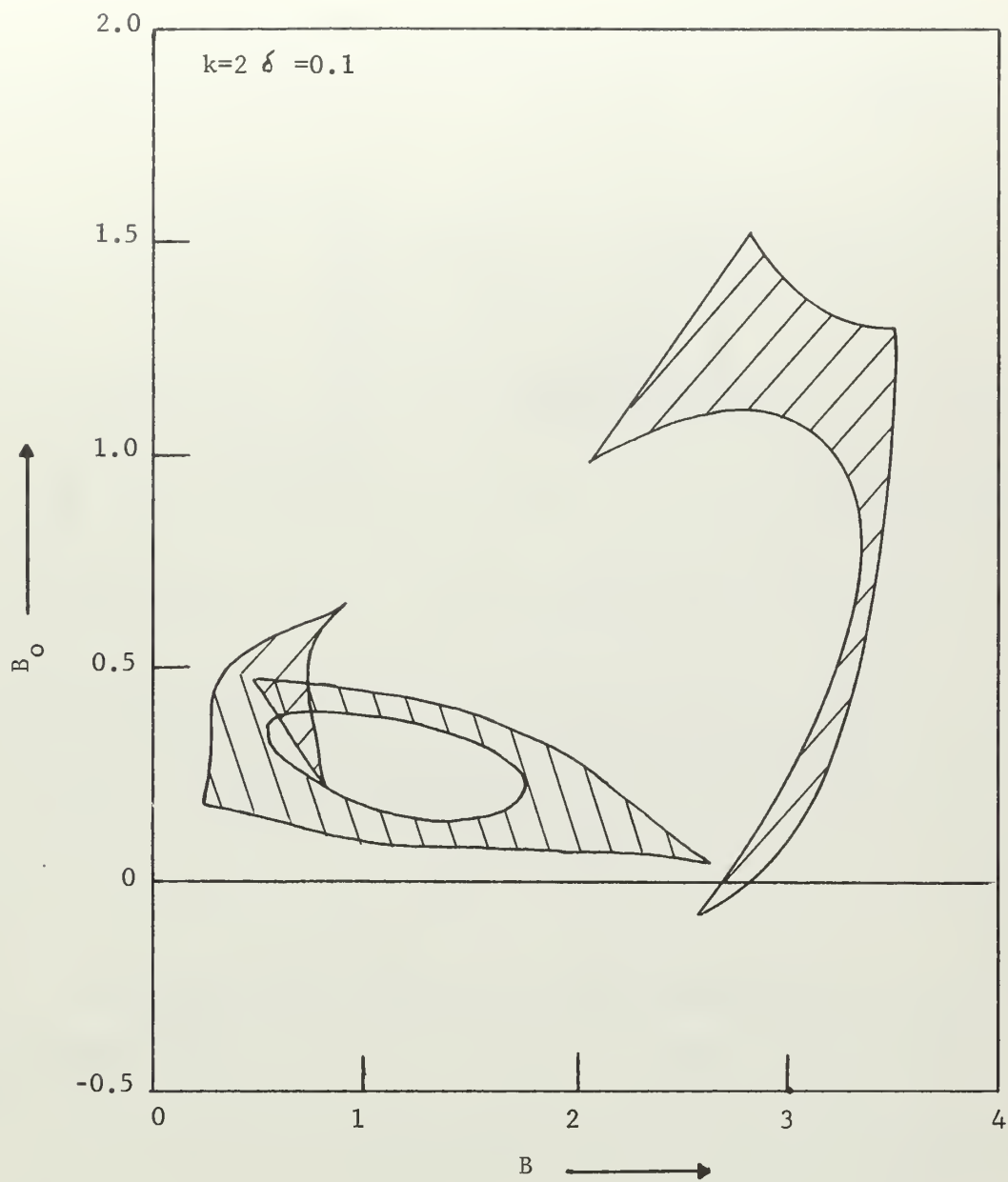


Figure 2-6. Region in which the 1/2-harmonic is sustained (calculated).

One-half harmonics are also witnessed in the electric circuit of Figure 2-7 due to the presence of a saturable-core inductor  $L$

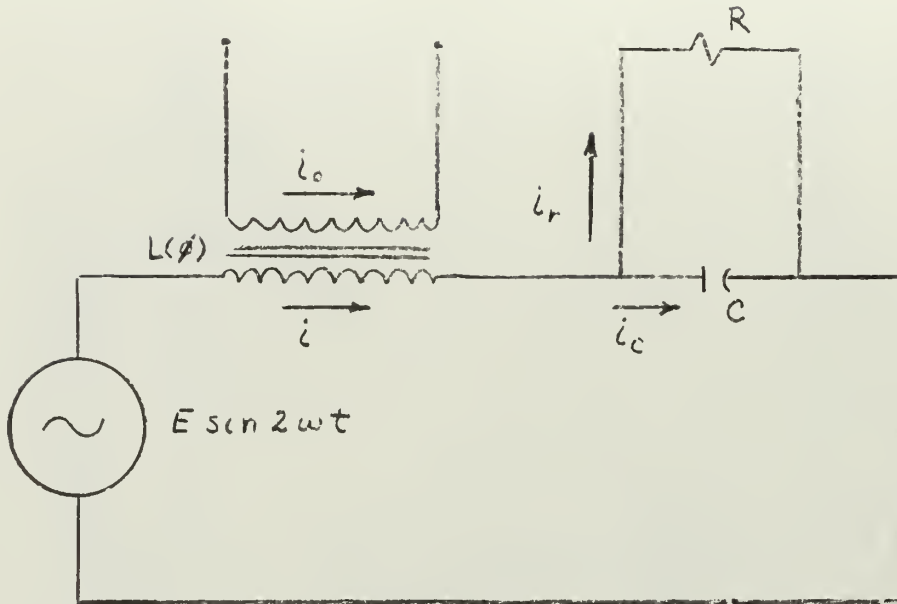


Figure 2-7. Oscillatory circuit containing reactor with direct current superposed.

under the impression of an alternating voltage  $E \sin 2\omega t$ . The secondary winding is provided on the core so that asymmetry is afforded to the nonlinear characteristic by forcing a constant DC current flow through it.

Using the notation of Figure 2-7 we have the equation

$$\begin{aligned} n \frac{d\phi}{dt} + R i_r &= E \sin 2\omega t \\ R i_r &= \frac{1}{C} \int i_c dt \\ i &= i_r + i_c \end{aligned} \tag{2-11}$$

where  $n$  is the number of turns in the primary winding and  $\phi$  is the magnetic flux in the core.

The non dimensional variables  $u$ ,  $u_0$ , and  $v$  are introduced in place of  $i$ ,  $i_0$ , and  $\phi$  by the relation

$$i = I_n u \quad i_0 = I_n u_0 \quad \phi = \Phi_n v \quad (2-12)$$

where  $I_n$  and  $\Phi_n$  are appropriate base quantities of the current and flux. Neglecting hysteresis the saturation curve has the form

$$u + u_0 = c_1 v + c_3 v^3 + c_5 v^5 + c_7 v^7 + \dots \quad (2-13)$$

The base quantities  $I_n$  and  $\Phi_n$  may be fixed by the relations

$$n \omega^2 C \Phi_n = I_n \quad c_1 + c_3 + c_5 + c_7 + \dots = 1$$

By eliminating  $i_r$  and  $i_c$  in equations (2-11) one obtains

$$\frac{d^2 v}{d\tau^2} + k \frac{dv}{d\tau} + c_1 v + c_3 v^3 + c_5 v^5 + \dots = B \cos 2\omega \tau + B_0$$

where  $\tau = \omega t - 1/2 \tan^{-1} k/2 \quad k = 1/\omega R C$

$$B = \frac{E}{n \omega \Phi_n} \sqrt{4 + k^2} \quad B_0 = u_0$$

In order that the experiment more closely agree with the analysis a composite reactor as described in section 2.1.1 is used, the saturation characteristics of which are described by

$$u + u_0 = c_1 v + c_3 v^3$$

Thus the differential equation of the electric circuit becomes

$$\frac{d^2 v}{d\tau^2} + k \frac{dv}{d\tau} + c_1 v + c_3 v^3 = B \cos 2\omega \tau + B_0$$

Figure 2-8 shows the experimental data obtained by varying the DC current in the secondary winding and the applied AC voltage.

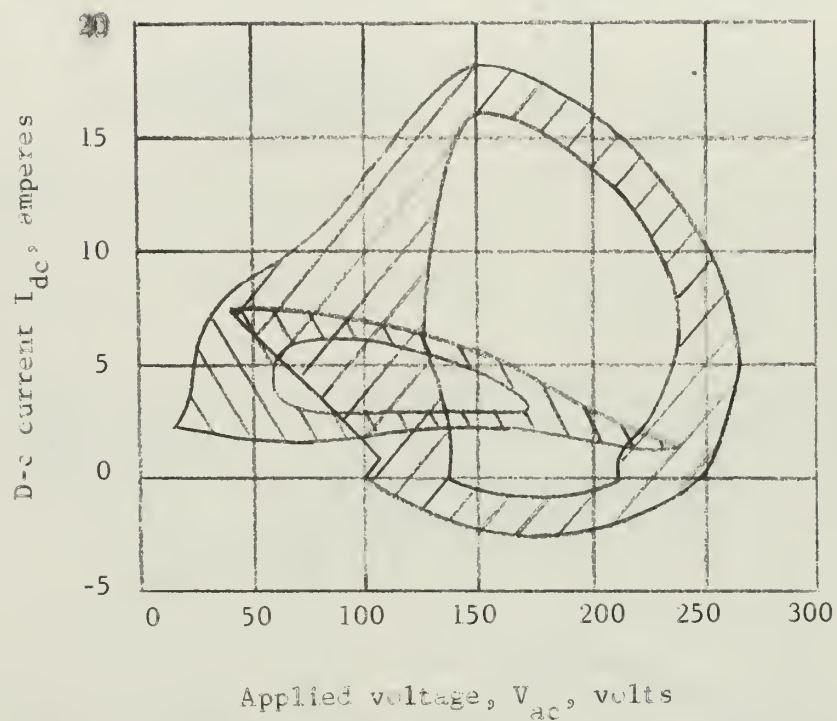


Figure 2-8. Region in which the 1/2-harmonic is sustained (experimental).

## 2.2 Subharmonics generated in a closed loop system with thyristors amplifiers.

It has been found that the problem of subharmonics is not limited merely to those cases described in the foregoing discussion. Dr. F. Fallside and Dr. A. R. Farmer have investigated the occurrence of subharmonics in systems which employ thyristors to create a power amplifier.<sup>11</sup>

Power amplifiers that use thyristors, thyatrons, magnetic amplifiers and mercury-arc converters are well known. Like other types of controlled-rectifier amplifiers, the thyristor amplifier is a discontinuous element since the input signal to the amplifier controls the output at discrete instants of time only. The output waveform is characterised by step changes in voltage and hence is rich in ripple.

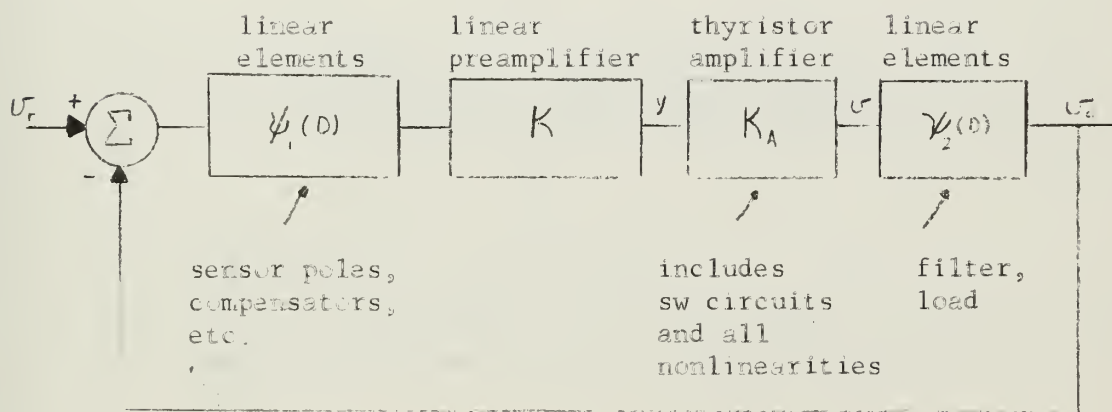


Figure 2-9. General control loop.

When used in a control loop such as Figure 2-9, the thyristor can be most simply treated as a continuous element, represented by its incremental DC gain between its steady-state input and its mean

output, and the ripple voltage due to the output wave can be disregarded. This is satisfactory for low bandwidth systems where the maximum component frequency of amplifier input signals is much less than the amplifier sampling frequency. Also, the large time constants incorporated into the linear filter is sufficient to ensure that only a negligible amount of ripple is fed back.

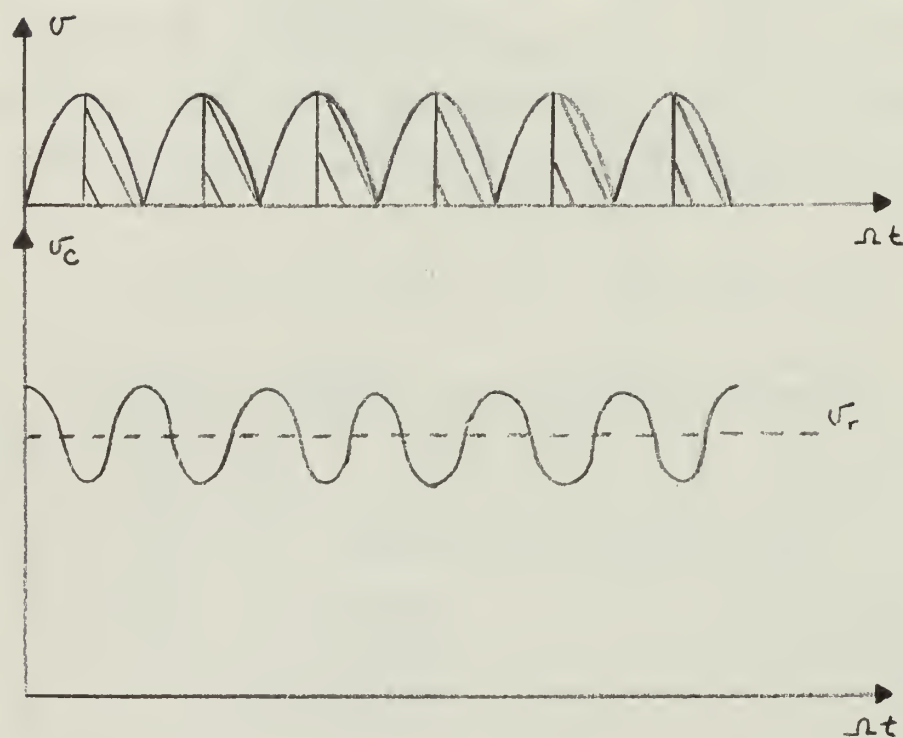


Figure 2-10. Waveforms of 2-phase power supply, stable operation.

In wide band applications such as current-control loops the simple approach is not valid. In such systems enough gain must be used so that appreciable ripple is fed back into the amplifier input, and, under certain conditions, a self oscillation of the loop, known as ripple instability can result. The frequency of the oscillation occurs at an integral submultiple of the basic ripple frequency, i.e., a subharmonic, and manifests itself in the amplifier as a periodic variation in the firing pattern.

The waveform of Figure 2-10 shows the behavior of the typical stable operation of a 2-phase regulated power supply.

Figure 2-11 Shows the ripple instability introduced when the loop gain is increased by the preamplifier.

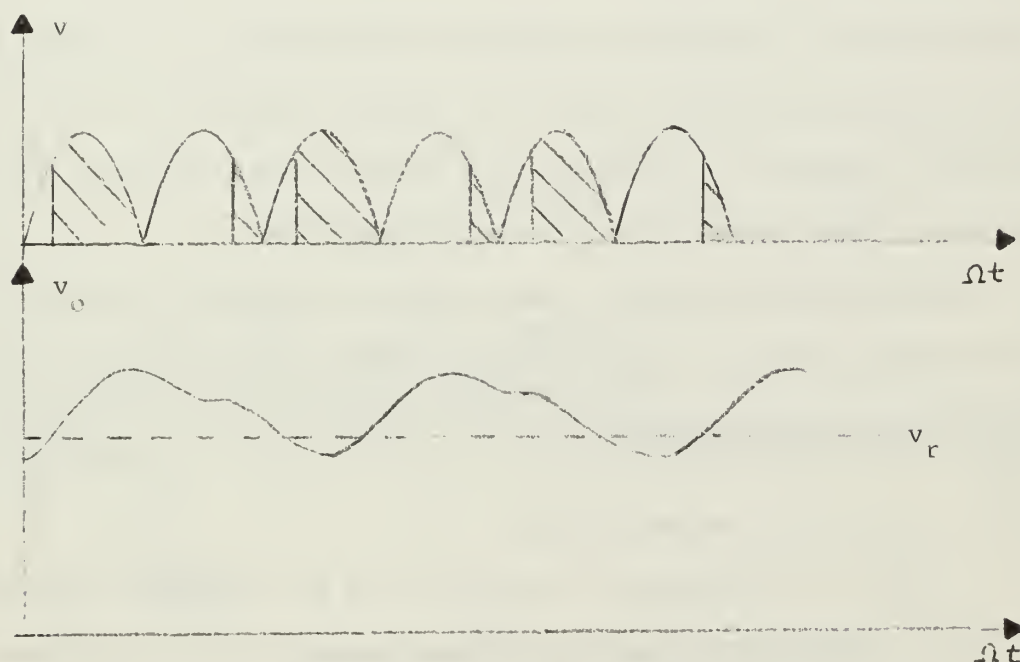


Figure 2-11. Waveforms of 2-phase power supply, presence of ripple instability.



Ripple instability cannot be predicted by a simple linearized approach to system design and a more accurate analysis must be used.

#### 2.2.1 Amplifier characteristics

A thyristor amplifier may be generally represented by the m-phase arrangement of cells shown in Figure 2-12. The output voltage waveform of the amplifier for a constant input  $y$  is assumed to be as shown in Figure 2-13 for a resistive or diode clamped load.

There are many types of firing circuits for thyristor amplifiers and the sinewave reference type is considered here. This type of firing has an advantage in that it produces a linear DC gain characteristic for the relation between the amplifier input  $y$  and the mean output voltage  $v_o$ . In this particular circuit, the input to the firing circuit of each phase consists of the amplifier input plus a phased sinusoidal reference signal of constant amplitude at the excitation frequency. A gate pulse is passed to the thyristor when this total input passes through zero going positive.

The Fallside and Farmer paper proceeds to analyze this particular amplifier by two means, an impulse method and a Master Describing Function method.

#### 2.2.2. Analysis by impulse method

Since the subharmonic of order  $1/2$  is the simplest oscillation to analyze by the impulse method so that it only will be considered here.

The unbalanced-amplifier output waveform characteristic of  $1/2$ -order subharmonic instability is shown in Figure 2-14a. This

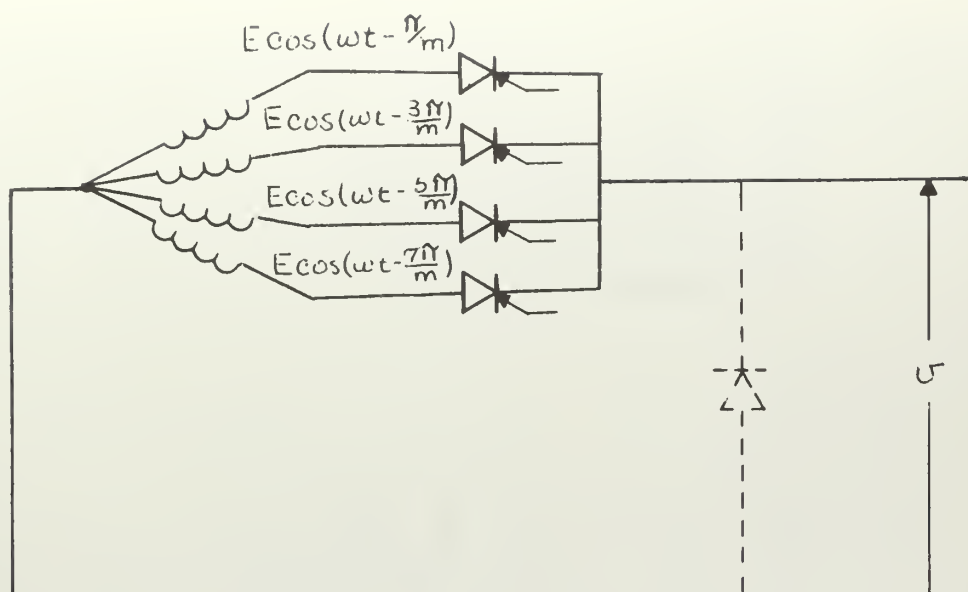


Figure 2-12. Generalized arrangement of m-phase amplifier

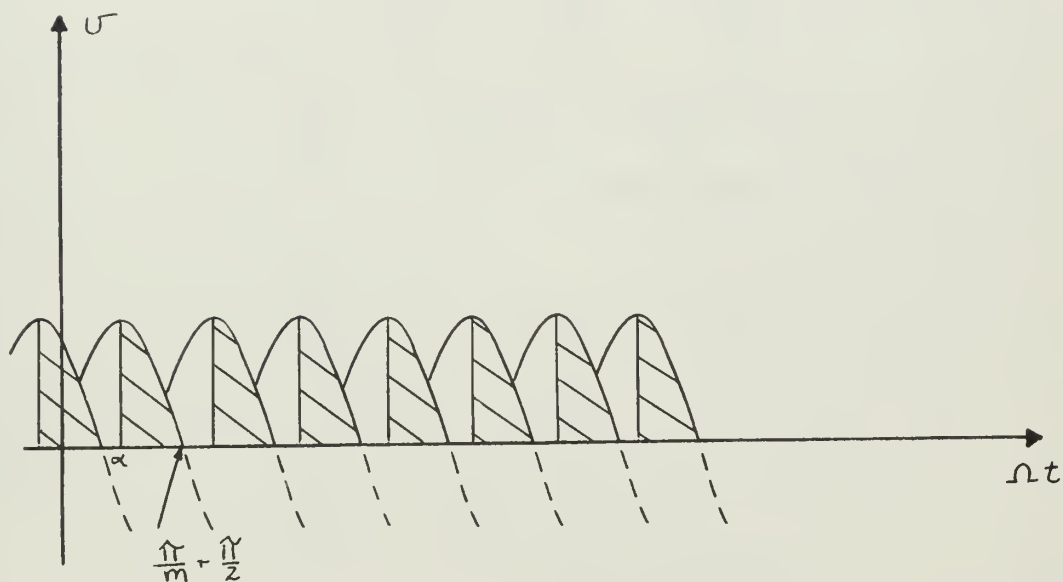


Figure 2-13. Output waveforms of m-phase amplifier, resistive or diode-clamped load.

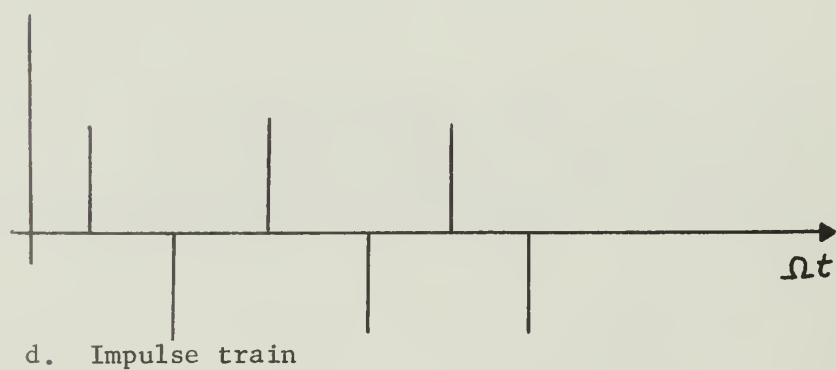
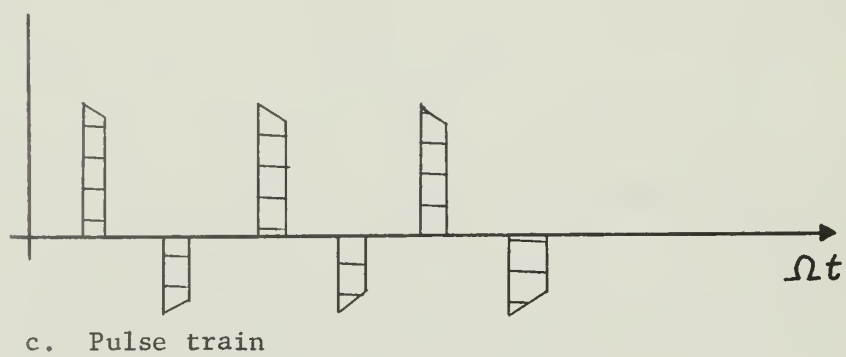
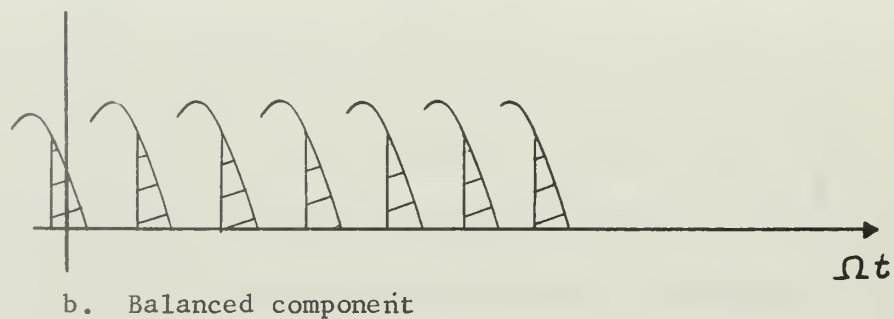
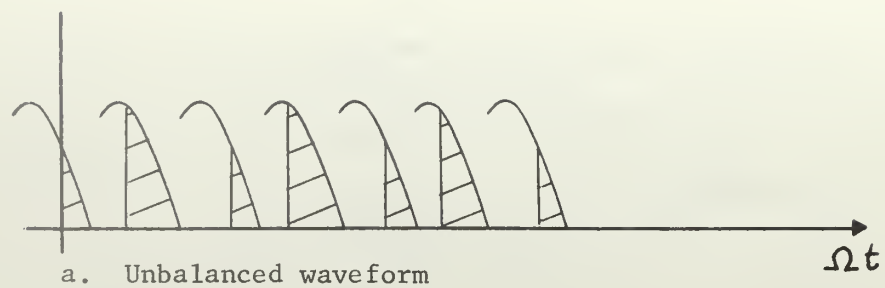


Figure 2-14. Unbalanced operation of a thyristor amplifier

waveform is considered to have two parts; the balanced component of Figure 2-14b and the pulse train of Figure 2-14c, alternating at the subharmonic frequency of  $m\Omega/2$ . The pulse train which is representative of the imbalance has no net DC output and injects a signal of frequency  $m\Omega/2$  into the loop. A portion of this signal, attenuated and smoothed by the filter, is fed back into the amplifier input and the oscillation may thus be maintained. For any appreciable oscillation about the mean firing angle  $\alpha$ , the positive and negative pulses are different both in amplitude and duration. However, for diminishingly smaller amounts of imbalance, the pulse train becomes in the limit, a symmetrical impulse train of Figure 2-14c, and represents the conditions at the onset of instability. By examining the system equations under these conditions it is possible to formulate a general condition for the loop to sustain a subharmonic of infinitesimal amplitude.

Referring to the linear control loop of Fig. 2-9, assuming stable, balanced operating conditions, the amplifier output can be written as the Fourier series

$$v = v(\alpha) + \sum_{n=1}^{\infty} c_n(\alpha) \sin(nm\Omega t + \phi) \quad (2-14)$$

The input to the thyristor amplifier is

$$y = K \psi_1(D) \{ v_r - \psi_2(D) v \} \quad (2-15)$$

and the equation of the firing circuits at any firing instant is

$$y + X \cos(\Omega t - \pi/m - \rho) = 0 \quad (2-16)$$

where

$$\Omega t = \alpha + \frac{2\pi k}{m} \quad (k = 0, 1, 2, \dots, \infty) \quad (2-17)$$

and

$$\rho = \frac{2\pi k}{m} + \pi - \frac{\pi}{m} \quad (2-18)$$

Substituting for  $y$  Equation (2-16) becomes

$$K \psi_1(D) v_r - K \psi_1(D) \psi_2(D) v + \bar{X} \cos(\Omega t - \frac{\pi}{m} - \rho) = 0 \quad (2-19)$$

Considering steady state operation where  $v_r$  is constant, the operator  $D$  may be replaced by  $j\omega$ , after substituting for  $e$ ,  $\Omega t$ , and  $\rho$  Equation (2-19) becomes

$$\begin{aligned} K \psi_1(j\omega) v_r - K \psi_1(j\omega) \psi_2(j\omega) v_0(\alpha) \\ = K \sum_{n=1}^{\infty} z_n c_n(\alpha) \sin \left\{ nm \left( \alpha + \frac{2\pi k}{m} \right) + \phi_n + \theta_n \right\} \\ - \bar{X} \cos \alpha = 0 \end{aligned} \quad (2-20)$$

The operator  $\psi_1(D)$  and  $\psi_2(D)$  have been replaced by  $\psi_1(j\omega)$  and  $\psi_2(j\omega)$  is the amplitude and  $\theta_n$  the phase of the expression at a frequency  $\omega = nm\Omega$ .

If one now assumed an infinitesimal amplitude of subharmonic oscillation, the system equations must be modified by the pulse train  $\Delta v$ , assuming the pulses have a duration  $\Delta \alpha$

$$\Delta v = \sum_{l=1/2}^{\infty} \frac{2m\Delta \alpha}{\pi} \sin \frac{\pi}{m} \sin \alpha \cos lm \left( \Omega t - \alpha - \frac{2\pi k}{m} \right) \quad (2-21)$$

where

$$l = n - 1/2 \quad (n = 1, 2, \dots, \infty)$$

The firing instants now become  $\Omega t = (\alpha - \Delta\alpha) + \frac{2\pi k}{m}$ , thus the firing circuit equations becomes

$$\begin{aligned}
 & K \psi_1(j\omega) \psi_r - K \psi_1(j\omega) \psi_2(j\omega) \psi_c(\alpha) \\
 & - K \sum_{\ell=1/2}^{\infty} Z_{\ell} \frac{2mE\Delta\alpha}{\pi} \sin \frac{\pi}{m} \sin \alpha \cos \left\{ \ell m \left( \frac{2\pi k}{m} \right. \right. \\
 & \left. \left. + \alpha - \Delta\alpha - \frac{2\pi k}{m} - \alpha \right) + \Theta_{\ell} \right\} - K \sum_{n=1}^{\infty} Z_n C_n(\alpha) \sin \left\{ nm(\alpha \right. \\
 & \left. - \Delta\alpha + \frac{2\pi k}{m}) + \phi_n + \Theta_n \right\} - \bar{X} \cos(\alpha - \Delta\alpha) = 0.
 \end{aligned} \tag{2-22}$$

Assuming  $\Delta\alpha \rightarrow 0$ , the terms which represent balanced operation may be removed by subtracting Eq. (2-20). The conditions by which subharmonics may exist is seen as

$$\begin{aligned}
 & K \left\{ \sum_{\ell=1/2}^{\infty} Z_{\ell} \frac{2mE\Delta\alpha}{\pi} \sin \frac{\pi}{m} \sin \alpha \cos \Theta_{\ell} \right. \\
 & \left. - \sum_{n=1}^{\infty} Z_n C_n(\alpha) nm \Delta\alpha \cos(nm\alpha + \phi_n + \Theta_n) \right\} \\
 & + \bar{X} \Delta\alpha \sin \alpha = 0.
 \end{aligned}$$

Dividing through by  $\bar{X} \Delta\alpha \sin \alpha$ , and introducing the DC gain

$$K_A = \frac{mE}{\pi \bar{X}} \sin \frac{\pi}{m}, \text{ this reduces to}$$

$$\begin{aligned}
 & G_c \left\{ \sum_{\ell=1/2}^{\infty} 2 Z_{\ell} \cos \Theta_{\ell} - \sum_{n=1}^{\infty} \frac{Z_n C_n(\alpha) nm}{\bar{X} K_A \sin \alpha} \cos(nm\alpha \right. \\
 & \left. + \Theta_n + \phi_n) \right\} + 1 = 0.
 \end{aligned} \tag{2-23}$$

This may be written more simply as

$$G_C \left\{ \sum_{l=1/2}^{\infty} 2z_l \cos \theta_l - \sum_{n=1}^{\infty} z_n C_n \cos(\gamma_n + \theta_n) \right\} + 1 = 0 \quad (2-24)$$

where  $C_n = \frac{c_n(\alpha) n m}{\bar{I} K_A \cos(\alpha - \pi/m)}$

and  $\gamma_n = n m \alpha + \phi_n.$

In summary, the critical loop gain for ripple instability at a subharmonic of order 1/2 can be calculated from the impulse-analysis criterion of Eq. (2-24) for any given thyristor amplifier, in any linear control system to any degree of accuracy, by taking sufficient terms in the summation. In Eq. (2-24),  $C_n$  and  $\gamma_n$  depend the amplifier used and its mean firing angle or output voltage; the terms  $z_l$ ,  $z_n$ ,  $\theta_l$  and  $\theta_n$  define the remainder of the control loop through  $\psi_1(j\omega)$   $\psi_2(j\omega)$ .

### 2.2.3 Describing function for infinitesimal subharmonic input signals of order 1/2.

The Fallside and Farmer paper also presents a describing function approach to the analysis of the conditions for sustentation of subharmonics of order 1/2, considering the subharmonics appear as infinitesimal amplitudes. Again for a constant input the firing circuit equation is

$$y + \bar{I} \cos(\Omega t - \pi/m - \rho) = 0 \quad (2-16)$$

and at the firing instants

$$\Omega t = \alpha + \frac{2\pi k}{m} \quad (k = 0, 1, 2, \dots, \infty) \quad (2-17)$$



If a sinusoidal signal of infinitesimal amplitude  $\Delta y$ , frequency  $m\Omega/2$  and some arbitrary phase  $\mu$  is added to  $y$ , the firing equations become

$$y + \Delta y \cos\left(\frac{m\Omega t}{2} + \mu\right) + X \cos(\Omega t - \tilde{\pi}/m - \Gamma) = 0$$

and

$$\Omega t = \alpha \pm \Delta\alpha + \frac{2\tilde{\pi}k}{m}$$

After subtracting Eqn. (2-16), the incremental firing angle and the input subharmonic signal amplitude  $\Delta y$  are related by

$$\begin{aligned} \Delta y \cos\left\{\frac{m}{2}\left(\alpha - \Delta\alpha + \frac{2\tilde{\pi}k}{m}\right) + \mu\right\} \\ = -\Delta\alpha X \sin\left(\alpha + \frac{2\tilde{\pi}k}{m} - \frac{\tilde{\pi}}{m} - \Gamma\right). \end{aligned} \quad (2-25)$$

The addition of a subharmonic signal to the input of the amplifier in turn produces an alternating impulse train at the amplifier output. (Fig. 2-14d) This impulse train has a component of subharmonic frequency given by

$$U_{1/2} = \frac{2mE}{\pi} \Delta\alpha \sin \frac{\tilde{\pi}}{m} \sin \alpha \cos\left(\frac{m\Omega}{2}t - \frac{m\alpha}{2} - \tilde{\pi}k\right)$$

Substituting from Eq. (2-25) for  $\Delta y$  and assuming  $\Delta\alpha \ll 1$ ,

$$U_{1/2} = 2K_A \cos \psi \cos\left(\frac{m\Omega}{2}t + \mu - \psi\right)$$

where

(2-26)

$$\psi = \frac{m}{2}\left(\alpha + \frac{2\tilde{\pi}k}{m}\right) + \mu.$$

Thus, for input signals of infinitesimal amplitude at subharmonic frequency  $\frac{m\Omega}{2}$ , the amplifier has a gain of  $2K_A \cos \psi$  and introduces a phase shift  $\psi$ .



The amplifier can then be characterized by the describing function,

$$N\left(j \frac{m\Omega}{2}\right) = \frac{v_{1/2}}{\cos\left(\frac{m\Omega}{2} + \mu\right)} = \left| 2K_A \cos \psi \right| \angle -\psi \quad (2-27)$$

This is shown in Fig. 2-15, and is a circle of radius  $K_A$ , centered on  $(K_A, j0)$ . The normalized version  $\bar{N}\left(j \frac{m\Omega}{2}\right)$  is a circle of unit radius centered on  $(1, j0)$ .

This describing function may be used to test for ripple instability at the subharmonic frequency  $\frac{m\Omega}{2}$  and the procedure can be seen in Fig. 2-16. First the open-loop frequency locus  $KK_A \psi_1(\omega) \psi_2(\omega)$  is plotted; then the normalized describing function  $\bar{N}\left(j \frac{m\Omega}{2}\right)$  is superimposed, as a unit circle, centered upon the point on the frequency locus corresponding to  $\omega = \frac{m\Omega}{2}$ . Using conventional assumptions, the system will be unstable and oscillate at the subharmonic frequency  $\frac{m\Omega}{2}$  if the circle encloses the point  $(-1, j0)$ ; the critical condition being

$$2KK_A \bar{z}_{1/2} \cos \Theta_{1/2} + 1 = 0 \quad (2-28)$$

Referring to Eqn. (2-24), this is the condition which was obtained from merely the first term of the exact impulse criterion.

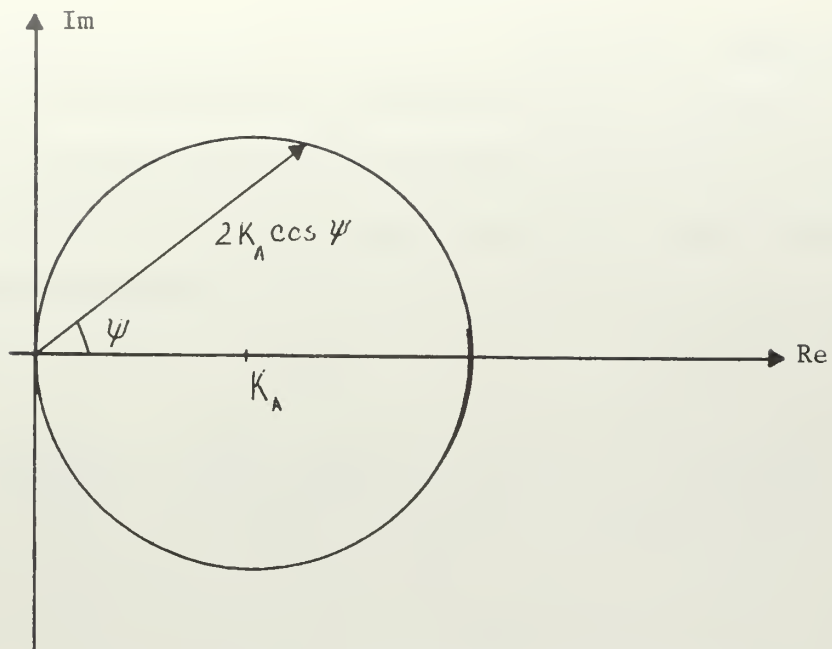


Figure 2-15. Describing function for thyristor amplifiers with subharmonic input signals of order  $1/2$ .

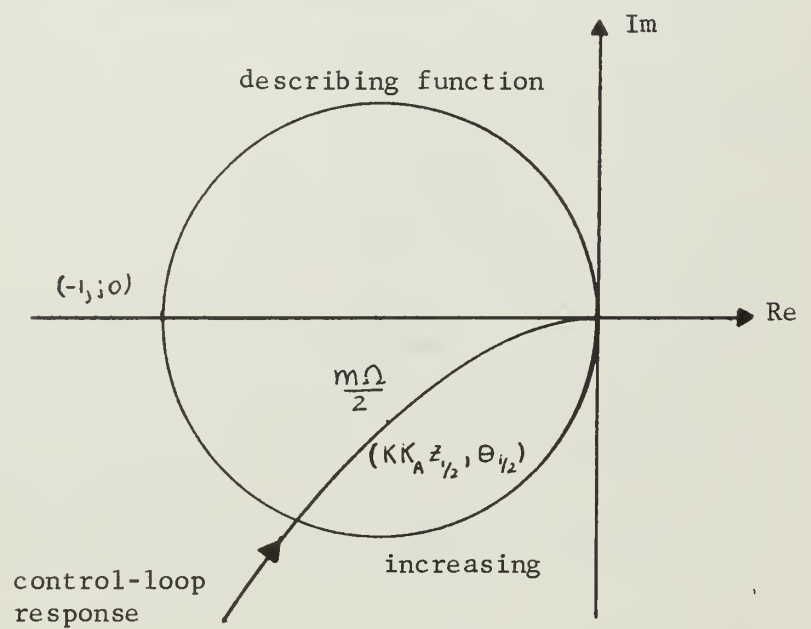


Figure 2-16. Use of describing function to test for ripple instability.

### 3. Description of system

In chapter 2, the SCR amplifier that was discussed was one that employed a phase firing scheme of control. The thyristors were fired individually when the current through each one attained a certain phase in relation to a reference sinusoid. The thyristor amplifier that is the concern of this paper employs a different method of operation.

The specific system under investigation is a polyphase, thyristor, AC to DC rectifier, operating under forced limit cycling conditions. The block diagram for the model of the system appears in Figure 3-1.

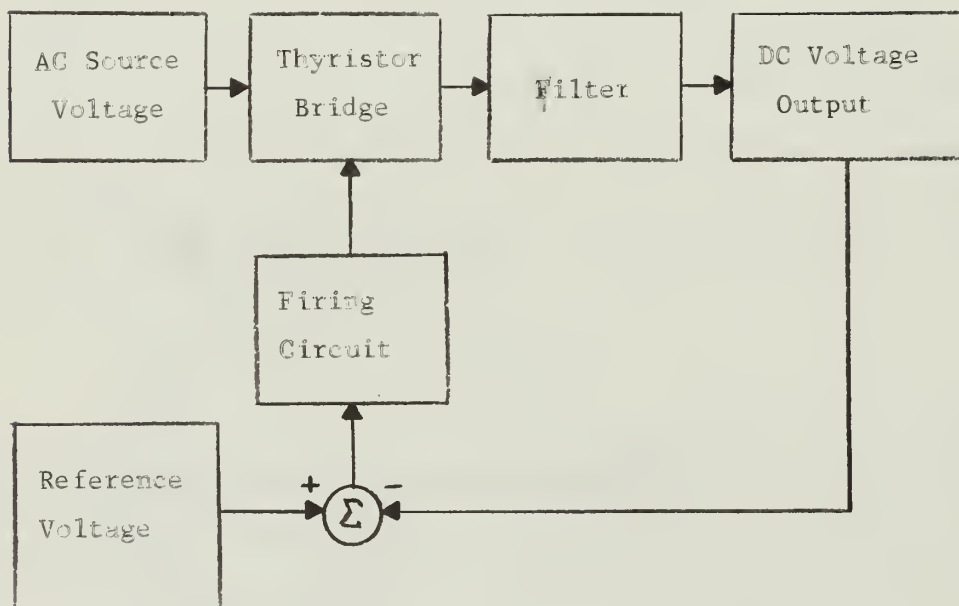


Figure 3-1. Block diagram for Regulated Thyristor Power Supply.

This block diagram may be simplified into the system of Figure 3-2 where  $G_1$  is included to take into account any gain that may be associated with the comparator, firing circuits and compensation that

may be added to the system and is completely linear.  $G_2$  is the linear transfer function of the filter and load. All of the nonlinearities of the firing circuit and bridge are lumped into the single describing function  $N$ . The nature of this describing function is developed in Leszczynski's thesis not considering ripple instability.<sup>10</sup>

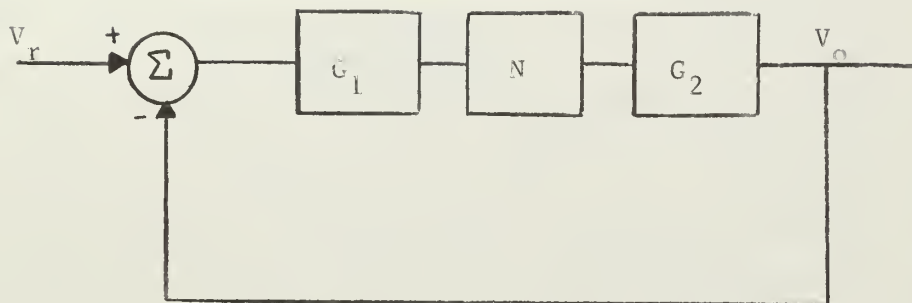


Figure 3-2. Simplified block diagram.

In the phase firing scheme, for polyphase rectifications, it is required that there be separate firing circuits for each individual thyristor as well as phasing and timing circuits to ensure proper sequence of firing. Hence, a three-phase, full wave rectifier would require six separate firing circuits.

So as to simplify the control philosophy and to curtail the expense of six separate firing circuits, the method considered here is to control the entire polyphase bridge as a unit with one firing circuit. In this way the gates of all the thyristors in the bridge are connected in series and are pulsed simultaneously with one pulse. (A simplified circuit diagram can be seen in Figure 3-3.) However, only those thyristors whose current has a phase between 0 and 180 degrees will fire immediately as the pulse goes ON. As the phase

of the current in the remaining thyristors traverse through 0 degrees they too will fire as long as the ON pulse is maintained at the thyristor gates. Figure 3-4 illustrates the sequence as the six thyristors are pulsed ON. As a result, when the firing signal is ON, the entire bridge is on and acts as a conventional diode bridge.

A slightly different aspect is presented when the bridge is pulsed OFF, or the bias is removed from the thyristor gates. When the OFF pulse is received, a time delay occurs before the bridge is completely cut off. This is due to the fact that the thyristor, like its gas tube counterpart, the thyatron, is not cut off until its shut off conditions have been met, i.e., the bias has been removed and the collector voltage goes negative with respect to the emitter. Figure 3-5 shows the sequence as the six thyristors are pulsed OFF. The time delay  $\tau$  occurs between the time the OFF signal is received and the last thyristor cuts off.

A summary of the system operation is as follows. Assume that the desired output is a certain voltage and the output voltage is below this reference level. The rectifier bridge is then supplied with an ON signal and the bridge output is a three-phased, full-wave, rectified voltage which is fed to the filter. The filter then attenuates the harmonics of this voltage and provides a relatively smooth DC voltage at the output. When the DC output rises above the reference level the bridge is pulsed off. Because the shut off conditions of each thyristor must be met, a time delay occurs before the bridge turns off. In the OFF state the input voltage to the filter is essentially zero since the reverse current is virtually blocked off by a clamping diode. The bridge thus remains in its OFF

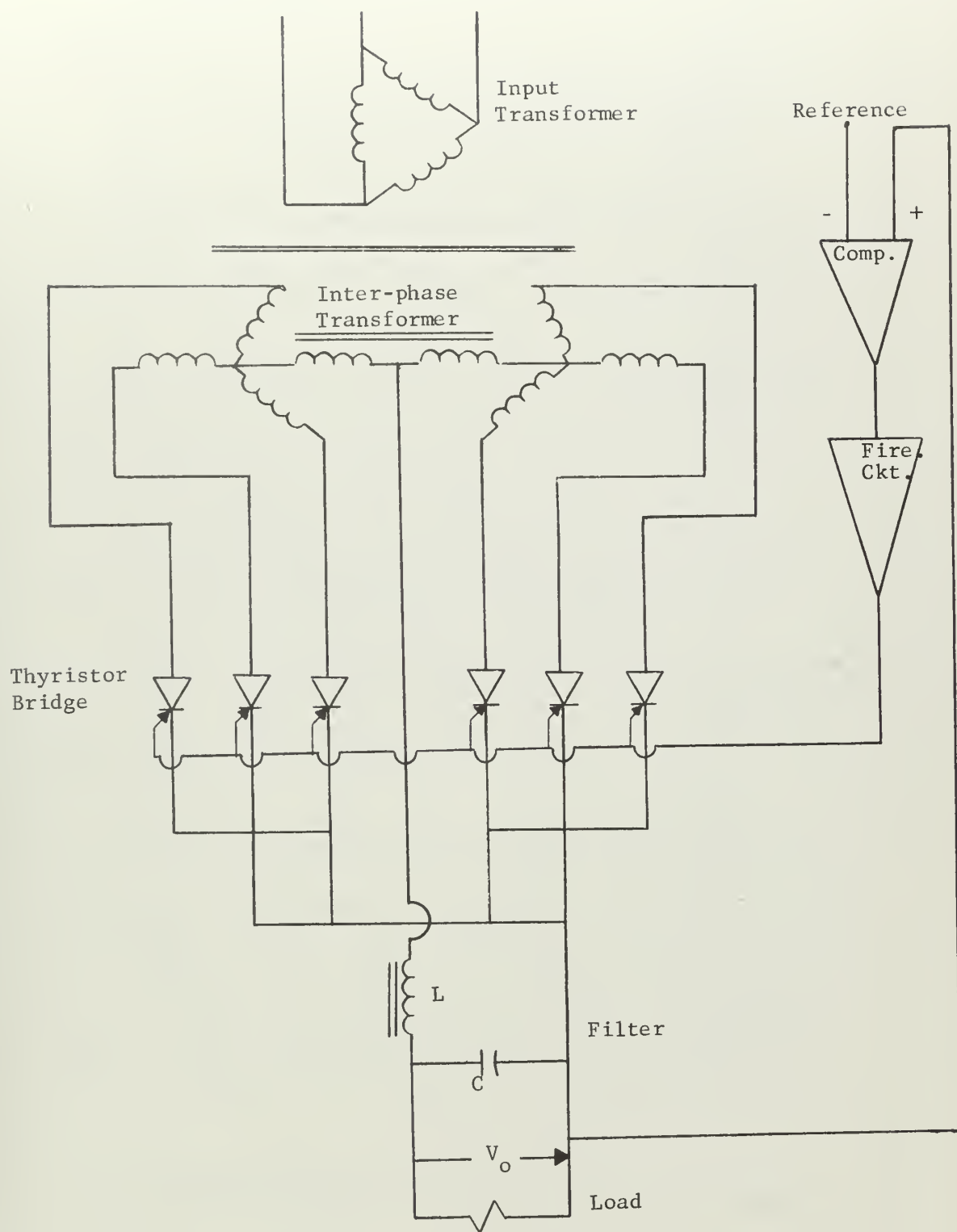


Figure 3-3. Three-phase, full-wave, forced limit-cycle, regulator.

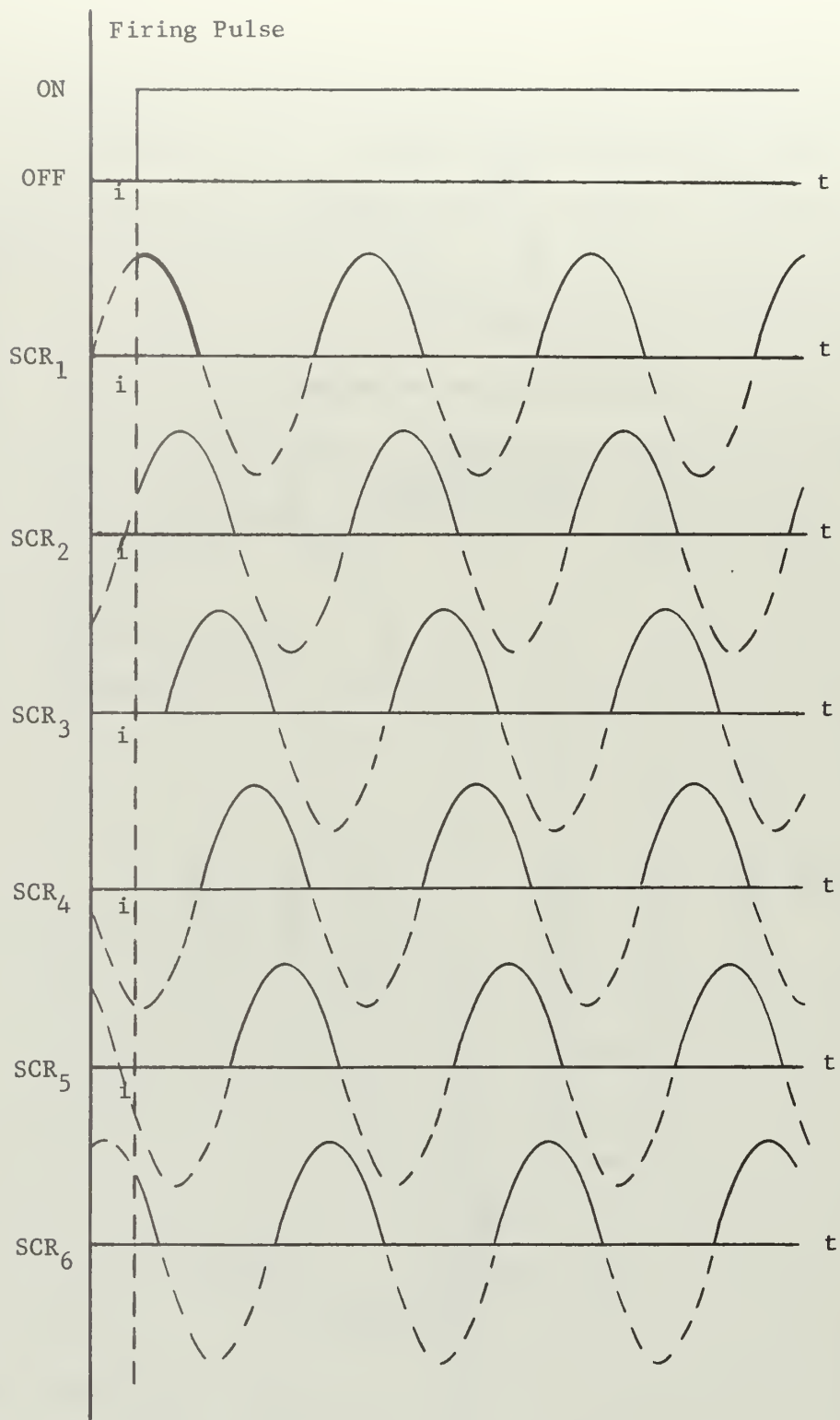


Figure 3-4. Firing sequence of thyristor bridge.



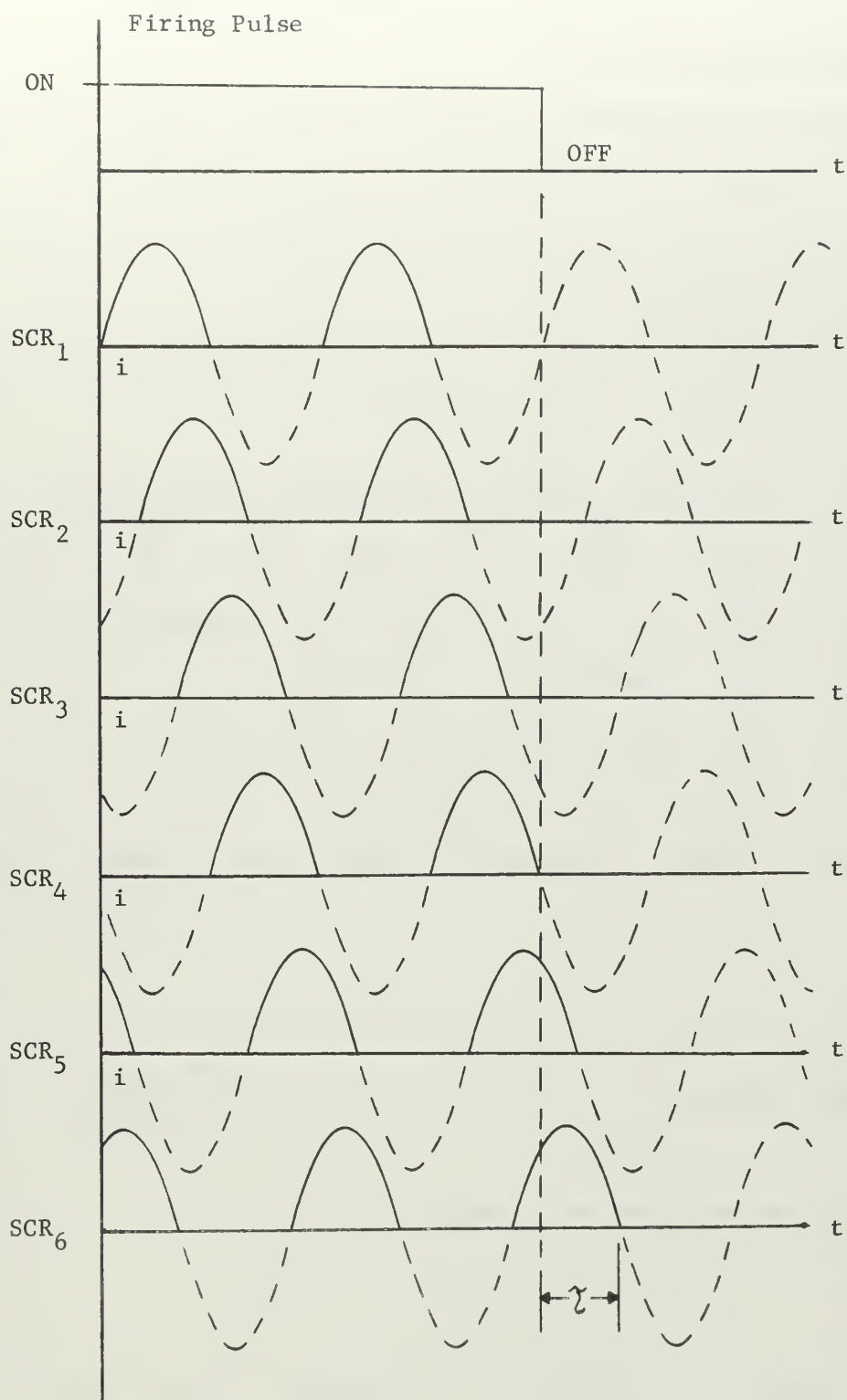


Figure 3-5. Cut-off sequence of thyristor bridge.



state until the output voltage drops below the reference, whereupon the cycle repeats itself.

Leszczynski's thesis shows that the output of the power supply is a DC voltage with a ripple that is a non-sinusoidal limit cycle, with a fundamental frequency different from the AC supply voltage or any of its harmonics.

The input to the filter can be shown as a series of pulses, one of which appears in Figure 3-6 below.

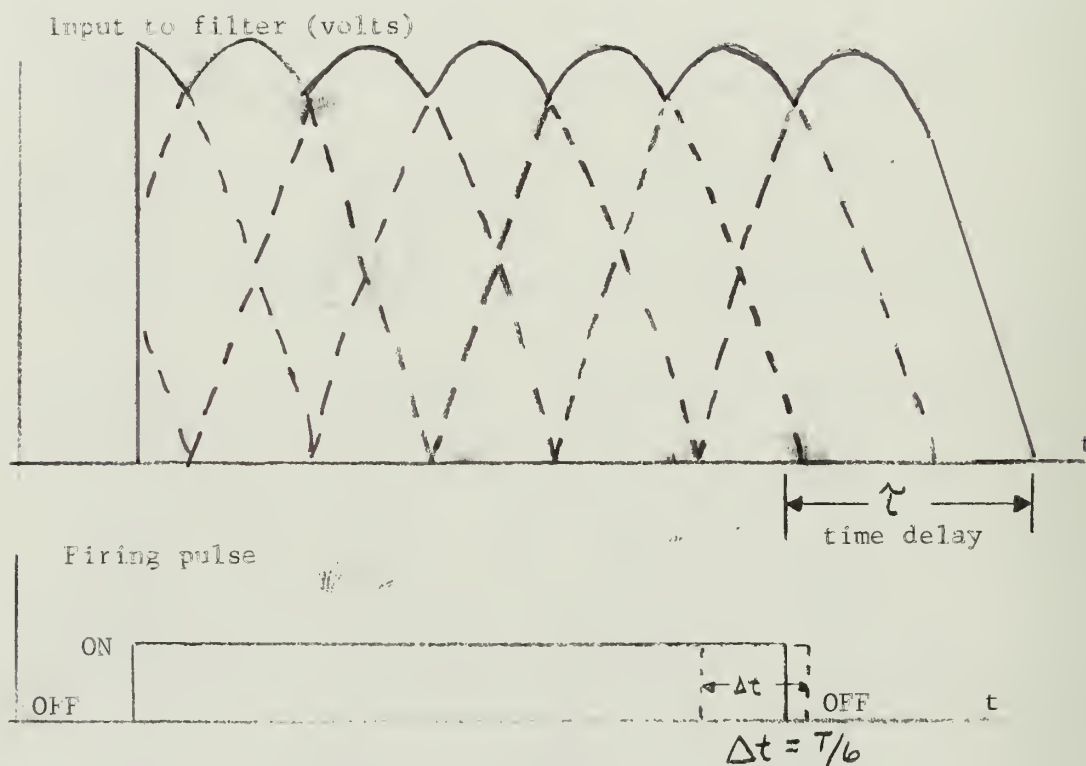


Figure 3-6. Thyristor bridge output pulse

Suppose that the period of the supply voltage is  $T$  seconds. By examining figure 3-6 it can be seen that, depending upon the length of the firing pulse, there is a period of  $T/6$ , the time that exists between one thyristor's firing and the next thyristor's firing, in

which the cut off of the firing pulse will not vary the elapsed time of the output pulse of the thyristor bridge. It is also seen that the time delay  $\tau$  can vary from  $T/3$  to  $T/2$  seconds in length, or

$$T/3 < \tau < T/2$$

It is this variation in  $\tau$  that might give some insight into the problem of ripple instability in a forced limit-cycling regulator and will be examined more carefully in the next section.

### 3.1 Preliminary investigation into ripple instability.

It was seen in the preceding section that the output of the thyristor bridge under steady-state operating conditions is a series of pulses that take the form of the pulse shown in figure 3-6.

If one assumes that the ripple of the DC output of the filter is a limit-cycle that closely approximates a sinuoid, with a fundamental frequency  $f_1$  and a fundamental period  $T_1$ , then the length of the firing pulse would be  $T_1/2$  or the length of time that  $V_o$  is less than  $V_r$  in one limit-cycle period  $T_1$ .

Figure 3-7a is a replica of figure 3-6 in which the firing pulse is  $T_1/2$  seconds long and the thyristor bridge pulse length is  $t_1$  seconds. Figure 3-7b shows the firing pulse still to be  $T_1/2$  seconds but displaced in time from the first firing pulse by  $\epsilon$  seconds. The resulting pulse formed by the thyristor bridge is  $t_2$  seconds which can be seen to be less than  $t_1$ .

Suppose one used this sine wave limit cycle over a long period of time to generate a train of pulses that might be obtained from the thyristor bridge under steady-state operating conditions. Assume that the bridge is pulsed on when the sine wave is greater than its

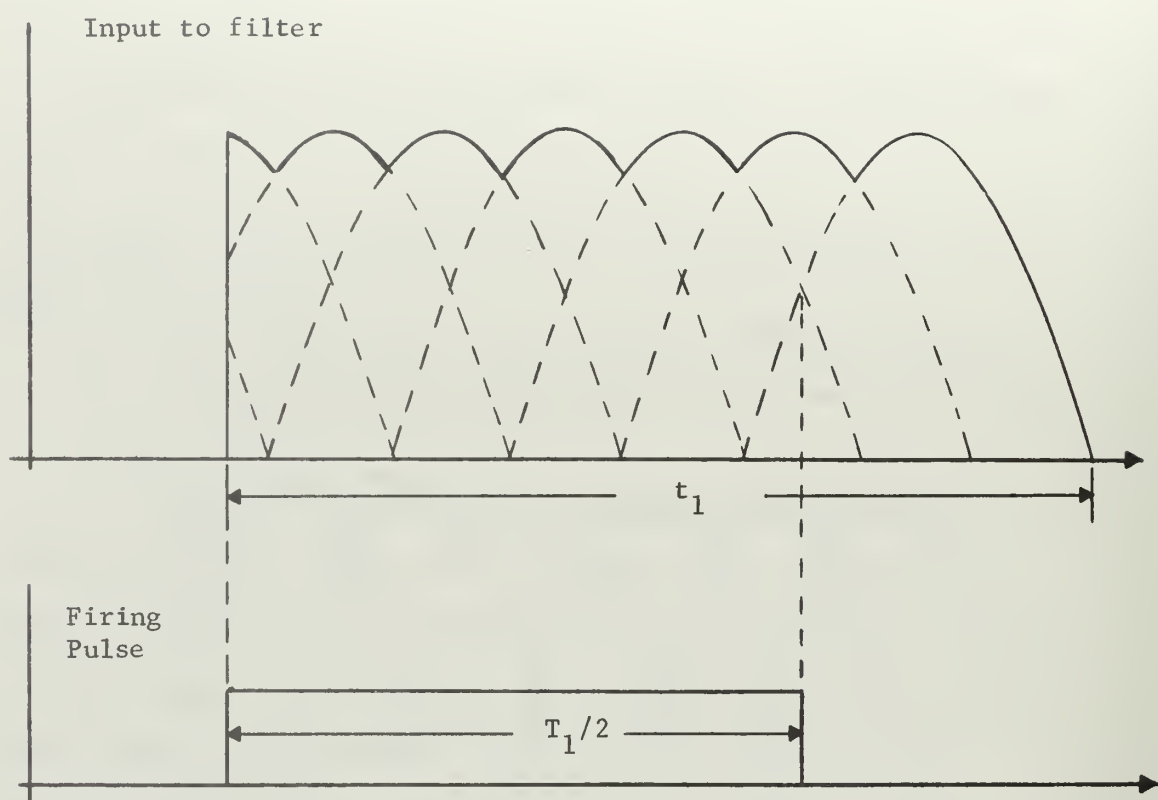


Figure 3-7a.

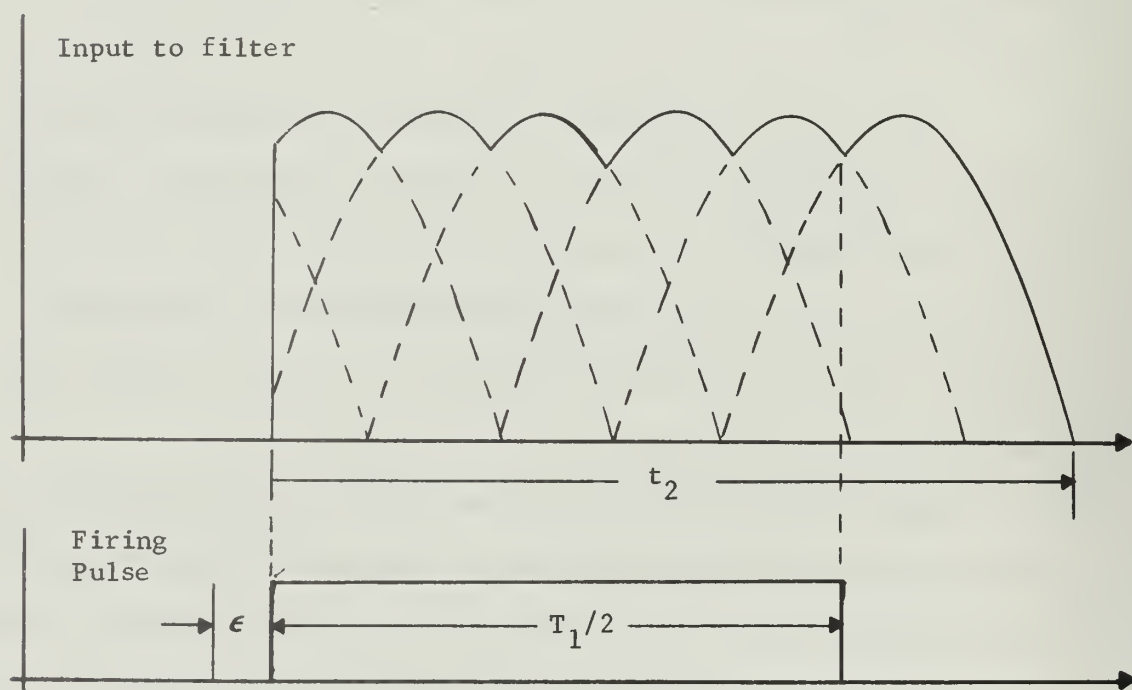


Figure 3-7b.

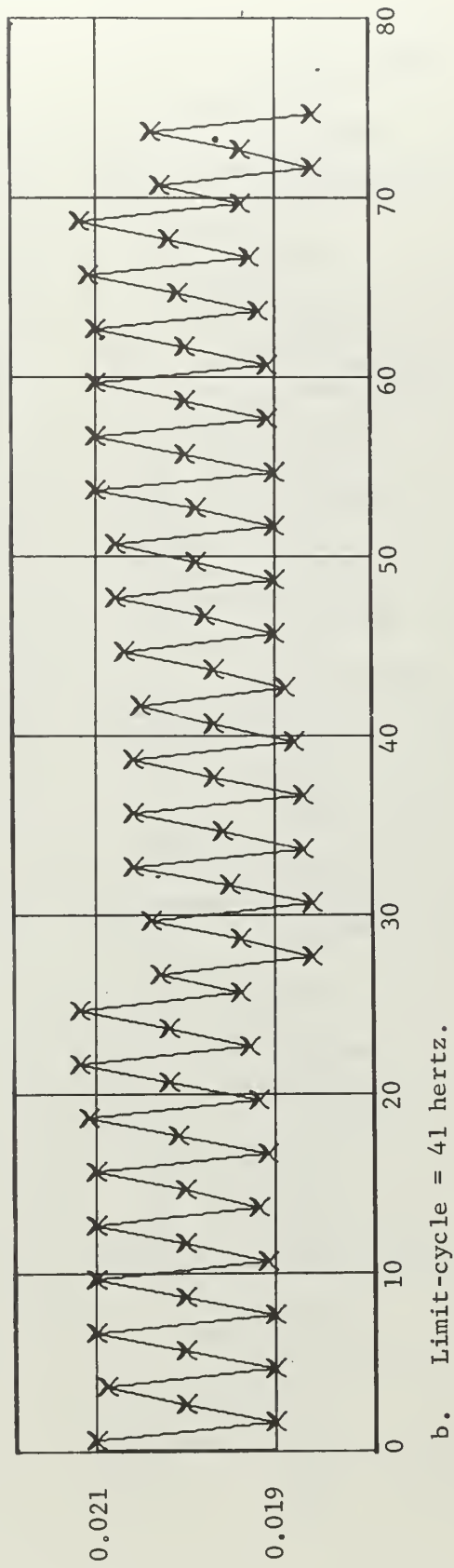
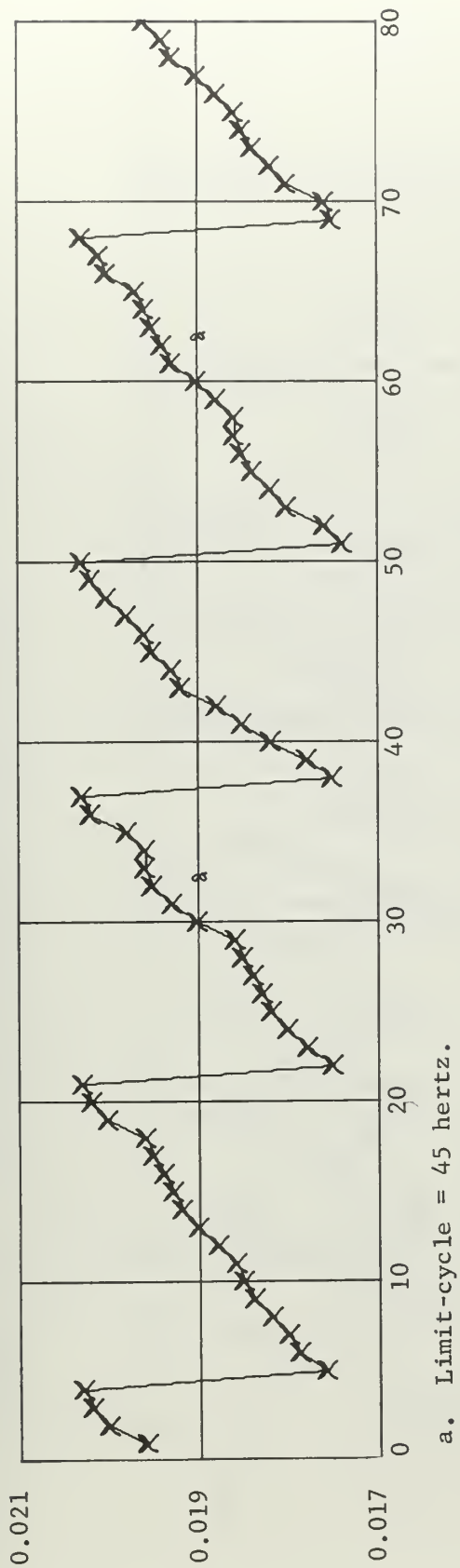


Figure 3-8. Pulse Width in Seconds vs Number of Pulse.

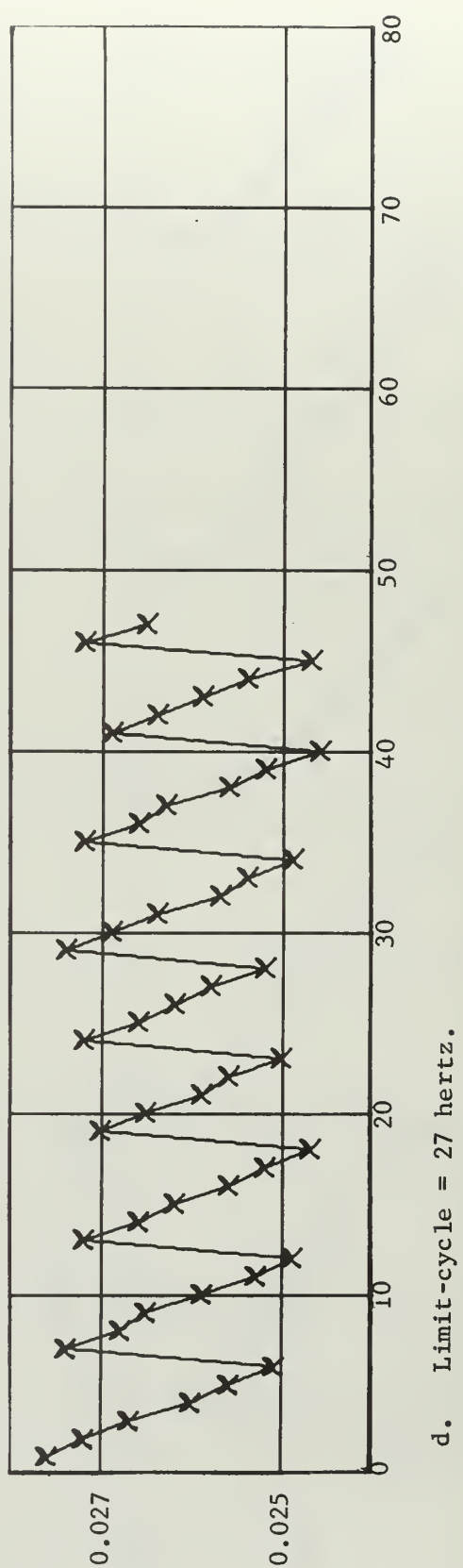
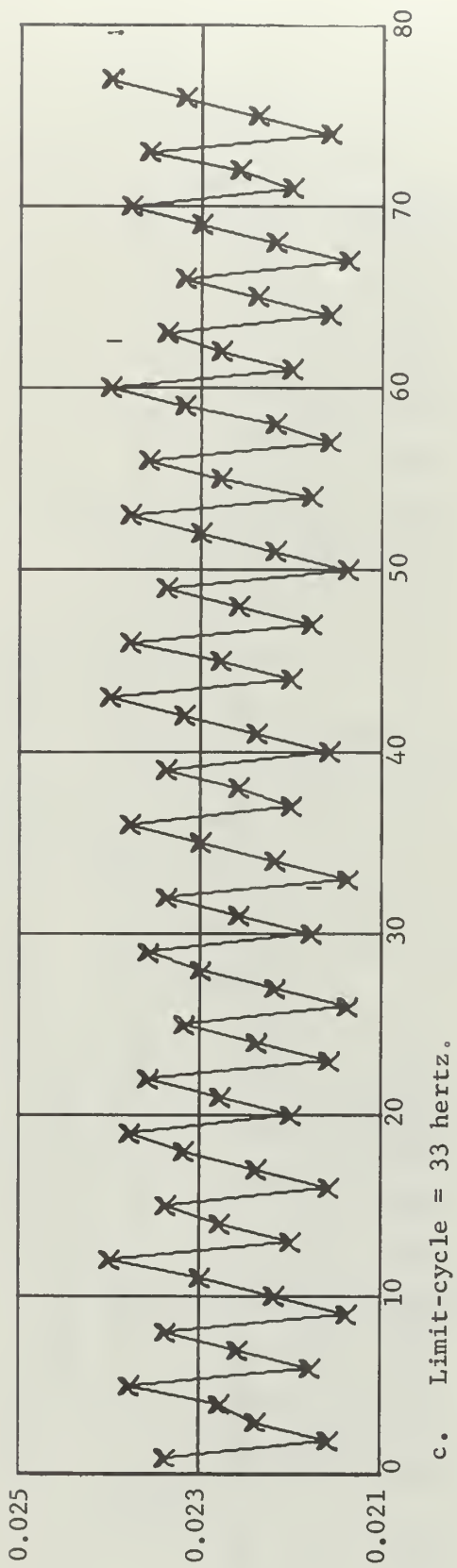
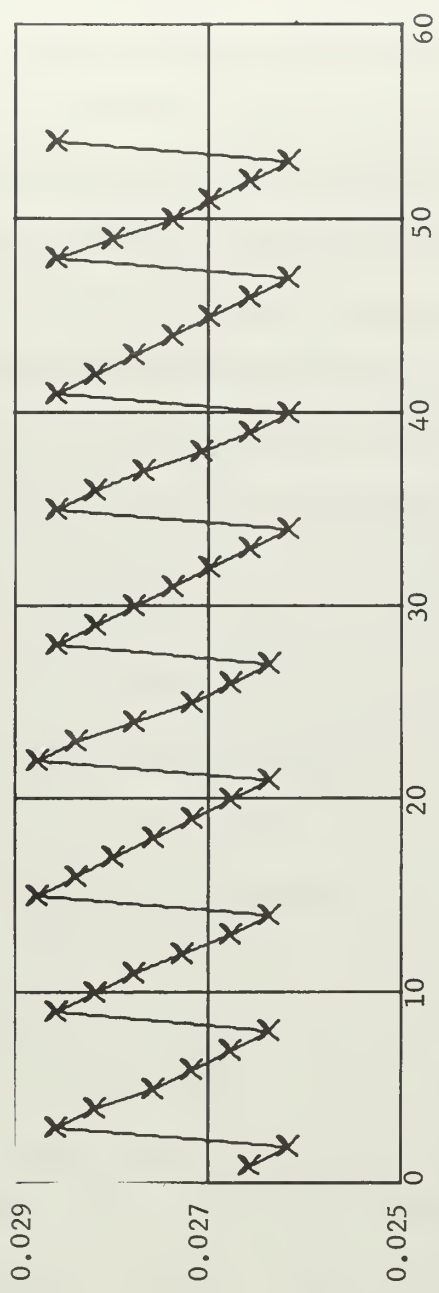


Figure 3-8. Pulse Width in Seconds vs Number of Pulse.



e. Limit-cycle = 25 hertz.

Figure 3-8. Pulse Width in Seconds vs Number of Pulse

mean value and is shut off when the sine wave goes below its mean, so as to simulate the frequency of the error signal becoming greater or less than zero. Observed over fifty or sixty cycles of the frequency  $f_1$  one notes that the pulse train from the bridge takes on an obvious pattern as can be seen in figure 3-8a-e.

Observe that the period of repetition of the pattern established by this means is some times many times greater than the limit cycle period  $T_1$  but in all cases is an integral multiple of the limit-cycle period. If one were to write a Fourier Series representation of this pulse train, as complicated as it might be, the fundamental frequency in each case would be a subharmonic of the sine wave that generated it. Hence, it can be seen that a pulse train generated by a sinusoidal signal with frequency  $f_1$  presents energy to the filter that contains subharmonics of the generating signal.

This, of course, is not irrevocable proof that subharmonics do exist in the output because it is known that the limit-cycle is not a true sinusoid and also one does not know what form of pulse train is generated by a limit-cycle in which ripple instability does exist, but one must admit to a definite possibility that subharmonics of the limit-cycle frequency might be present in the output.

The next step would be to simulate the system on an analog or digital computer, if not the actual plant itself, and in fact see if subharmonics are present in the output and under what conditions they exist. This is indeed what will be done in the next chapter.



#### 4. Synthesis of the forced limit-cycling regulator.

The system under study was successfully synthesized in Leszczynski's thesis by a digital computer program utilizing Fortran IV language and the Naval Postgraduate School IBM 360 Computer Facility. In the program the firing circuit and SCR bridge was simulated by logic statement manipulation and the output of the linear filter was obtained by calling a library subroutine INTEG 2 which gives a Runge-Kutta solution to a group of differential equations, in this case the state variable equations developed from the dynamics of the linear filter (see Appendix I). The linear filter is assumed to be as shown in Figure 4-1. The transfer function for the filter and load is developed as follows:

$$\begin{aligned} V_{in} &= V_L + V_C & i_L &= i_C + i_R \\ &= L \frac{di_L}{dt} + V_C & &= C \frac{dV_C}{dt} + \frac{V_C}{R} \\ \frac{dV_C}{dt} &= \frac{1}{L} (V_{in} - V_C) & \frac{dV_C}{dt} &= \frac{i_L}{C} - \frac{V_C}{RC} \end{aligned}$$

where  $V_C = V_0$

Choosing the state variables as

$$\begin{aligned} x_1 &= V_0 & \dot{x}_1 &= x_2/C - x_1/RC \\ x_2 &= i_L & \dot{x}_2 &= V_{in}/L - x_1/L \end{aligned}$$

a signal flow graph of the linear system is shown in Figure 4-2.

Using Mason's gain rule the transfer function in Laplace notation is:

$$T(S) = \frac{V_0}{V_{in}} = \frac{1/LC}{S^2 + 1/RC S + 1/LC}$$



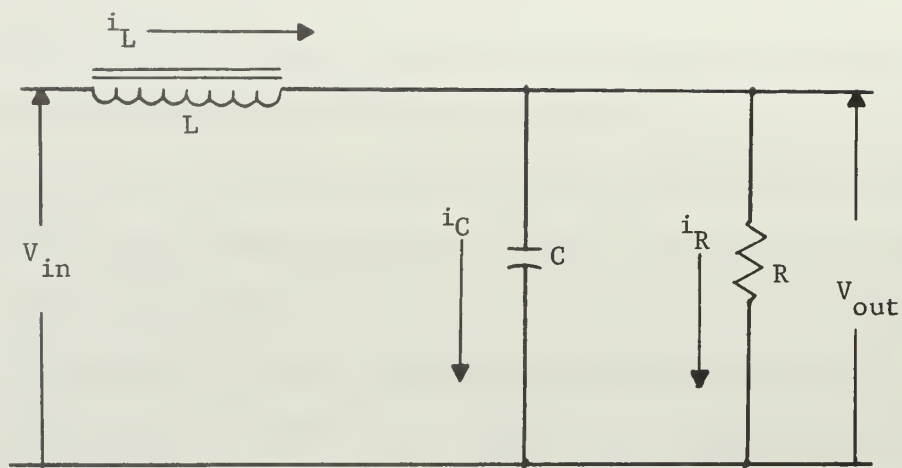


Figure 4-1. Filter and load.

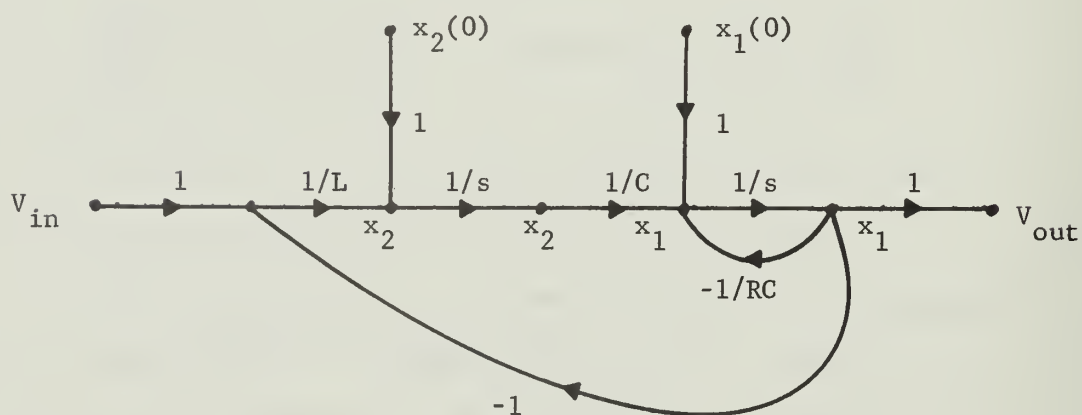


Figure 4-2. Signal flow graph for linear system.

The feedback path between the error signal and the firing circuit is known in the actual system to contain a dead zone. Figure 4-3 is the dead zone that was assumed in simulation of this system, with  $\alpha$  being the width of the dead zone. In the program a gain C(6) is introduced into the feedback path to provide amplification to the error signal prior to the dead zone and has the ability of defeating the effects of the dead zone if used properly as will be seen in the experimental results.

In conducting the experiment the supply voltage was considered to be a three-phase 60 cycle AC source with a peak amplitude of 65 volts. The value of the inductance and capacitance of the linear filter were kept constant throughout the experiment at 0.0005 henries and 0.1 farads respectively.

Thus, the experimental data was collected using the following factors as variables:

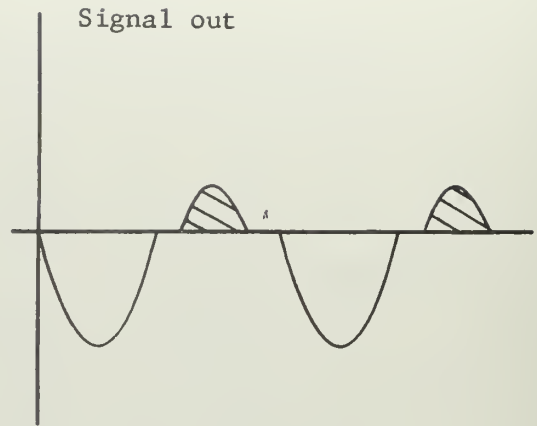
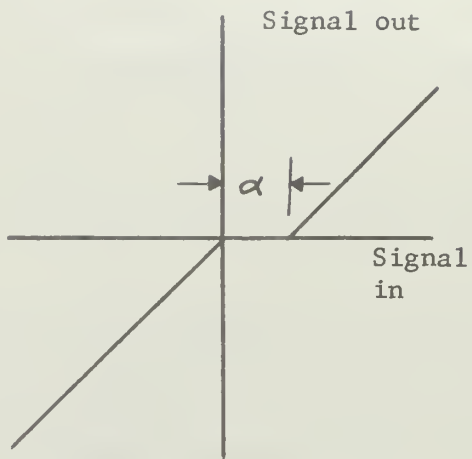
C(4) - The value of the load resistance in ohms

C(5) - The value of the reference voltage

C(6) - The amount of error signal amplification

C(7) - The width of the dead zone ( $\alpha$ )

Using a step size of 0.00002222 seconds it was found that in most cases by setting the initial conditions close to the desired reference voltage the transient died out within the first 0.1 second and the effect of ripple instability could be successfully observed from 0.1 to 0.2 seconds. Thus, the graphs that are shown begin at 0.097687 seconds and continue to 0.19702 seconds. The effects of manipulating the several variables can well be seen during this time frame in most cases.



NOTE: The shaded areas denote the period in which the SCR bridge is ON.

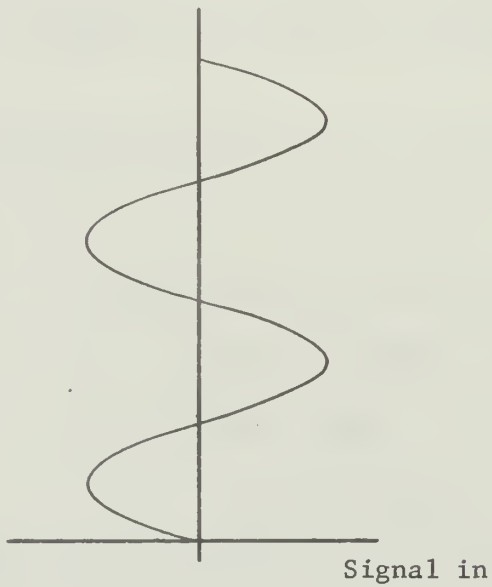


Figure 4-3. The dead zone characteristics of the feedback system.

#### 4.1 Experimental results

The first concern was to find out if the output of the filter actually contained some subharmonic ripple, so taking time intervals of 0.1 seconds the simulation program was run until the transient had obviously died away and the steady state output was examined. Fig. 4-4b. shows the steady state output of the regulator with the load equal to 1.6 ohms and the reference voltage set at 60.0 volts. (The dead zone in each case is set at 0.0 volts unless otherwise noted on the graphs.)

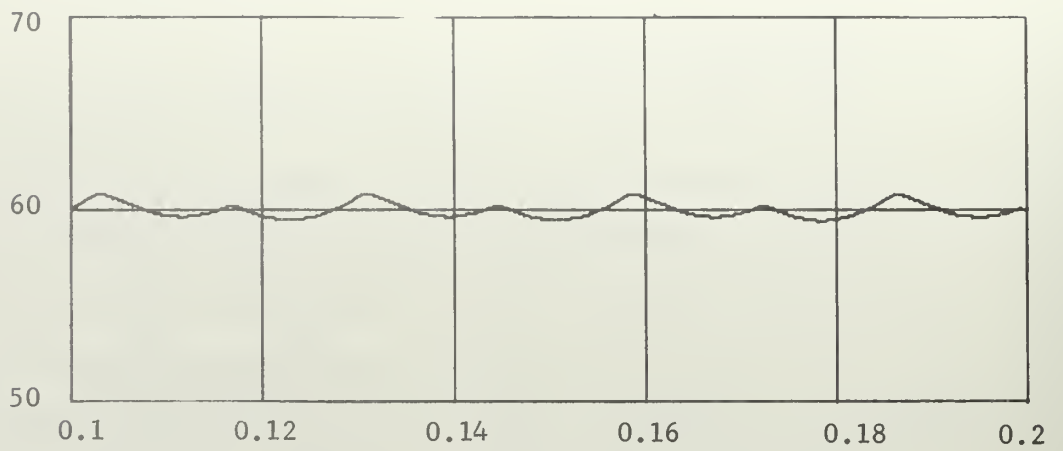
The load resistance was subsequently doubled and then halved to see the respective results on the output. Those results can be seen in Fig. 4-4a and c. Fig. 4-5 shows the input pulse train for the corresponding time period.

In Fig. 4-6a the reference voltage with the load set at 3.2 ohms was dropped to 58.0 volts. Fig. 4-6b presents the results when the error signal was doubled but zero dead zone was considered.

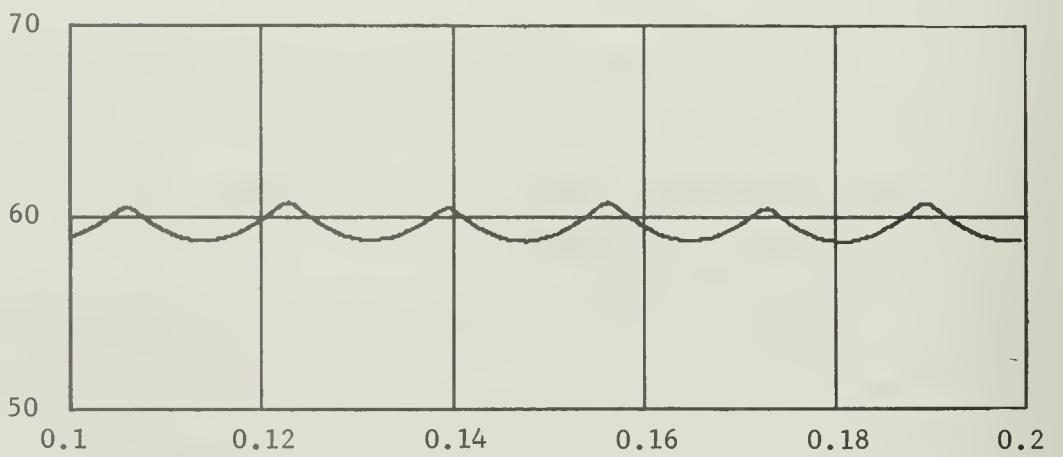
Keeping the load resistance at 0.8 ohms, the reference voltage was dropped in steps from 65.0 volts to 48.0 volts. These results appear in Figs. 4-8, 4-9, and 4-10.

Using the values of  $R=0.8$  ohms and  $V_{ref}=60.0$  volts the system was examined assuming the dead zone to be 0.5 volts. These results were compared to the results obtained by setting  $V_{ref}=60.5$  volts and the dead zone set at 0.0. Fig. 4-11 shows this comparison.

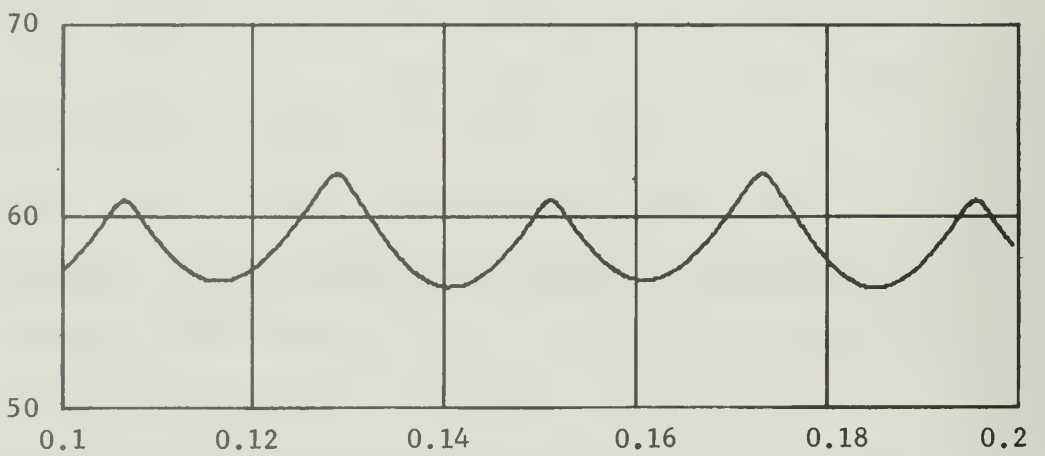
Figure 4-13 is a comparison between the results obtained by setting  $V_{ref}=62.0$  volts and the dead zone at 0.0 and setting  $V_{ref}=60.0$  volts and dead zone equal to 2.0 volts. The error signal was then amplified by a factor of 1.5 and compared to the preceding experiments.



a.  $R=3.2$  Ohms  $V_{ref}=60.0$  Volts

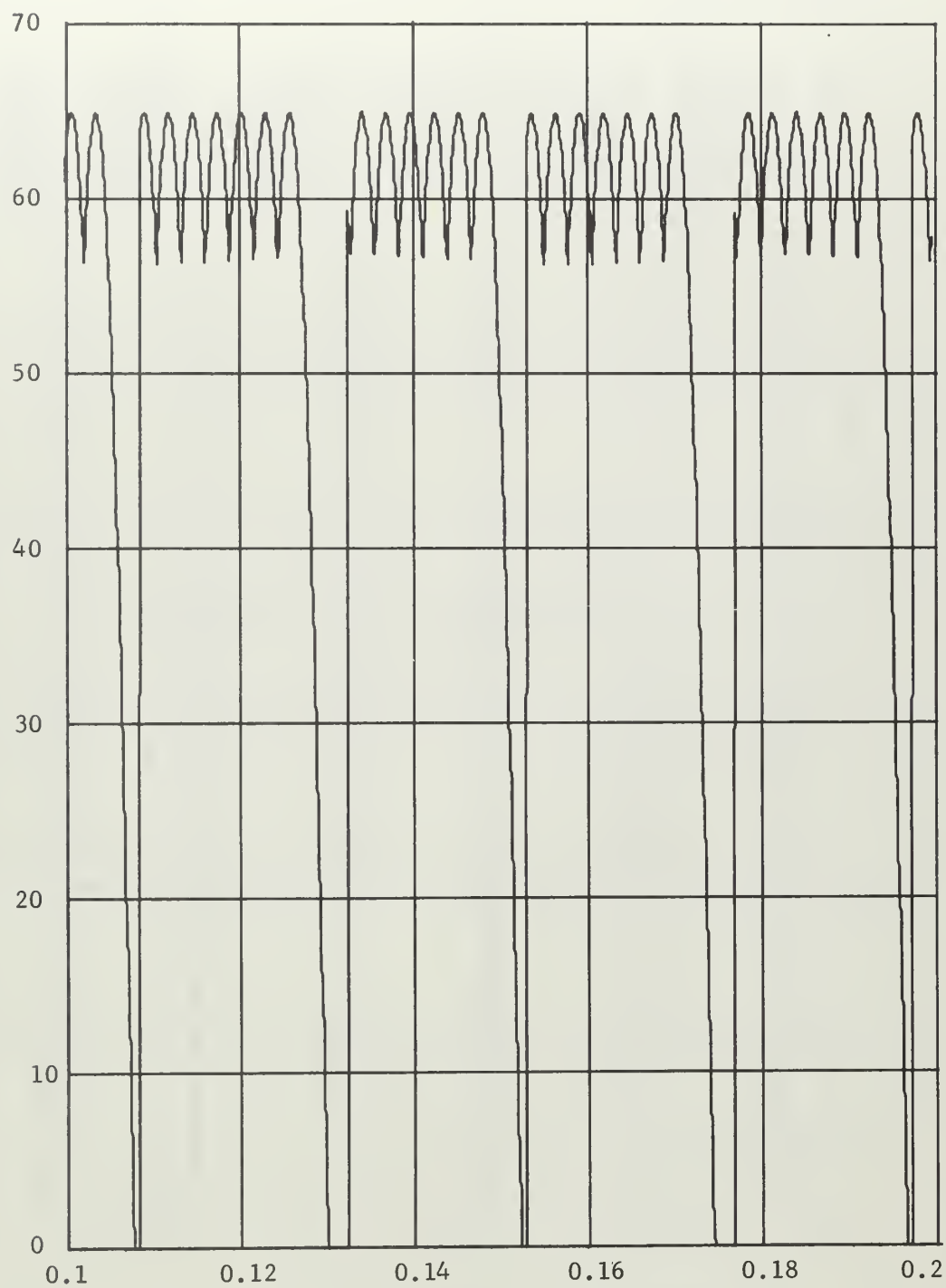


b.  $R=1.6$  Ohms  $V_{ref}=60.0$  Volts



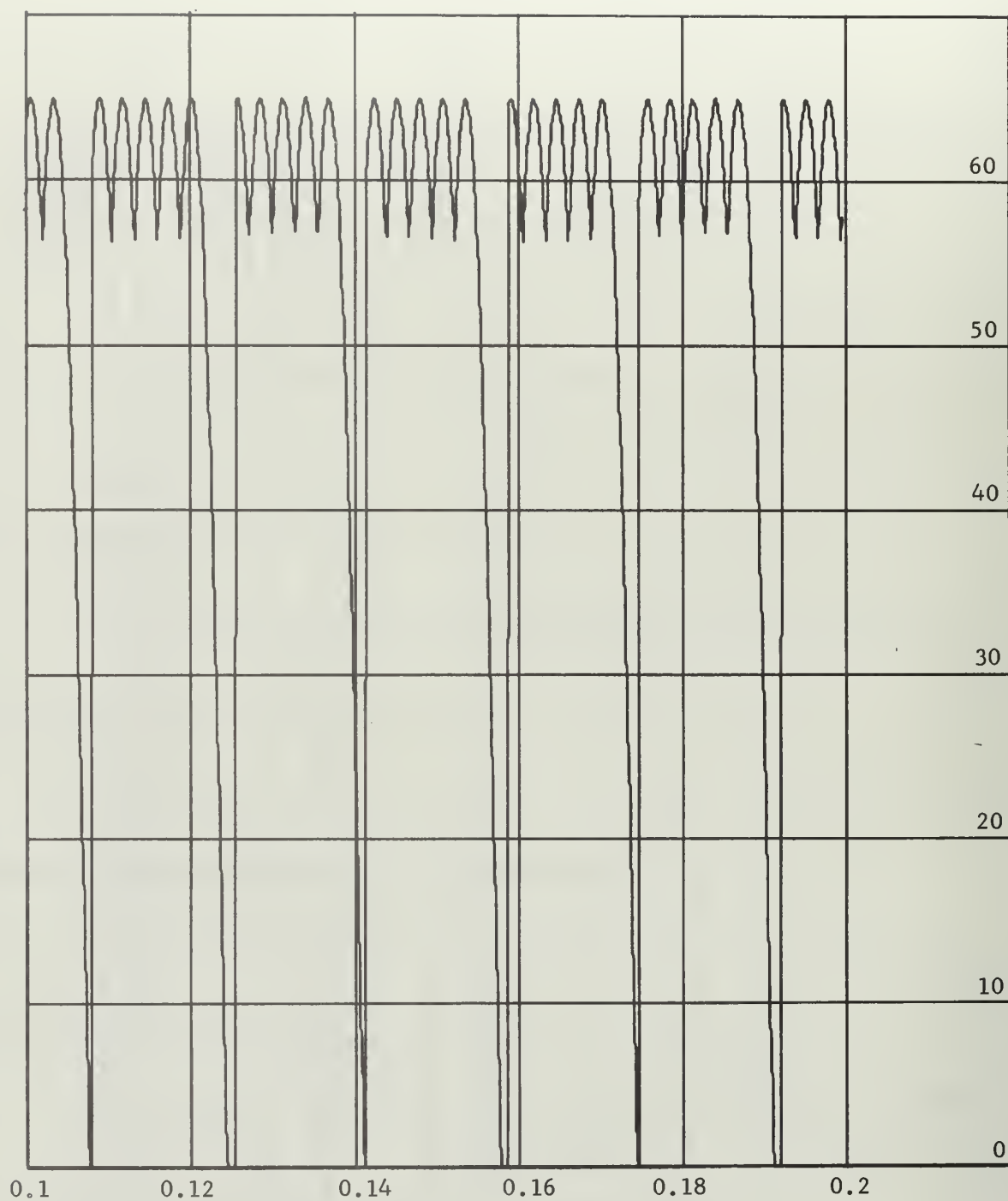
c.  $R=0.8$  Ohms  $V_{ref}=60.0$  Volts

Figure 4-4.  $V_{out}$  vs. Time



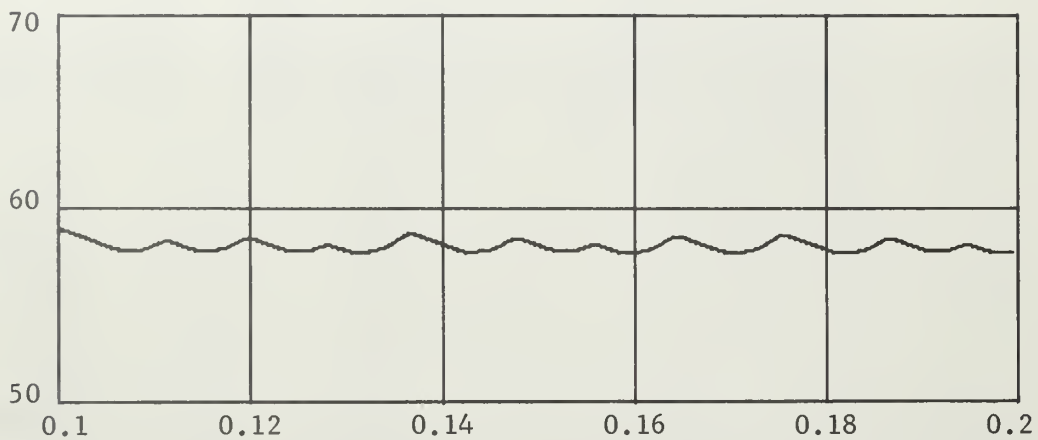
a.  $R=0.8$  Ohms  $V_{ref}=60.0$  Volts

Figure 4-5.  $V_{in}$  vs. Time

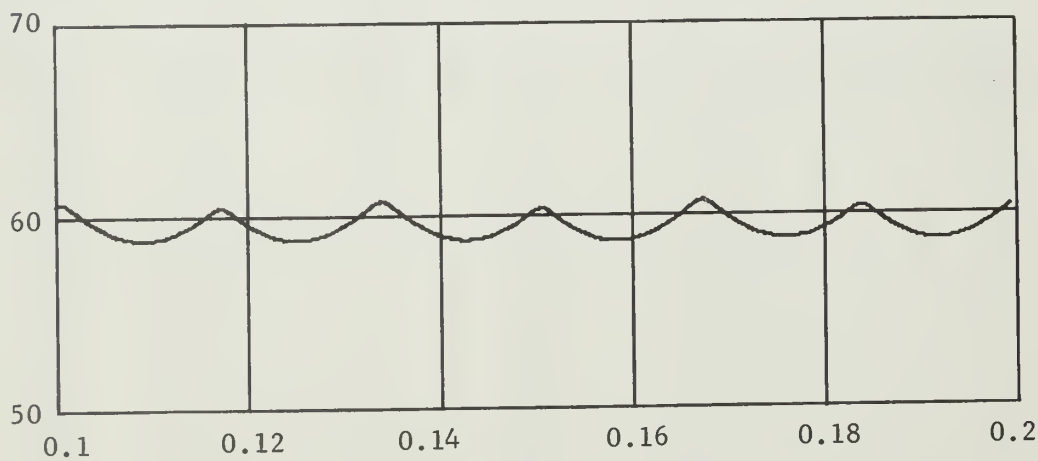


b.  $R=1.6$  Ohms  $V_{ref}=60.0$  Volts

Figure 4-5.  $V_{in}$  vs. Time



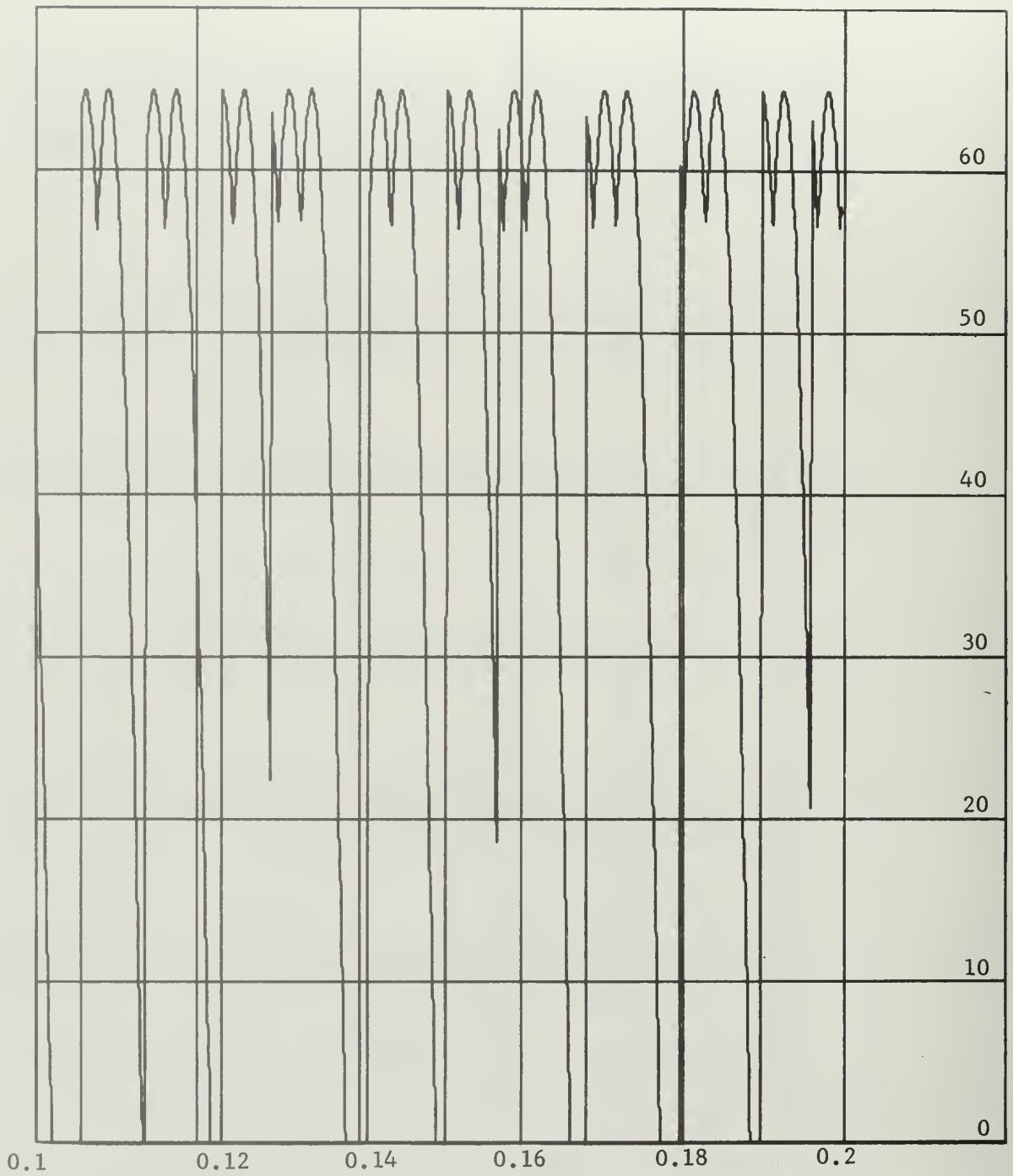
a.  $R=3.2$  Ohms  $V_{ref}=58.0$  Volts



b.  $R=1.6$  Ohms  $V_{ref}=60.0$  Volts  $C(6)=C(8)=2.0$

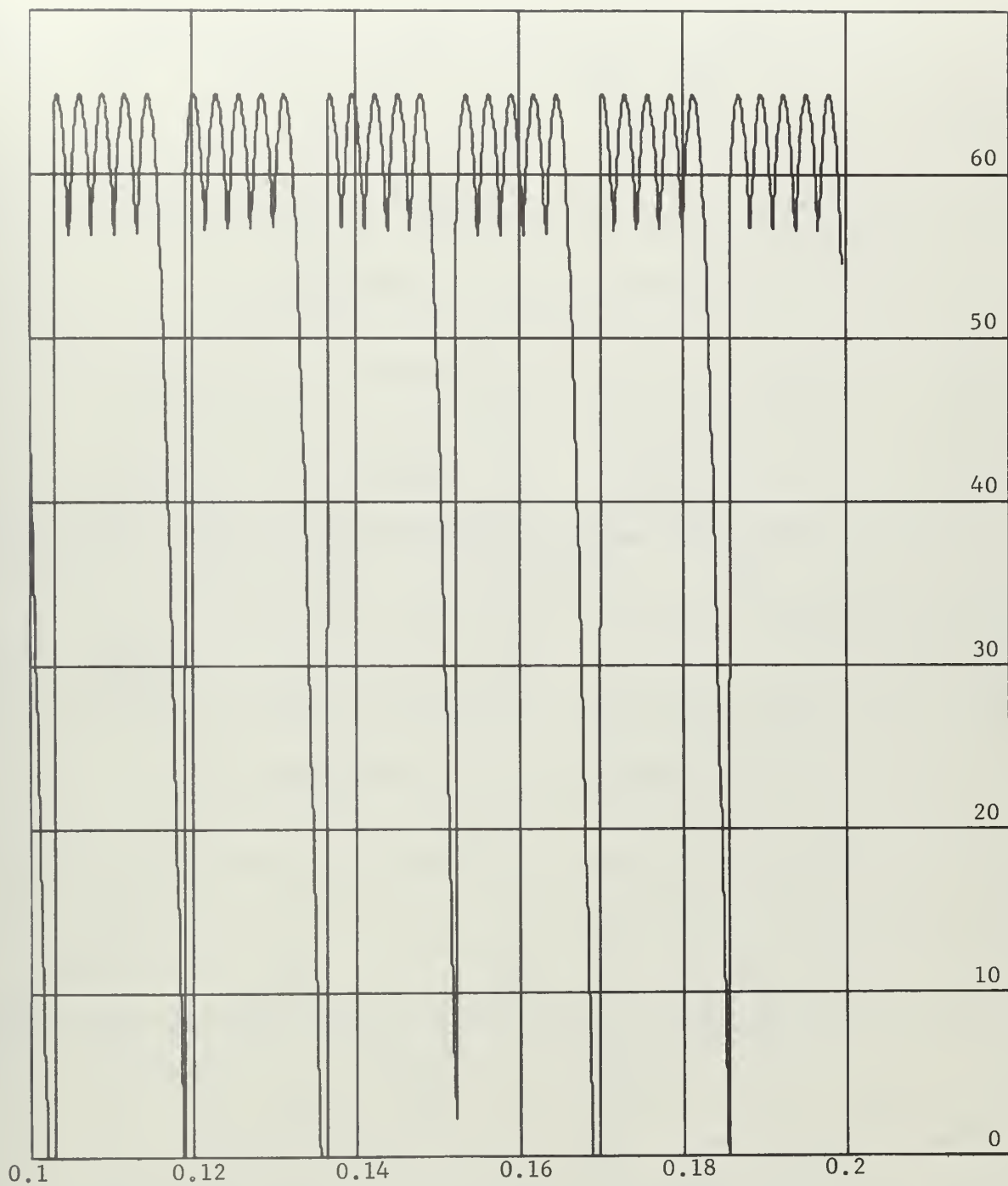
Figure 4-6.  $V_{out}$  vs. Time.





a.  $R=3.2$  Ohms  $V_{ref}=58.0$  Volts

Figure 4-7.  $V_{in}$  vs. Time



b.  $R=1.6$  Ohms

$V_{ref}=60.0$  Volts

$C(6)=C(8)=2.0$

Figure 4-7.  $V_{in}$  vs. Time

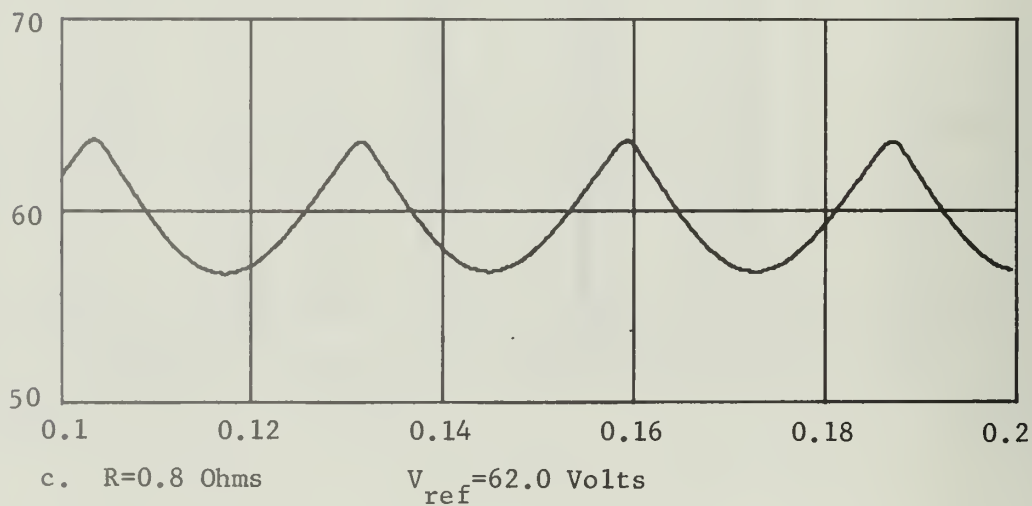
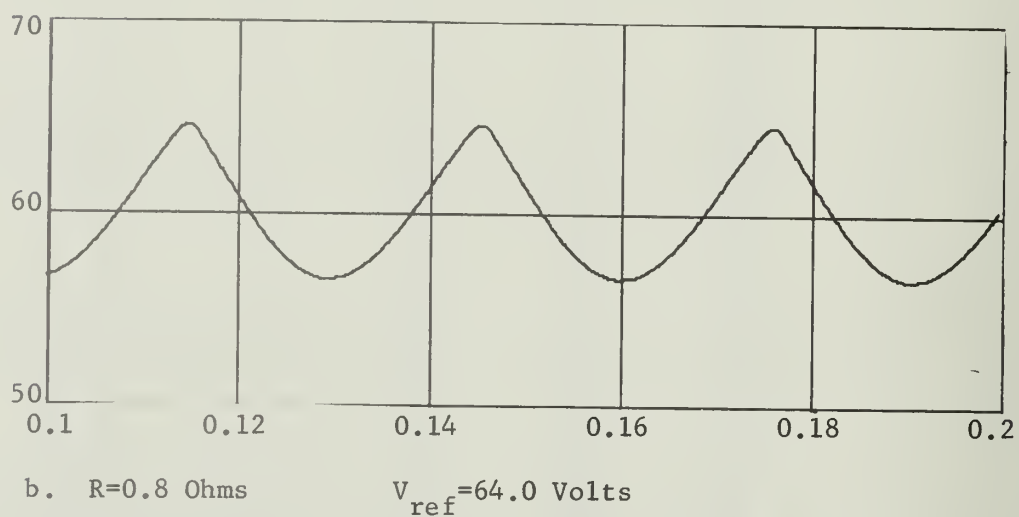
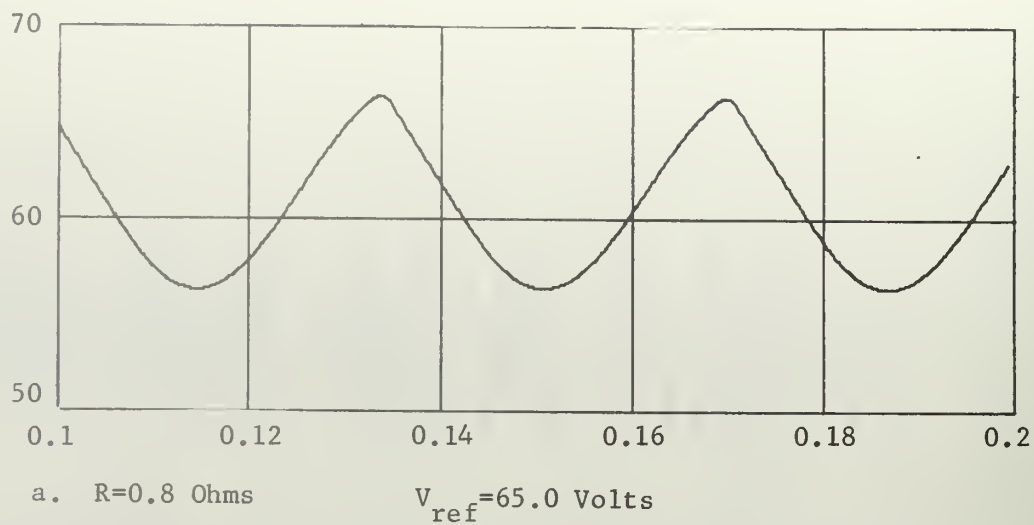
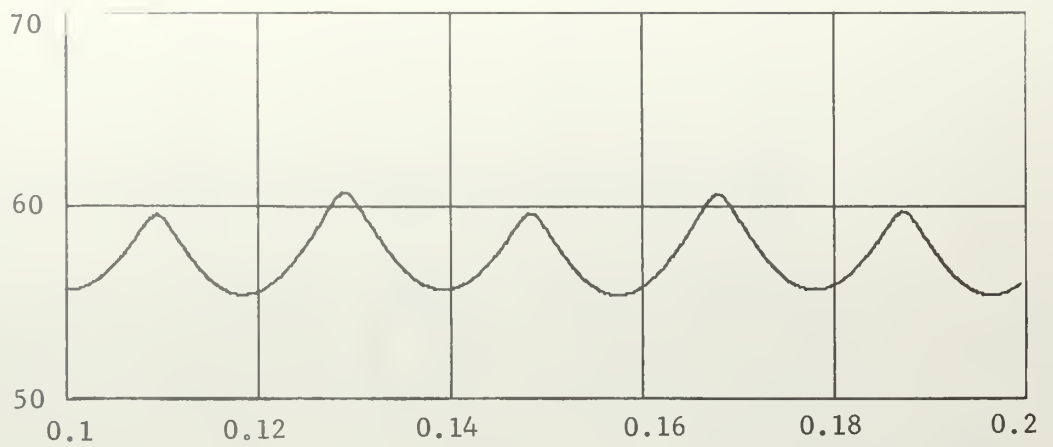
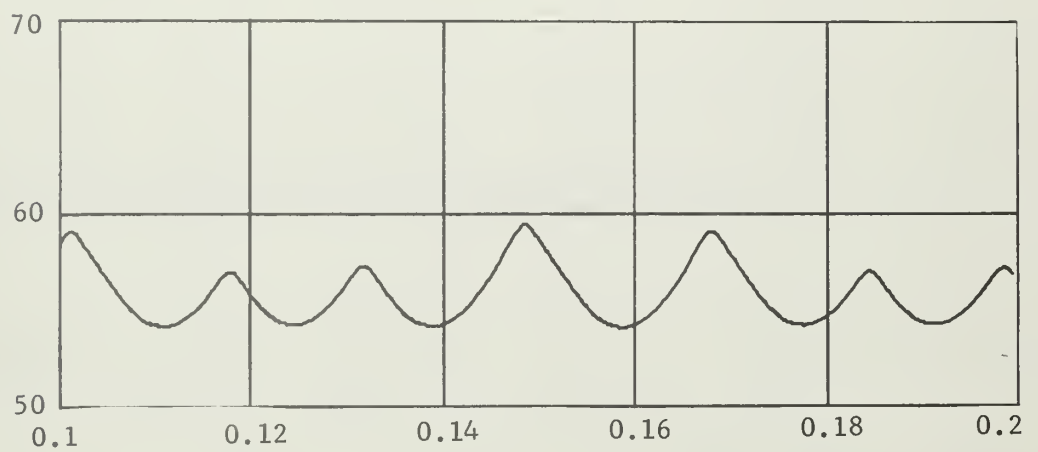


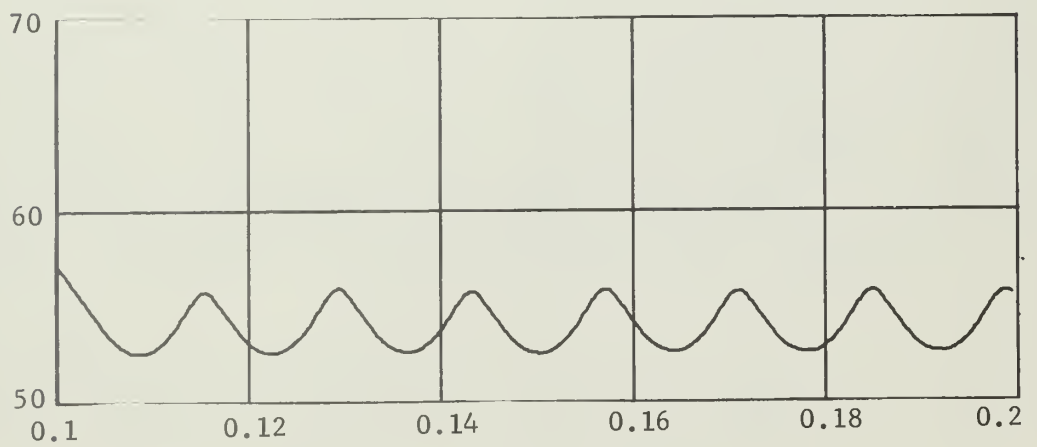
Figure 4-8.  $V_{out}$  vs. Time



a.  $R=0.8$  Ohms  $V_{ref}=58.0$  Volts

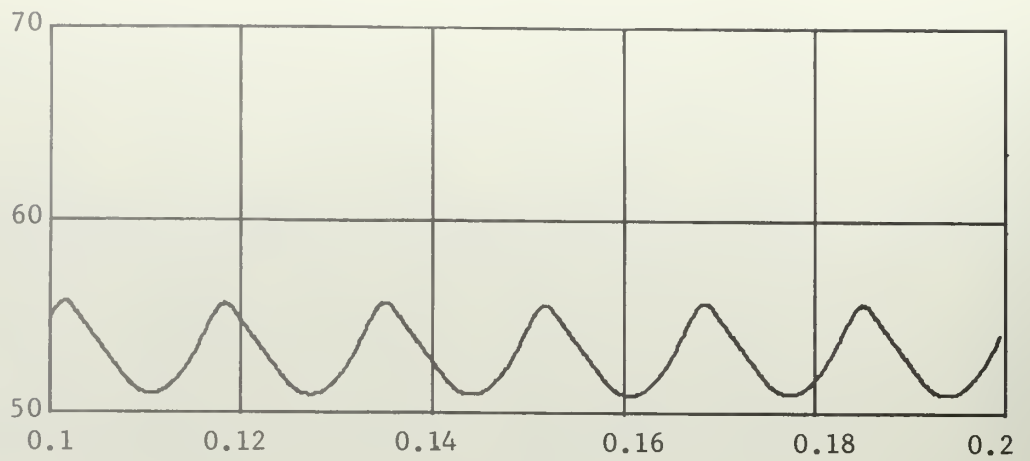


b.  $R=0.8$  Ohms  $V_{ref}=56.0$  Volts

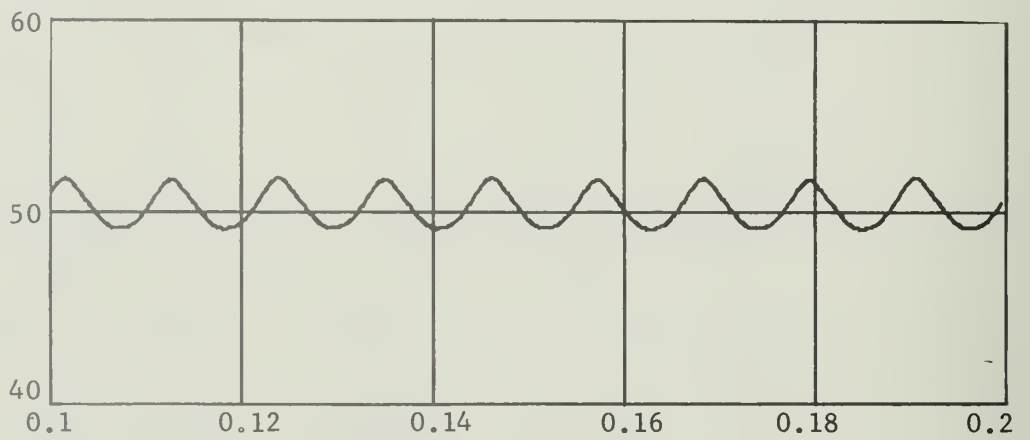


c.  $R=0.8$  Ohms  $V_{ref}=54.0$  Volts

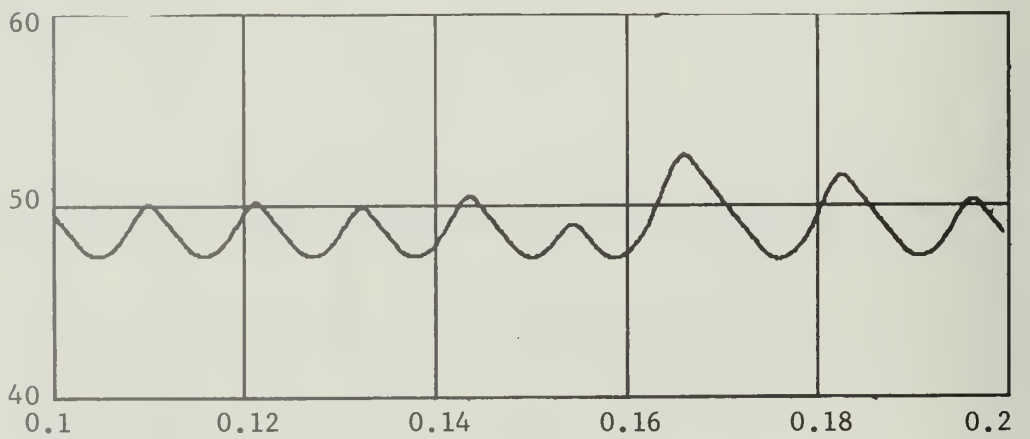
Figure 4-9.  $V_{out}$  vs. Time



a.  $R=0.8$  Ohms  $V_{ref}=52.0$  Volts

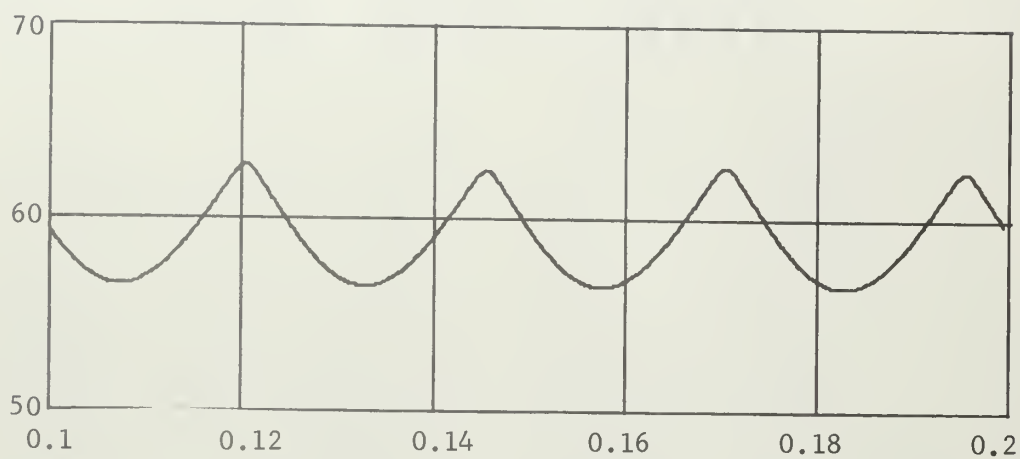


b.  $R=0.8$  Ohms  $V_{ref}=50.0$  Volts

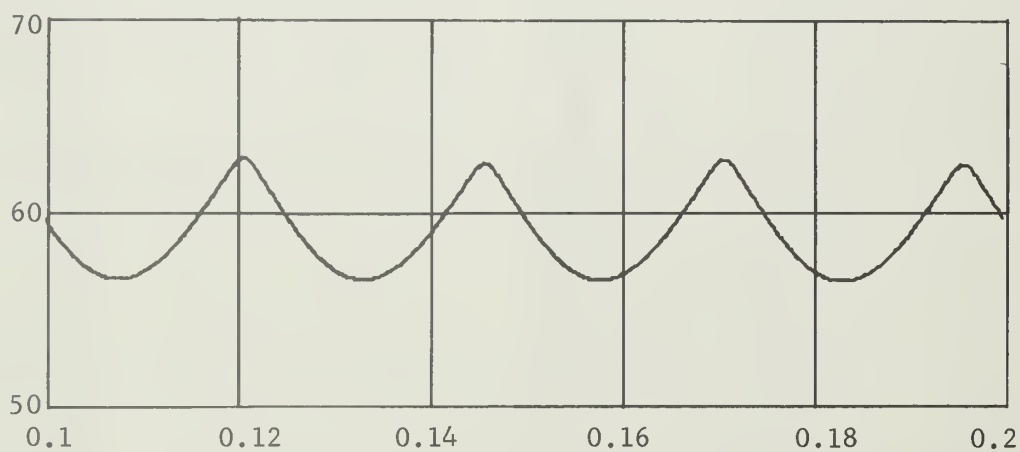


c.  $R=0.8$  Ohms  $V_{ref}=48.0$  Volts

Figure 4-10.  $V_{out}$  vs. Time



a.  $R=0.8$  Ohms  $V_{ref}=60.0$  Volts  $\text{Alpha}=0.5$



b.  $R=0.8$  Ohms  $V_{ref}=60.5$  Volts  $\text{Alpha}=0.0$

Figure 4-11.  $V_{out}$  vs. Time

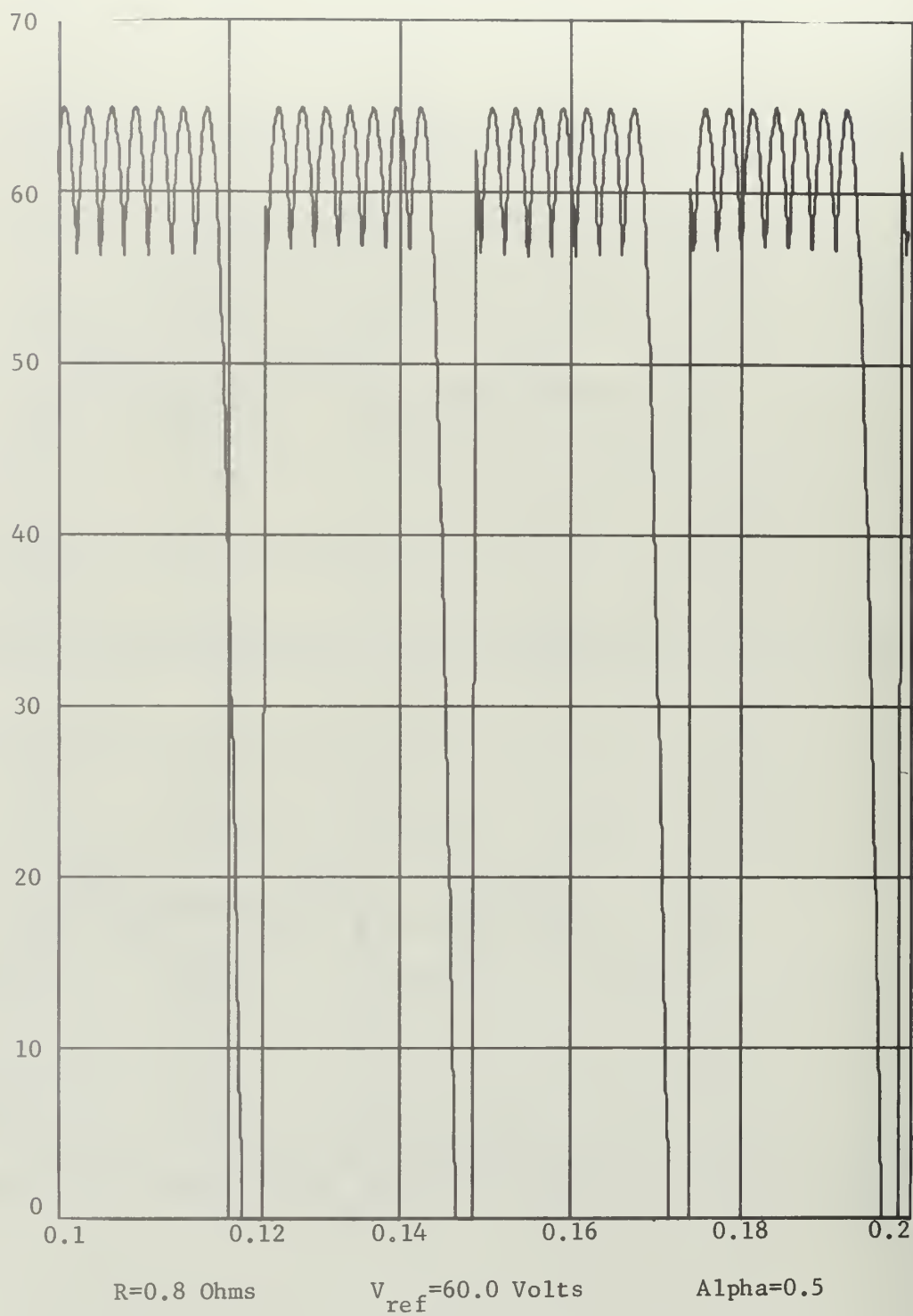
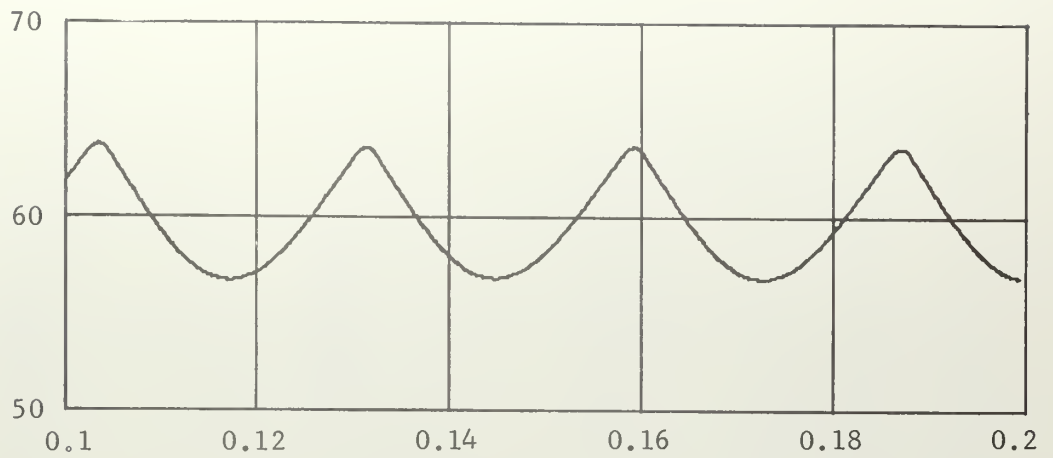


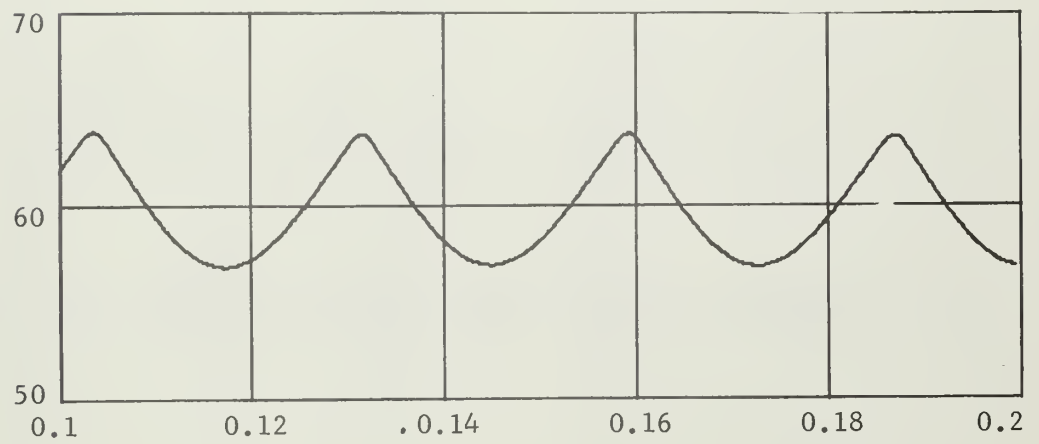
Figure 4-12.  $V_{in}$  vs. Time



a.  $R=0.8$  Ohms

$V_{ref}=62.0$

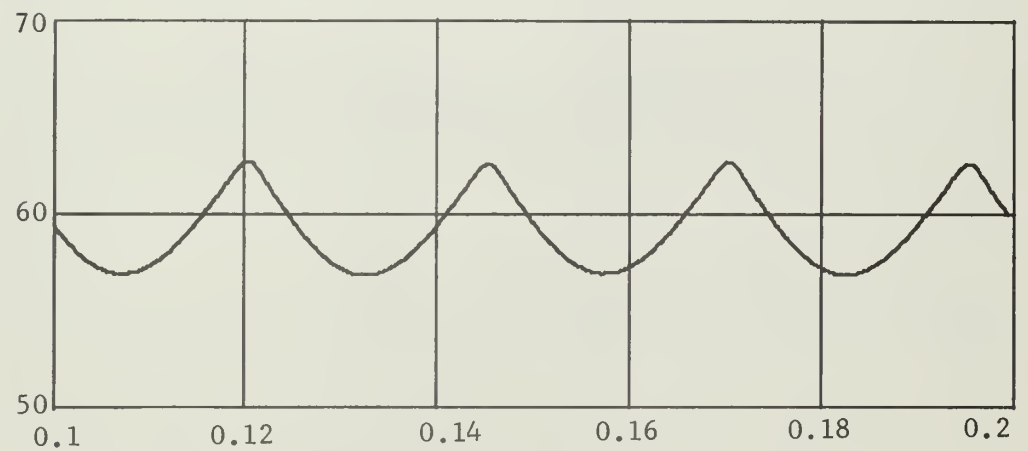
$\text{Alpha}=0.0$



b.  $R=0.8$  Ohms

$V_{ref}=60.0$  Volts

$\text{Alpha}=2.0$



c.  $R=0.8$  Ohms

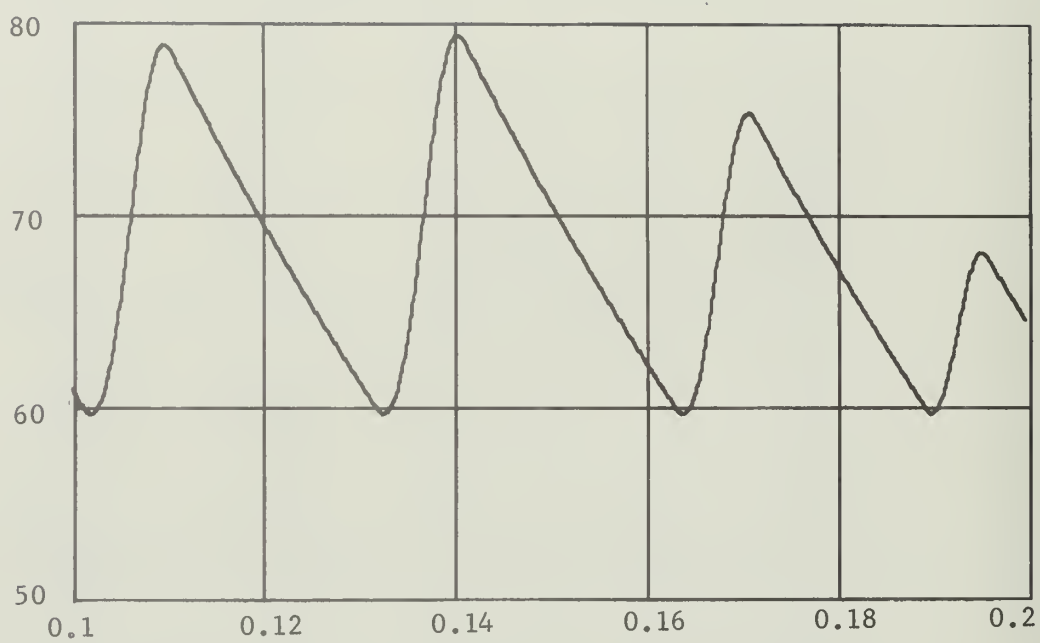
$V_{ref}=60.0$  Volts

$\text{Alpha}=2.0$

$C(6)=1.5$

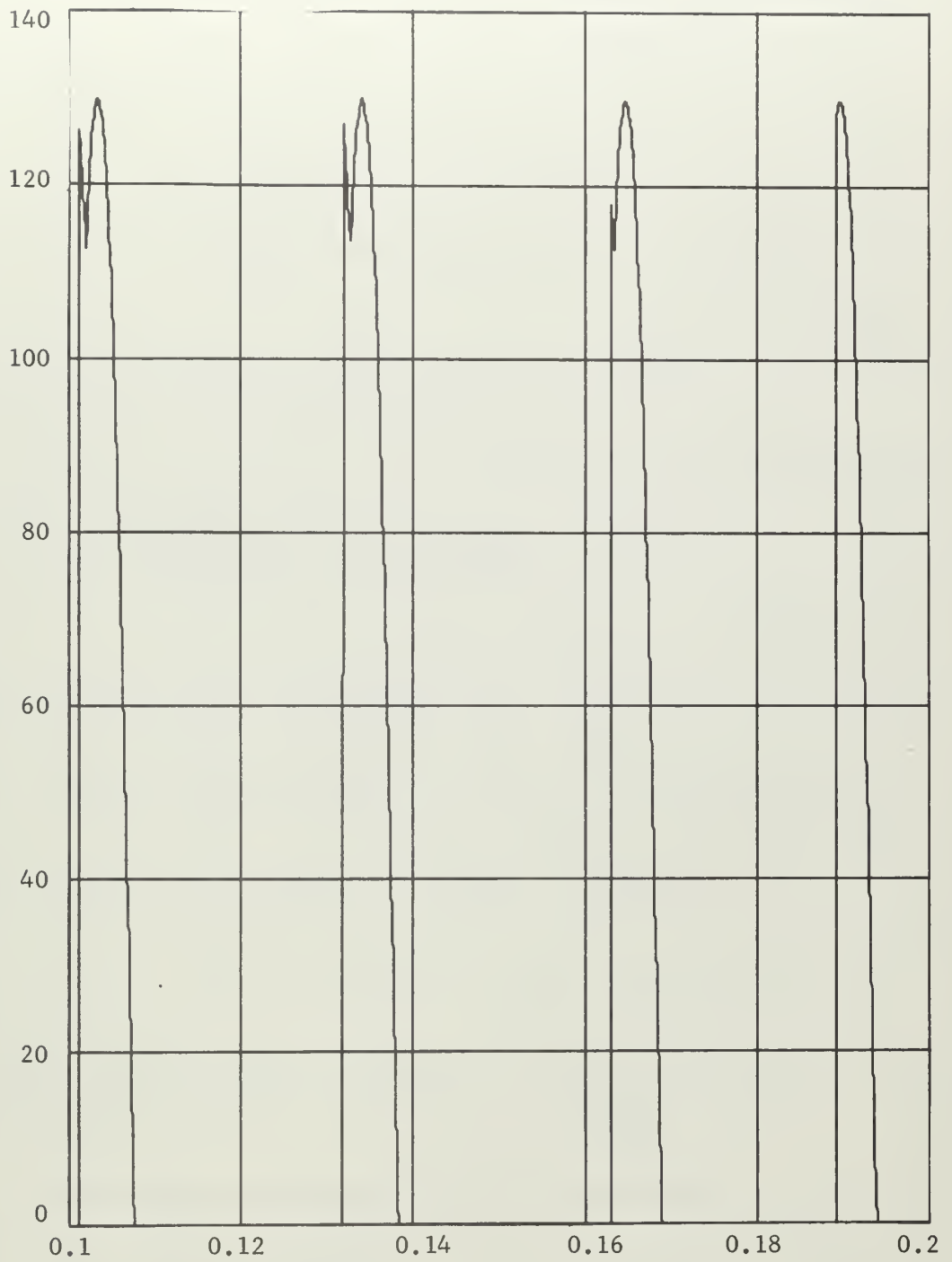
Figure 4-13.  $V_{out}$  vs. Time





b.  $R=0.8$  Ohms  $V_{ref}=60.0$  Volts  
 Input Voltage Amplitude  $C(1)=130.0$  Volts

Figure 4-14.  $V_{out}$  vs. Time



$R=0.8$  Ohms

$V_{ref}=60.0$  Volts

Input Voltage Amplitude  $C(1)=130.0$  Volts

Figure 4-15.  $V_{in}$  vs. Time

Finally the system was examined when the pulse train was amplified by a factor of 2.0 before going into the filter and the results were compared to setting the source voltage to double its original value. These experimental results appear in Fig. 4-14.

#### 4.1 Summary and analysis of the experimental data.

The transfer function for the linear filter as stated previously is:

$$T(j\omega) = \frac{1/LC}{(j\omega)^2 + (j\omega)/RC + 1}$$

In the Bode form this becomes,

$$T(j\omega) = \frac{1}{LC(j\omega)^2 + (j\omega)L/R + 1}$$

In decibels,

$$T(j\omega)_{db} = -20 \log \left| LC(j\omega)^2 + L/R(j\omega) + 1 \right|$$

Comparing this to the normal form of the Bode plot equation

$$T(j\omega)_{db} = -20 \log \left| (j\omega/\omega_n)^2 + 2\zeta/\omega_n (j\omega) + 1 \right|.$$

it can be seen that

$$\omega_n = \frac{1}{\sqrt{LC}} \quad 2\zeta/\omega_n = L/R \quad \text{and} \quad \zeta = 1/2R \sqrt{\frac{L}{C}}$$

so that for the values of L and C used in this experiment

$$\omega_n = \frac{1}{\sqrt{(.0005)(.1)}} = \frac{141 \text{ rad/sec}}{\underline{\hspace{1cm}}} = \underline{\underline{22.4 \text{ hertz}}}$$

and

$$\zeta = 1/2R \sqrt{\frac{.0005}{.1}} = \frac{0.03535534}{R}$$

hence, for

$$R=3.2 \quad \zeta = 0.0110485$$

$$R=1.6 \quad \zeta = 0.0220970$$

$$R=0.8 \quad \zeta = 0.0441940$$

Using these three values of load resistance the Bode diagrams for the linear filter response can be seen in Figure 4-16.

Table 4-1 is a tabular summary of the results of the experiment in which the reference voltage was kept constant at 60.0 volts and the value of the load resistance was varied. In Table 4-1,

- R = Value of the load resistance in ohms.
- $f_{LC}$  = Frequency of the fundamental limit-cycle in hertz
- $f_{SUB}$  = Frequency of the obvious subharmonic in hertz
- $V_{P1}$  = Peak to peak amplitude of the larger spike in the output.
- $V_{P2}$  = Peak to peak amplitude of the smallest spike in the output.
- $\zeta$  = Damping coefficient

$V_{ref}=60.0$ Volts					
R	$f_{LC}$	$f_{SUB}$	$V_{P1}$	$V_{P2}$	$\zeta$
3.2	72.7	36.3	1.195	0.739	.011
1.6	59.3	29.7	1.959	1.724	.022
0.8	45.06	22.53	5.904	4.192	.044

Table 4-1.

The values of the subharmonic frequencies are noted for each case on the Bode diagrams of Figure 4-16.

Table 4-2 is a tabulated summary of the experiment in which the load resistance was held constant at 0.8 ohms and the reference voltage was decreased.

<u>R = 0.8 Ohms</u>				
<u>V<sub>ref</sub></u>	<u>f<sub>LC</sub></u>	<u>f<sub>SUB</sub></u>	<u>V<sub>p1</sub></u>	<u>V<sub>p2</sub></u>
65.0	27.56	0	10.004	-----
64.0	32.91	0	8.001	-----
62.0	35.79	17.89	6.927	6.844
60.0	45.06	22.53	5.904	4.192
58.0	51.79	25.89	5.003	4.232
56.0	60.13	15.03*	4.997	-----
54.0	51.79	36.36	3.301	3.240
52.0**	60.93	30.47	4.410	4.709
50.0	90.25	45.13	2.592	2.551
48.0	99.99	?	-----	-----
* 1/4-order subharmonic				
** Data does not follow pattern.				

Table 4-2.

Because the physical system is known to contain a dead zone in the feedback path, Table 4-3 is a comparison of the system's response when a dead zone is assumed and the system's response when no dead zone is considered.

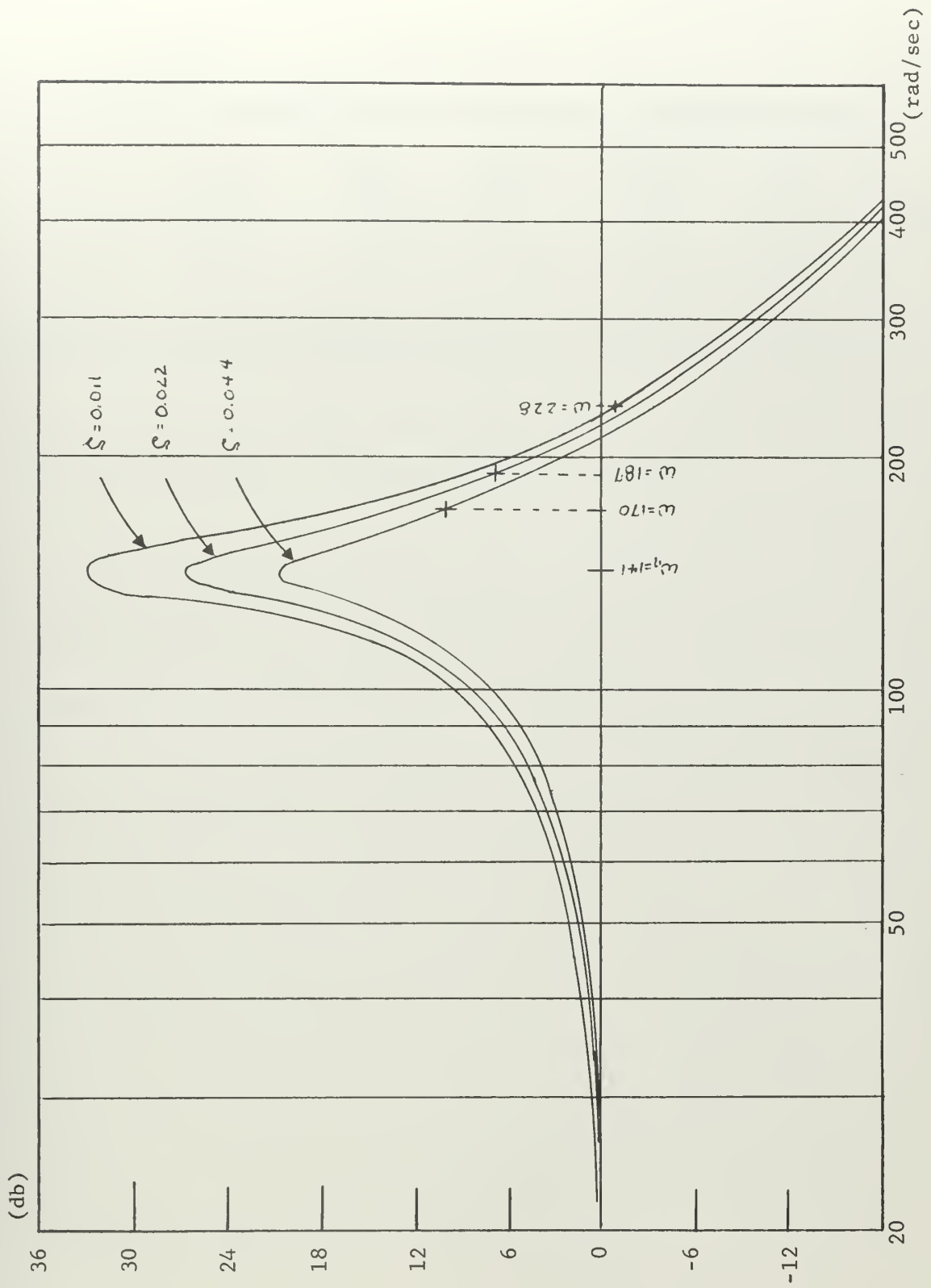


Figure 4-16. Response of Linear Filter  
Gain in(db's) vs. frequency in radians/sec.

<u>V<sub>ref</sub></u>	<u>Alpha</u>	<u>f<sub>LC</sub></u>	<u>f<sub>SUB</sub></u>	<u>V<sub>p1</sub></u>	<u>V<sub>p2</sub></u>
60.0	0.0	45.06	22.53	5.904	4.192
60.0	0.5	40.27	20.13	6.259	6.014
60.0	2.0	35.79	17.89	6.927	6.844

Table 4-3.

## 5. Conclusions

The main conclusion that can be drawn by examination of the experimental data is that under certain conditions the forced limit-cycling regulator discussed will support subharmonic ripple instability. The other object of the investigation, that of determining the exact causes for the subharmonic sustentation, was not clearly achieved and the conclusions that might be drawn toward this end are somewhat speculative and will appear in the next section in a discussion of the recommendations for further study in this area.



## 6. Recommended areas for further study

One tentative conclusion that might possibly be reached in reviewing the experimental results is that the subharmonic that is sustained in the system is dependent upon the numerics of the components of the filter that is employed. The filter in this case was both simple and a little unrealistic but it did bring the interesting observation that the subharmonic that was the most evident in the output was one that was quite near the resonant frequency of the linear filter. Examining the results presented in Figure 4-4 one can see that although the damping of the linear filter is increased as the load resistance is lowered, the amplitude of the subharmonic is increased. This might be explained by the Bode diagram of Figure 4-16 where it can be seen that as the load is reduced the limit-cycle frequency is also reduced and its  $1/2$ -order subharmonic is moved closer to the resonant frequency of the filter.

In Figure 4-9b, where the resistance is 0.8 ohms and the reference voltage is 56.0 volts, the  $1/4$ -order subharmonic of the limit-cycle is more evident than the  $1/2$ -order subharmonic as was the case with the rest of the results. This also could be due to the fact that this order subharmonic was closer to the resonant peak than was the  $1/2$ -order subharmonic.

Based on the above philosophy, a recommendation for further study would be to refine and design the filter to produce a desired limit-cycle whose subharmonics are well attenuated by the linear filter.

It can be noted in Table 4-3 that as the dead zone in the feedback path was increased the limit-cycle frequency decreased and

its 1/2-order subharmonic moved away from the filter's resonant peak. Any further work should also include a more detailed study of the effects of the dead zone on the system.

Another area for study that was touched on briefly but in no extensive detail was the matter of varying the supply voltage and studying its effect on the ripple instability.

In the realm of mathematical analysis several of the references noted in the bibliography suggest that a possible method of predicting the performance of the system would be to employ a Dual Input Describing Function or even a Multiple Input Describing Function. Surely, any further study should give some consideration to these analytical methods in attempting to understand ripple instability in this system.

## BIBLIOGRAPHY

1. West, J. C., Douce, J. L., and Livesly, R. K., "The Dual Input Describing Function and its use in the Analysis of Nonlinear Feedback Systems", Proc. IEEE, Vol. 103, Part B., p 463 (1956).
2. West, J. C., and Douce, J. L., "The Mechanism of Subharmonic Generation in a Feedback System", Proc. IEEE, Vol. 102, Part B., p 569 (1956).
3. West, J. C., Analytical Techniques for Nonlinear Control Systems, D. Van Nostrand, 1960.
4. Hayashi, C., Forced Oscillations in Nonlinear Systems, Nippon Printing and Publishing Co., Ltd., Osaka, Japan, 1953.
5. Hayashi, C., "Subharmonic Oscillations in Nonlinear Systems", Journal of Applied Physics, 24:344-348 (1953).
6. Hayashi, C., Nonlinear Oscillations in Physical Systems, McGraw-Hill, New York, New York, 1964.
7. Ludeke, C. A., "The Generation and Extinction of Subharmonics", Symposium on Nonlinear Circuit Analysis, 2:215-233 (1953).
8. Gelb, S., and Vander Velde, W. E., Multiple-Input Describing Functions and Nonlinear System Design, McGraw-Hill, New York, New York, 1958.
9. Cunningham, W. J., Introduction to Nonlinear Design, McGraw-Hill, New York, New York, 1958.
10. Leszczynski, V. J., Analysis of a Forced Limit-Cycling Regulator, Thesis, Naval Postgraduate School, 1968.
11. Fallside, F. and Farmer, A. R., "Ripple Instability in Closed-Loop Systems with Thyristor Amplifiers", Proc. IEEE., Vol. 114, No. 1, pp 139-152 (January 1967).
12. Thaler, G. J. and Brown, R. G., Analysis and Design of Feedback Control Systems, McGraw-Hill, New York, New York, 1960.

## APPENDIX I

Computer program for simulation of system with numerical data for the conditions when the reference voltage is held constant at 60.0 volts and the load resistance is 3.2 ohms, 1.6 ohms and 0.8 ohms.

```

C *****-----*****-----*****-----*****-----
C
C      C(1)=MAXIMUM VALUE OF INPUT SINE WAVE
C      C(2)=VALUE OF FILTER INDUCTANCE IN HENRIES
C      C(3)=VALUE OF FILTER CAPICITANCE IN FARADS
C      C(4)=VALUE OF LOAD RESISTANCE IN OHMS
C      C(5)=REFERENCE VOLTAGE
C      C(6)=GAIN OF AMPLIFIER BEFORE DEAD ZONE
C      C(7)=MAGNITUDE OF DEAD ZONE
C      C(8)=GAIN OF AMPLIFIER AFTER DEAD ZONE
C *****-----*****-----*****-----*****-----
C
C      DIMENSION X(30),XDOT(30),C(15)
C      C(10)=1.
C      IBP=1
C      X(5)=61.094
C      PI=3.141592
C      X(8)=IBP
C      X(10)=0.0
1  CALL INTEG2(T,X,XDOT,C)
C      X(10)=T-C.097687
C      XMAX=C(1)*SIN(PI/3.)
C      THA=2.0*PI*60.0*T
C      PHASEA=ABS(C(1)*SIN(THA))
C      PHASEB=ABS(C(1)*SIN(THA+2.0*PI/3.))
C      PHASEC=ABS(C(1)*SIN(THA+PI/3.))
C      X(6)=AMAX1(PHASEA,PHASEB,PHASEC)
C      IF(PHASEA.GE.XMAX)IPH=1
C      IF(PHASEB.GE.XMAX)IPH=2
C      IF(PHASEC.GE.XMAX)IPH=3
206 ERROR=X(1)-C(5)
C      X(9)=IPH
C      VK1=C(6)*ERROR
C      IF(VK1.GE.C(7))VDZ=VK1-C(7)
C      IF(VK1.LT.C(7))VDZ=0.0
C      IF(VK1.LT.0.0)VDZ=VK1
C      VK2=VDZ*C(8)
C      GO TO(100,101,102,103,104),IBP
100 CONTINUE
C      IF(VK2)207,207,208
207 IBP=1
C      VIN=X(6)
C      X(5)=VIN
C      X(7)=0.
C      X(3)=(1./C(2))*(VIN-X(1))
C      XDOT(2)=X(3)
C      IF(X(2).LT.-0.01) X(2)=-0.01
C      X(4)=(1./C(3))*X(2)-(1./(C(3)*C(4)))*X(1)
C      XDOT(1)=X(4)
C      VLAST=VIN
C      X(8)=IBP
C      GO TO 1
208 IF(VIN.LT.VLAST)GO TO 207
C      GO TO(101,102,103),IPH
101 VIN=PHASEA
C      IF(VK2)207,207,105
105 CONTINUE
C      X(7)=1.
C      X(5)=VIN
C      IF(VIN-.75)300,301,301
300 VIN=0.0
C      X(5)=VIN
C      IBP=5
C      GO TO 302
301 IBP=2
302 X(3)=(1./C(2))*(VIN-X(1))
C      IF(X(2).LT.-0.01)X(3)=0.0
C      XDOT(2)=X(3)

```

```

IF(X(2).LT.-0.(1)) X(2)=-0.01
X(4)=(1./C(3))*X(2)-(1./C(3)*C(4))*X(1)
XDOT(1)=X(4)
VLAST=VIN
X(8)=IBP
GO TO 1
102 VIN=PHASER
IF(VK2)207,207,106
106 CONTINUE
X(7)=2.
X(5)=VIN
IF(VIN-.75)303,304,304
303 VIN=0.0
X(5)=VIN
IBP=5
GO TO 305
304 IBP=3
305 X(3)=(1./C(2))*(VIN-X(1))
IF(X(2).LT.-0.(1))X(3)=0.0
XDOT(2)=X(3)
IF(X(2).LT.-0.(1)) X(2)=-0.01
X(4)=(1./C(3))*X(2)-(1./C(3)*C(4))*X(1)
XDOT(1)=X(4)
VLAST=VIN
X(8)=IBP
GO TO 1
103 VIN=PHASEC
IF(VK2)207,207,107
107 CONTINUE
X(7)=3.
X(5)=VIN
IF(VIN-.75)306,307,307
306 VIN=0.0
X(5)=VIN
IBP=5
GO TO 308
307 IBP=4
308 X(3)=(1./C(2))*(VIN-X(1))
IF(X(2).LT.-0.(1))X(3)=0.0
XDOT(2)=X(3)
IF(X(2).LT.-0.(1)) X(2)=-0.01
X(4)=(1./C(3))*X(2)-(1./C(3)*C(4))*X(1)
XDOT(1)=X(4)
VLAST=VIN
X(8)=IBP
GO TO 1
104 VIN=0.0
X(7)=4.
X(5)=VIN
X(3)=(1./C(2))*(VIN-X(1))
IF(X(2).LT.-0.(1))X(3)=0.0
XDOT(2)=X(3)
IF(X(2).LT.-0.(1)) X(2)=-0.01
X(4)=(1./C(3))*X(2)-(1./C(3)*C(4))*X(1)
XDOT(1)=X(4)
IBP=5
IF(VK2)309,309,310
309 IBP=1
310 CONTINUE
X(8)=IBP
GO TO 1
END

```

# INPUT DATA RECORD

ORDER OF EQUATIONS = 2  
INITIAL TIME = 0.9769E-01  
FINAL TIME = 0.2000E 00  
STEP SIZE = 0.2222E-04

THE NON-ZERO CONSTANTS, C(I), ARE

C( 1) = 0.6500E 02  
C( 2) = 0.5000E-03  
C( 3) = 0.1000E 00  
C( 4) = 0.3200E 01  
C( 5) = 0.6000E 02  
C( 6) = 0.1000E 01  
C( 8) = 0.1000E 01

THE NON-ZERO INITIAL CONDITIONS ARE

X( 1) = 0.6006E 02  
X( 2) = 0.3786E 02

THE COLUMN HEADINGS AND THE CORRESPONDING VARIABLES ARE

TIME	X( 0)
VIN	X( 5)
VOUT	X( 1)



HYDE,W.H. B16 R=3.2OHMS, VREF=60.0VOLTS

TIME	VIN	VOUT
0.97687E-01	0.61094E 02	0.60059E 02
0.98130E-01	0.63935E 02	0.60148E 02
0.98574E-01	0.64994E 02	0.60251E 02
0.99017E-01	0.64240E 02	0.60372E 02
0.99461E-01	0.61695E 02	0.60507E 02
0.99904E-01	0.57430E 02	0.60647E 02
0.10035E 00	0.51563E 02	0.60773E 02
0.10079E 00	0.44258E 02	0.60862E 02
0.10123E 00	0.35720E 02	0.60885E 02
0.10168E 00	0.26186E 02	0.60819E 02
0.10212E 00	0.15921E 02	0.60734E 02
0.10256E 00	0.52118E 01	0.60650E 02
0.10301E 00	0.0	0.60566E 02
0.10345E 00	0.0	0.60481E 02
0.10390E 00	0.0	0.60397E 02
0.10434E 00	0.0	0.60313E 02
0.10478E 00	0.0	0.60229E 02
0.10523E 00	0.0	0.60146E 02
0.10567E 00	0.0	0.60062E 02
0.10611E 00	0.61829E 02	0.59978E 02
0.10656E 00	0.64304E 02	0.59901E 02
0.10700E 00	0.64986E 02	0.59840E 02
0.10744E 00	0.63856E 02	0.59799E 02
0.10789E 00	0.60945E 02	0.59773E 02
0.10833E 00	0.56335E 02	0.59751E 02
0.10877E 00	0.60885E 02	0.59723E 02
0.10922E 00	0.63823E 02	0.59698E 02
0.10966E 00	0.64982E 02	0.59690E 02
0.11010E 00	0.64329E 02	0.59701E 02
0.11055E 00	0.61882E 02	0.59730E 02
0.11099E 00	0.57710E 02	0.59768E 02
0.11143E 00	0.59822E 02	0.59799E 02
0.11188E 00	0.63218E 02	0.59829E 02
0.11232E 00	0.64852E 02	0.59873E 02
0.11276E 00	0.64677E 02	0.59936E 02
0.11321E 00	0.62699E 02	0.60016E 02
0.11365E 00	0.58973E 02	0.60107E 02
0.11409E 00	0.53602E 02	0.60192E 02
0.11454E 00	0.46737E 02	0.60251E 02
0.11498E 00	0.38568E 02	0.60255E 02
0.11543E 00	0.29324E 02	0.60186E 02
0.11587E 00	0.19262E 02	0.60102E 02
0.11631E 00	0.86633E 01	0.60019E 02
0.11676E 00	0.57348E 02	0.59935E 02
0.11720E 00	0.61640E 02	0.59852E 02
0.11764E 00	0.64213E 02	0.59769E 02
0.11809E 00	0.64996E 02	0.59700E 02
0.11853E 00	0.63966E 02	0.59651E 02
0.11897E 00	0.61152E 02	0.59619E 02
0.11942E 00	0.56634E 02	0.59592E 02



HYDE, W.H. B16 R=3.20HMS, VREF=60.0VOLTS

TIME	VIN	VOUT
0.11986E 00	0.60671E 02	0.59559E 02
0.12030E 00	0.63706E 02	0.59529E 02
0.12075E 00	0.64965E 02	0.59516E 02
0.12119E 00	0.64413E 02	0.59524E 02
0.12163E 00	0.62065E 02	0.59550E 02
0.12208E 00	0.57985E 02	0.59586E 02
0.12252E 00	0.59583E 02	0.59617E 02
0.12296E 00	0.63075E 02	0.59647E 02
0.12341E 00	0.64808E 02	0.59690E 02
0.12385E 00	0.64735E 02	0.59753E 02
0.12429E 00	0.62856E 02	0.59835E 02
0.12474E 00	0.59225E 02	0.59928E 02
0.12518E 00	0.58379E 02	0.60018E 02
0.12562E 00	0.62321E 02	0.60103E 02
0.12607E 00	0.64525E 02	0.60195E 02
0.12651E 00	0.64930E 02	0.60304E 02
0.12696E 00	0.63525E 02	0.60430E 02
0.12740E 00	0.60348E 02	0.60568E 02
0.12784E 00	0.55489E 02	0.60704E 02
0.12829E 00	0.49082E 02	0.60819E 02
0.12873E 00	0.41307E 02	0.60887E 02
0.12917E 00	0.32380E 02	0.60878E 02
0.12962E 00	0.22549E 02	0.60796E 02
0.13006E 00	0.12091E 02	0.60711E 02
0.13050E 00	0.12949E 01	0.60627E 02
0.13095E 00	0.0	0.60542E 02
0.13139E 00	0.0	0.60458E 02
0.13183E 00	0.0	0.60374E 02
0.13228E 00	0.0	0.60290E 02
0.13272E 00	0.0	0.60206E 02
0.13316E 00	0.0	0.60122E 02
0.13361E 00	0.0	0.60039E 02
0.13405E 00	0.62926E 02	0.59956E 02
0.13449E 00	0.64759E 02	0.59883E 02
0.13494E 00	0.64786E 02	0.59828E 02
0.13538E 00	0.63007E 02	0.59793E 02
0.13582E 00	0.59471E 02	0.59770E 02
0.13627E 00	0.58111E 02	0.59746E 02
0.13671E 00	0.62147E 02	0.59716E 02
0.13715E 00	0.64450E 02	0.59696E 02
0.13760E 00	0.64956E 02	0.59693E 02
0.13804E 00	0.63650E 02	0.59711E 02
0.13849E 00	0.60570E 02	0.59744E 02
0.13893E 00	0.56770E 02	0.59780E 02
0.13937E 00	0.61246E 02	0.59808E 02
0.13982E 00	0.64015E 02	0.59842E 02
0.14026E 00	0.64998E 02	0.59891E 02
0.14070E 00	0.64170E 02	0.59960E 02
0.14115E 00	0.61552E 02	0.60045E 02
0.14159E 00	0.57217E 02	0.60135E 02

HYDE,W.H. B16 R=3.20HMS, VREF=60.7VOLTS

TIME	VIN	VOUT
0.14203E 00	0.51287E 02	0.60213E 02
0.14248E 00	0.43927E 02	0.60255E 02
0.14292E 00	0.35343E 02	0.60232E 02
0.14336E 00	0.25772E 02	0.60150E 02
0.14381E 00	0.15483E 02	0.60066E 02
0.14425E 00	0.58522E 02	0.59983E 02
0.14469E 00	0.59090E 02	0.59809E 02
0.14514E 00	0.62772E 02	0.59816E 02
0.14558E 00	0.64704E 02	0.59736E 02
0.14602E 00	0.64833E 02	0.59674E 02
0.14647E 00	0.63153E 02	0.59632E 02
0.14691E 00	0.59712E 02	0.59603E 02
0.14735E 00	0.57837E 02	0.59575E 02
0.14780E 00	0.61967E 02	0.59541E 02
0.14824E 00	0.64368E 02	0.59517E 02
0.14868E 00	0.64975E 02	0.59511E 02
0.14913E 00	0.63770E 02	0.59526E 02
0.14957E 00	0.60787E 02	0.59557E 02
0.15002E 00	0.56473E 02	0.59593E 02
0.15046E 00	0.61041E 02	0.59622E 02
0.15090E 00	0.63907E 02	0.59656E 02
0.15135E 00	0.64991E 02	0.59706E 02
0.15179E 00	0.64263E 02	0.59777E 02
0.15223E 00	0.61743E 02	0.59864E 02
0.15268E 00	0.57501E 02	0.59958E 02
0.15312E 00	0.59996E 02	0.60045E 02
0.15356E 00	0.63321E 02	0.60132E 02
0.15401E 00	0.64881E 02	0.60230E 02
0.15445E 00	0.64631E 02	0.60346E 02
0.15489E 00	0.62579E 02	0.60477E 02
0.15534E 00	0.58782E 02	0.60617E 02
0.15578E 00	0.53346E 02	0.60748E 02
0.15622E 00	0.46423E 02	0.60850E 02
0.15667E 00	0.38205E 02	0.60894E 02
0.15711E 00	0.28921E 02	0.60850E 02
0.15755E 00	0.18831E 02	0.60765E 02
0.15800E 00	0.82169E 01	0.60681E 02
0.15844E 00	0.0	0.60596E 02
0.15888E 00	0.0	0.60512E 02
0.15933E 00	0.0	0.60428E 02
0.15977E 00	0.0	0.60344E 02
0.16021E 00	0.0	0.60260E 02
0.16066E 00	0.0	0.60176E 02
0.16110E 00	0.0	0.60092E 02
0.16154E 00	0.0	0.60008E 02
0.16199E 00	0.63794E 02	0.59927E 02
0.16243E 00	0.64978E 02	0.59859E 02
0.16288E 00	0.64351E 02	0.59811E 02
0.16332E 00	0.61929E 02	0.59780E 02
0.16376E 00	0.57781E 02	0.59757E 02

HYDE, W.H. B16 R=3.20HMS, VREF=60.0VOLTS

TIME	VIN	VOUT
0.16421E 00	0.59761E 02	0.59729E 02
0.16465E 00	0.63182E 02	0.59700E 02
0.16509E 00	0.64841E 02	0.59685E 02
0.16554E 00	0.64693E 02	0.59689E 02
0.16598E 00	0.62740E 02	0.59713E 02
0.16642E 00	0.59037E 02	0.59748E 02
0.16687E 00	0.58576E 02	0.59780E 02
0.16731E 00	0.62448E 02	0.59807E 02
0.16775E 00	0.64578E 02	0.59845E 02
0.16820E 00	0.64908E 02	0.59901E 02
0.16864E 00	0.63428E 02	0.59976E 02
0.16908E 00	0.60179E 02	0.60064E 02
0.16953E 00	0.55253E 02	0.60151E 02
0.16997E 00	0.48786E 02	0.60219E 02
0.17041E 00	0.40957E 02	0.60241E 02
0.17086E 00	0.31988E 02	0.60188E 02
0.17130E 00	0.22126E 02	0.60104E 02
0.17174E 00	0.11648E 02	0.60021E 02
0.17219E 00	0.56709E 02	0.59937E 02
0.17263E 00	0.60615E 02	0.59854E 02
0.17307E 00	0.63675E 02	0.59771E 02
0.17352E 00	0.64960E 02	0.59695E 02
0.17396E 00	0.64433E 02	0.59639E 02
0.17441E 00	0.62110E 02	0.59602E 02
0.17485E 00	0.58055E 02	0.59574E 02
0.17529E 00	0.59521E 02	0.59541E 02
0.17574E 00	0.63038E 02	0.59509E 02
0.17618E 00	0.64796E 02	0.59489E 02
0.17662E 00	0.64748E 02	0.59490E 02
0.17707E 00	0.62895E 02	0.59512E 02
0.17751E 00	0.59288E 02	0.59546E 02
0.17795E 00	0.58312E 02	0.59578E 02
0.17840E 00	0.62277E 02	0.59607E 02
0.17884E 00	0.64507E 02	0.59646E 02
0.17928E 00	0.64937E 02	0.59703E 02
0.17973E 00	0.63557E 02	0.59780E 02
0.18017E 00	0.60405E 02	0.59872E 02
0.18061E 00	0.56988E 02	0.59965E 02
0.18106E 00	0.61396E 02	0.60050E 02
0.18150E 00	0.64091E 02	0.60140E 02
0.18194E 00	0.65000E 02	0.60244E 02
0.18239E 00	0.64096E 02	0.60367E 02
0.18283E 00	0.61405E 02	0.60504E 02
0.18327E 00	0.57002E 02	0.60643E 02
0.18372E 00	0.51009E 02	0.60768E 02
0.18416E 00	0.43594E 02	0.60853E 02
0.18460E 00	0.34963E 02	0.60869E 02
0.18505E 00	0.25358E 02	0.60799E 02
0.18549E 00	0.15045E 02	0.60715E 02
0.18594E 00	0.43128E 01	0.60630E 02

HYDE, W. H. B16 R=3.20HMS, VREF=60.0VOLTS

TIME		VIN		VOUT	
0.18638E	00	0.0		0.60546E	02
0.18682E	00	0.0		0.60462E	02
0.18727E	00	0.0		0.60377E	02
0.18771E	00	0.0		0.60294E	02
0.18815E	00	0.0		0.60210E	02
0.18860E	00	0.0		0.60126E	02
0.18904E	00	0.0		0.60042E	02
0.18948E	00	0.62101E	02	0.59959E	02
0.18993E	00	0.64430E	02	0.59881E	02
0.19037E	00	0.64961E	02	0.59821E	02
0.19081E	00	0.63681E	02	0.59781E	02
0.19126E	00	0.60626E	02	0.59755E	02
0.19170E	00	0.56695E	02	0.59732E	02
0.19214E	00	0.61195E	02	0.59703E	02
0.19259E	00	0.63988E	02	0.59679E	02
0.19303E	00	0.64997E	02	0.59671E	02
0.19347E	00	0.64194E	02	0.59684E	02
0.19392E	00	0.61601E	02	0.59714E	02
0.19436E	00	0.57290E	02	0.59751E	02
0.19480E	00	0.60169E	02	0.59781E	02
0.19525E	00	0.63422E	02	0.59813E	02
0.19569E	00	0.64907E	02	0.59858E	02
0.19613E	00	0.64581E	02	0.59922E	02
0.19658E	00	0.62456E	02	0.60004E	02
0.19702E	00	0.58588E	02	0.60095E	02

# INPUT DATA RECORD

ORDER OF EQUATIONS = 2  
INITIAL TIME = 0.9769E-01  
FINAL TIME = 0.2000E 00  
STEP SIZE = 0.2222E-04

THE NON-ZERO CONSTANTS, C(I), ARE

C( 1) = 0.6500E 02  
C( 2) = 0.5000E-03  
C( 3) = 0.1000E 00  
C( 4) = 0.1600E 01  
C( 5) = 0.6000E 02  
C( 6) = 0.1000E 01  
C( 8) = 0.1000E 01

THE NON-ZERO INITIAL CONDITIONS ARE

X( 1) = 0.5897E 02  
X( 2) = 0.4501E 02

THE COLUMN HEADINGS AND THE CORRESPONDING VARIABLES ARE

TIME	X( 0)
VIN	X( 5)
VOUT	X( 1)



HYDE, W.H. B1 R=1.6 OHMS, VREF= 60.0 VOLTS.

TIME	VIN	VOUT
0.97687E-01	0.61094E 02	0.58968E 02
0.98130E-01	0.63935E 02	0.59010E 02
0.98574E-01	0.64994E 02	0.59072E 02
0.99017E-01	0.64240E 02	0.59155E 02
0.99461E-01	0.61695E 02	0.59258E 02
0.99904E-01	0.57430E 02	0.59370E 02
0.10035E 00	0.60055E 02	0.59476E 02
0.10079E 00	0.63356E 02	0.59584E 02
0.10123E 00	0.64890E 02	0.59706E 02
0.10168E 00	0.64614E 02	0.59848E 02
0.10212E 00	0.62537E 02	0.60008E 02
0.10256E 00	0.58716E 02	0.60176E 02
0.10301E 00	0.53258E 02	0.60338E 02
0.10345E 00	0.46315E 02	0.60470E 02
0.10390E 00	0.38080E 02	0.60546E 02
0.10434E 00	0.28784E 02	0.60533E 02
0.10478E 00	0.18685E 02	0.60402E 02
0.10523E 00	0.80639E 01	0.60234E 02
0.10567E 00	0.0	0.60067E 02
0.10611E 00	0.61829E 02	0.59900E 02
0.10656E 00	0.64304E 02	0.59739E 02
0.10700E 00	0.64986E 02	0.59596E 02
0.10744E 00	0.63856E 02	0.59474E 02
0.10789E 00	0.60945E 02	0.59369E 02
0.10833E 00	0.56335E 02	0.59270E 02
0.10877E 00	0.60885E 02	0.59166E 02
0.10922E 00	0.63823E 02	0.59069E 02
0.10966E 00	0.64982E 02	0.58990E 02
0.11010E 00	0.64329E 02	0.58934E 02
0.11055E 00	0.61882E 02	0.58899E 02
0.11099E 00	0.57710E 02	0.58876E 02
0.11143E 00	0.59822E 02	0.58850E 02
0.11188E 00	0.63218E 02	0.58827E 02
0.11232E 00	0.64852E 02	0.58822E 02
0.11276E 00	0.64677E 02	0.58840E 02
0.11321E 00	0.62699E 02	0.58880E 02
0.11365E 00	0.58973E 02	0.58934E 02
0.11409E 00	0.58642E 02	0.58989E 02
0.11454E 00	0.62490E 02	0.59042E 02
0.11498E 00	0.64595E 02	0.59109E 02
0.11543E 00	0.64900E 02	0.59196E 02
0.11587E 00	0.63394E 02	0.59305E 02
0.11631E 00	0.60121E 02	0.59429E 02
0.11676E 00	0.57348E 02	0.59555E 02
0.11720E 00	0.61640E 02	0.59675E 02
0.11764E 00	0.64213E 02	0.59802E 02
0.11809E 00	0.64996E 02	0.59946E 02
0.11853E 00	0.63966E 02	0.60108E 02
0.11897E 00	0.61152E 02	0.60285E 02
0.11942E 00	0.56634E 02	0.60464E 02

HYDE,W.H. B1 R=1.6 OHMS, VREF= 60.0 VOLTS.

TIME		VIN		VOUT	
0.11986E	00	0.50536E	02	0.60627E	02
0.12030E	00	0.43029E	02	0.60749E	02
0.12075E	00	0.34322E	02	0.60800E	02
0.12119E	00	0.24658E	02	0.60747E	02
0.12163E	00	0.14307E	02	0.60587E	02
0.12208E	00	0.35561E	01	0.60419E	02
0.12252E	00	0.0		0.60251E	02
0.12296E	00	0.0		0.60083E	02
0.12341E	00	0.64808E	02	0.59919E	02
0.12385E	00	0.64735E	02	0.59771E	02
0.12429E	00	0.62856E	02	0.59642E	02
0.12474E	00	0.59225E	02	0.59526E	02
0.12518E	00	0.58379E	02	0.59409E	02
0.12562E	00	0.62321E	02	0.59289E	02
0.12607E	00	0.64525E	02	0.59181E	02
0.12651E	00	0.64930E	02	0.59093E	02
0.12696E	00	0.63525E	02	0.59029E	02
0.12740E	00	0.60348E	02	0.58981E	02
0.12784E	00	0.57061E	02	0.58939E	02
0.12829E	00	0.61446E	02	0.58893E	02
0.12873E	00	0.64117E	02	0.58857E	02
0.12917E	00	0.65000E	02	0.58841E	02
0.12962E	00	0.64070E	02	0.58849E	02
0.13006E	00	0.61354E	02	0.58877E	02
0.13050E	00	0.56928E	02	0.58914E	02
0.13095E	00	0.60451E	02	0.58947E	02
0.13139E	00	0.63583E	02	0.58986E	02
0.13183E	00	0.64943E	02	0.59042E	02
0.13228E	00	0.64491E	02	0.59121E	02
0.13272E	00	0.62241E	02	0.59220E	02
0.13316E	00	0.58256E	02	0.59330E	02
0.13361E	00	0.59339E	02	0.59436E	02
0.13405E	00	0.62926E	02	0.59542E	02
0.13449E	00	0.64759E	02	0.59661E	02
0.13494E	00	0.64786E	02	0.59798E	02
0.13538E	00	0.63007E	02	0.59954E	02
0.13582E	00	0.59471E	02	0.60122E	02
0.13627E	00	0.54277E	02	0.60285E	02
0.13671E	00	0.47569E	02	0.60424E	02
0.13715E	00	0.39534E	02	0.60512E	02
0.13760E	00	0.30397E	02	0.60516E	02
0.13804E	00	0.20413E	02	0.60402E	02
0.13849E	00	0.98602E	01	0.60234E	02
0.13893E	00	0.0		0.60067E	02
0.13937E	00	0.61246E	02	0.59900E	02
0.13982E	00	0.64015E	02	0.59737E	02
0.14026E	00	0.64998E	02	0.59590E	02
0.14070E	00	0.64170E	02	0.59465E	02
0.14115E	00	0.61552E	02	0.59358E	02
0.14159E	00	0.57217E	02	0.59259E	02

HYDE,W.H. B1 R=1.6 OHMS, VREF= 60.0 VOLTS.

TIME		VIN		VOUT
0.14203E	00	0.60226E	02	0.59156E 02
0.14248E	00	0.63455E	02	0.59057E 02
0.14292E	00	0.64915E	02	0.58975E 02
0.14336E	00	0.64564E	02	0.58916E 02
0.14381E	00	0.62413E	02	0.58878E 02
0.14425E	00	0.58522E	02	0.58855E 02
0.14469E	00	0.59090E	02	0.58830E 02
0.14514E	00	0.62772E	02	0.58807E 02
0.14558E	00	0.64704E	02	0.58799E 02
0.14602E	00	0.64833E	02	0.58814E 02
0.14647E	00	0.63153E	02	0.58852E 02
0.14691E	00	0.59712E	02	0.58906E 02
0.14735E	00	0.57837E	02	0.58963E 02
0.14780E	00	0.61967E	02	0.59017E 02
0.14824E	00	0.64368E	02	0.59082E 02
0.14868E	00	0.64975E	02	0.59167E 02
0.14913E	00	0.63770E	02	0.59274E 02
0.14957E	00	0.60787E	02	0.59398E 02
0.15002E	00	0.56473E	02	0.59527E 02
0.15046E	00	0.61041E	02	0.59649E 02
0.15090E	00	0.63907E	02	0.59776E 02
0.15135E	00	0.64991E	02	0.59918E 02
0.15179E	00	0.64263E	02	0.60079E 02
0.15223E	00	0.61743E	02	0.60255E 02
0.15268E	00	0.57501E	02	0.60437E 02
0.15312E	00	0.51656E	02	0.60605E 02
0.15356E	00	0.44371E	02	0.60738E 02
0.15401E	00	0.35848E	02	0.60805E 02
0.15445E	00	0.26326E	02	0.60773E 02
0.15489E	00	0.16070E	02	0.60625E 02
0.15534E	00	0.53645E	01	0.60456E 02
0.15578E	00	0.0		0.60288E 02
0.15622E	00	0.0		0.60121E 02
0.15667E	00	0.64644E	02	0.59954E 02
0.15711E	00	0.64873E	02	0.59801E 02
0.15755E	00	0.63293E	02	0.59668E 02
0.15800E	00	0.59949E	02	0.59549E 02
0.15844E	00	0.57559E	02	0.59431E 02
0.15888E	00	0.61782E	02	0.59309E 02
0.15933E	00	0.64282E	02	0.59197E 02
0.15977E	00	0.64989E	02	0.59104E 02
0.16021E	00	0.63884E	02	0.59034E 02
0.16066E	00	0.60998E	02	0.58983E 02
0.16110E	00	0.56411E	02	0.58939E 02
0.16154E	00	0.60831E	02	0.58891E 02
0.16199E	00	0.63794E	02	0.58851E 02
0.16243E	00	0.64978E	02	0.58830E 02
0.16288E	00	0.64351E	02	0.58833E 02
0.16332E	00	0.61929E	02	0.58856E 02
0.16376E	00	0.57781E	02	0.58892E 02



HYDE, W.H. B1 R=1.6 OHMS, VREF= 60.0 VOLTS.

TIME	VIN	VOUT
0.16421E 00	0.59761E 02	0.58924E 02
0.16465E 00	0.63182E 02	0.58960E 02
0.16509E 00	0.64841E 02	0.59012E 02
0.16554E 00	0.64693E 02	0.59085E 02
0.16598E 00	0.62740E 02	0.59181E 02
0.16642E 00	0.59037E 02	0.59289E 02
0.16687E 00	0.58576E 02	0.59396E 02
0.16731E 00	0.62448E 02	0.59500E 02
0.16775E 00	0.64578E 02	0.59615E 02
0.16820E 00	0.64908E 02	0.59749E 02
0.16864E 00	0.63428E 02	0.59902E 02
0.16908E 00	0.60179E 02	0.60068E 02
0.16953E 00	0.55253E 02	0.60233E 02
0.16997E 00	0.48786E 02	0.60378E 02
0.17041E 00	0.40957E 02	0.60476E 02
0.17086E 00	0.31988E 02	0.60497E 02
0.17130E 00	0.22126E 02	0.60405E 02
0.17174E 00	0.11648E 02	0.60237E 02
0.17219E 00	0.84376E 00	0.60070E 02
0.17263E 00	0.60615E 02	0.59903E 02
0.17307E 00	0.63675E 02	0.59738E 02
0.17352E 00	0.64960E 02	0.59586E 02
0.17396E 00	0.64433E 02	0.59455E 02
0.17441E 00	0.62110E 02	0.59344E 02
0.17485E 00	0.58055E 02	0.59243E 02
0.17529E 00	0.59521E 02	0.59140E 02
0.17574E 00	0.63038E 02	0.59038E 02
0.17618E 00	0.64796E 02	0.58951E 02
0.17662E 00	0.64748E 02	0.58887E 02
0.17707E 00	0.62895E 02	0.58846E 02
0.17751E 00	0.59288E 02	0.58821E 02
0.17795E 00	0.58312E 02	0.58797E 02
0.17840E 00	0.62277E 02	0.58772E 02
0.17884E 00	0.64507E 02	0.58761E 02
0.17928E 00	0.64937E 02	0.58772E 02
0.17973E 00	0.63557E 02	0.58806E 02
0.18017E 00	0.60405E 02	0.58859E 02
0.18061E 00	0.56988E 02	0.58916E 02
0.18106E 00	0.61396E 02	0.58971E 02
0.18150E 00	0.64091E 02	0.59034E 02
0.18194E 00	0.65000E 02	0.59116E 02
0.18239E 00	0.64096E 02	0.59221E 02
0.18283E 00	0.61405E 02	0.59344E 02
0.18327E 00	0.57002E 02	0.59474E 02
0.18372E 00	0.60394E 02	0.59599E 02
0.18416E 00	0.63551E 02	0.59725E 02
0.18460E 00	0.64936E 02	0.59866E 02
0.18505E 00	0.64510E 02	0.60026E 02
0.18549E 00	0.62285E 02	0.60202E 02
0.18594E 00	0.58324E 02	0.60385E 02

HYDE,W.H. B1 R=1.6 OHMS, VREF= 60.0 VOLTS.

TIME	VIN	VOUT
0.18638E 00	0.52736E 02	0.60560E 02
0.18682E 00	0.45678E 02	0.60702E 02
0.18727E 00	0.37346E 02	0.60785E 02
0.18771E 00	0.27973E 02	0.60774E 02
0.18815E 00	0.17820E 02	0.60641E 02
0.18860E 00	0.71687E 01	0.60473E 02
0.18904E 00	0.0	0.60305E 02
0.18948E 00	0.0	0.60138E 02
0.18993E 00	0.64430E 02	0.59971E 02
0.19037E 00	0.64961E 02	0.59814E 02
0.19081E 00	0.63681E 02	0.59677E 02
0.19126E 00	0.60626E 02	0.59556E 02
0.19170E 00	0.56695E 02	0.59439E 02
0.19214E 00	0.61195E 02	0.59316E 02
0.19259E 00	0.63988E 02	0.59201E 02
0.19303E 00	0.64997E 02	0.59104E 02
0.19347E 00	0.64194E 02	0.59030E 02
0.19392E 00	0.61601E 02	0.58976E 02
0.19436E 00	0.57290E 02	0.58932E 02
0.19480E 00	0.60169E 02	0.58885E 02
0.19525E 00	0.63422E 02	0.58843E 02
0.19569E 00	0.64907E 02	0.58818E 02
0.19613E 00	0.64581E 02	0.58817E 02
0.19658E 00	0.62456E 02	0.58838E 02
0.19702E 00	0.58588E 02	0.58872E 02

INPUT DATA RECORD

ORDER OF EQUATIONS = 2  
INITIAL TIME = 0.9769E-01  
FINAL TIME = 0.2000E 00  
STEP SIZE = 0.2222E-04

THE NON-ZERO CONSTANTS, C(I), ARE  
C( 1) = 0.6500E 02  
C( 2) = 0.5000E-03  
C( 3) = 0.1000E 00  
C( 4) = 0.8000E 00  
C( 5) = 0.6000E 02  
C( 6) = 0.1000E 01  
C( 8) = 0.1000E 01

THE NON-ZERO INITIAL CONDITIONS ARE  
X( 1) = 0.5709E 02  
X( 2) = 0.1069E 03

THE COLUMN HEADINGS AND THE CORRESPONDING VARIABLES ARE

TIME	X( 0)
VIN	X( 5)
VOUT	X( 1)

HYDE,W.H. B3 R=0.8 OHMS, VREF=60.0

TIME	VIN	VOUT
0.97687E-01	0.61094E 02	0.57091E 02
0.98130E-01	0.63935E 02	0.57258E 02
0.98574E-01	0.64994E 02	0.57450E 02
0.99017E-01	0.64240E 02	0.57670E 02
0.99461E-01	0.61695E 02	0.57915E 02
0.99904E-01	0.57430E 02	0.58172E 02
0.10035E 00	0.60055E 02	0.58427E 02
0.10079E 00	0.63356E 02	0.58687E 02
0.10123E 00	0.64890E 02	0.58964E 02
0.10168E 00	0.64614E 02	0.59262E 02
0.10212E 00	0.62537E 02	0.59578E 02
0.10256E 00	0.58716E 02	0.59904E 02
0.10301E 00	0.53258E 02	0.60223E 02
0.10345E 00	0.46315E 02	0.60512E 02
0.10390E 00	0.38080E 02	0.60744E 02
0.10434E 00	0.28784E 02	0.60884E 02
0.10478E 00	0.18685E 02	0.60897E 02
0.10523E 00	0.80639E 01	0.60743E 02
0.10567E 00	0.0	0.60424E 02
0.10611E 00	0.0	0.60089E 02
0.10656E 00	0.64304E 02	0.59757E 02
0.10700E 00	0.64986E 02	0.59442E 02
0.10744E 00	0.63856E 02	0.59149E 02
0.10789E 00	0.60945E 02	0.58877E 02
0.10833E 00	0.56335E 02	0.58613E 02
0.10877E 00	0.60885E 02	0.58348E 02
0.10922E 00	0.63823E 02	0.58094E 02
0.10966E 00	0.64982E 02	0.57863E 02
0.11010E 00	0.64329E 02	0.57661E 02
0.11055E 00	0.61882E 02	0.57486E 02
0.11099E 00	0.57710E 02	0.57329E 02
0.11143E 00	0.59822E 02	0.57176E 02
0.11188E 00	0.63218E 02	0.57034E 02
0.11232E 00	0.64852E 02	0.56916E 02
0.11276E 00	0.64677E 02	0.56830E 02
0.11321E 00	0.62699E 02	0.56775E 02
0.11365E 00	0.58973E 02	0.56743E 02
0.11409E 00	0.58642E 02	0.56720E 02
0.11454E 00	0.62490E 02	0.56705E 02
0.11498E 00	0.64595E 02	0.56712E 02
0.11543E 00	0.64900E 02	0.56750E 02
0.11587E 00	0.63394E 02	0.56819E 02
0.11631E 00	0.60121E 02	0.56913E 02
0.11676E 00	0.57348E 02	0.57019E 02
0.11720E 00	0.61640E 02	0.57128E 02
0.11764E 00	0.64213E 02	0.57254E 02
0.11809E 00	0.64996E 02	0.57406E 02
0.11853E 00	0.63966E 02	0.57587E 02
0.11897E 00	0.61152E 02	0.57791E 02
0.11942E 00	0.56634E 02	0.58007E 02

HYDE,W.H. B3 R=0.8 OHMS, VREF=60.0

TIME	VIN	VOUT
0.11986E 00	0.60671E 02	0.58221E 02
0.12030E 00	0.63706E 02	0.58444E 02
0.12075E 00	0.64965E 02	0.58685E 02
0.12119E 00	0.64413E 02	0.58949E 02
0.12163E 00	0.62065E 02	0.59233E 02
0.12208E 00	0.57985E 02	0.59525E 02
0.12252E 00	0.59583E 02	0.59812E 02
0.12296E 00	0.63075E 02	0.60095E 02
0.12341E 00	0.64808E 02	0.60388E 02
0.12385E 00	0.64735E 02	0.60697E 02
0.12429E 00	0.62856E 02	0.61019E 02
0.12474E 00	0.59225E 02	0.61346E 02
0.12518E 00	0.53942E 02	0.61662E 02
0.12562E 00	0.47155E 02	0.61946E 02
0.12607E 00	0.39053E 02	0.62169E 02
0.12651E 00	0.29862E 02	0.62299E 02
0.12696E 00	0.19839E 02	0.62301E 02
0.12740E 00	0.92624E 01	0.62136E 02
0.12784E 00	0.0	0.61807E 02
0.12829E 00	0.0	0.61465E 02
0.12873E 00	0.0	0.61124E 02
0.12917E 00	0.0	0.60785E 02
0.12962E 00	0.0	0.60449E 02
0.13006E 00	0.0	0.60113E 02
0.13050E 00	0.56928E 02	0.59780E 02
0.13095E 00	0.60451E 02	0.59449E 02
0.13139E 00	0.63583E 02	0.59119E 02
0.13183E 00	0.64943E 02	0.58802E 02
0.13228E 00	0.64491E 02	0.58511E 02
0.13272E 00	0.62241E 02	0.58243E 02
0.13316E 00	0.58256E 02	0.57993E 02
0.13361E 00	0.59339E 02	0.57746E 02
0.13405E 00	0.62926E 02	0.57506E 02
0.13449E 00	0.64759E 02	0.57289E 02
0.13494E 00	0.64786E 02	0.57102E 02
0.13538E 00	0.63007E 02	0.56945E 02
0.13582E 00	0.59471E 02	0.56812E 02
0.13627E 00	0.58111E 02	0.56691E 02
0.13671E 00	0.62147E 02	0.56577E 02
0.13715E 00	0.64450E 02	0.56485E 02
0.13760E 00	0.64956E 02	0.56424E 02
0.13804E 00	0.63650E 02	0.56397E 02
0.13849E 00	0.60570E 02	0.56398E 02
0.13893E 00	0.56770E 02	0.56415E 02
0.13937E 00	0.61246E 02	0.56438E 02
0.13982E 00	0.64015E 02	0.56479E 02
0.14026E 00	0.64998E 02	0.56549E 02
0.14070E 00	0.64170E 02	0.56651E 02
0.14115E 00	0.61552E 02	0.56782E 02
0.14159E 00	0.57217E 02	0.56930E 02



HYDE, W.H. B3 R=0.8 OHMS, VREF=60.0

TIME	VIN	VOUT
0.14203E 00	0.60226E 02	0.57082E 02
0.14248E 00	0.63455E 02	0.57245E 02
0.14292E 00	0.64915E 02	0.57431E 02
0.14336E 00	0.64564E 02	0.57645E 02
0.14381E 00	0.62413E 02	0.57884E 02
0.14425E 00	0.58522E 02	0.58140E 02
0.14469E 00	0.59090E 02	0.58396E 02
0.14514E 00	0.62772E 02	0.58653E 02
0.14558E 00	0.64704E 02	0.58925E 02
0.14602E 00	0.64833E 02	0.59217E 02
0.14647E 00	0.63153E 02	0.59529E 02
0.14691E 00	0.59712E 02	0.59853E 02
0.14735E 00	0.54607E 02	0.60175E 02
0.14780E 00	0.47978E 02	0.60472E 02
0.14824E 00	0.40012E 02	0.60717E 02
0.14868E 00	0.30930E 02	0.60880E 02
0.14913E 00	0.20986E 02	0.60923E 02
0.14957E 00	0.10456E 02	0.60809E 02
0.15002E 00	0.0	0.60513E 02
0.15046E 00	0.0	0.60178E 02
0.15090E 00	0.63907E 02	0.59845E 02
0.15135E 00	0.64991E 02	0.59528E 02
0.15179E 00	0.64263E 02	0.59233E 02
0.15223E 00	0.61743E 02	0.58960E 02
0.15268E 00	0.57501E 02	0.58698E 02
0.15312E 00	0.59996E 02	0.58436E 02
0.15356E 00	0.63321E 02	0.58180E 02
0.15401E 00	0.64881E 02	0.57946E 02
0.15445E 00	0.64631E 02	0.57740E 02
0.15489E 00	0.62579E 02	0.57562E 02
0.15534E 00	0.58782E 02	0.57403E 02
0.15578E 00	0.58835E 02	0.57252E 02
0.15622E 00	0.62612E 02	0.57107E 02
0.15667E 00	0.64644E 02	0.56985E 02
0.15711E 00	0.64873E 02	0.56893E 02
0.15755E 00	0.63293E 02	0.56832E 02
0.15800E 00	0.59949E 02	0.56797E 02
0.15844E 00	0.57559E 02	0.56773E 02
0.15888E 00	0.61782E 02	0.56756E 02
0.15933E 00	0.64282E 02	0.56757E 02
0.15977E 00	0.64989E 02	0.56788E 02
0.16021E 00	0.63884E 02	0.56850E 02
0.16066E 00	0.60998E 02	0.56940E 02
0.16110E 00	0.56411E 02	0.57044E 02
0.16154E 00	0.60831E 02	0.57151E 02
0.16199E 00	0.63794E 02	0.57271E 02
0.16243E 00	0.64978E 02	0.57416E 02
0.16288E 00	0.64351E 02	0.57589E 02
0.16332E 00	0.61929E 02	0.57787E 02
0.16376E 00	0.57781E 02	0.58000E 02

HYDE,W.H. B3 R=0.8 OHMS, VREF=60.0

TIME	VIN	VOUT
0.16421E 00	0.59761E 02	0.58213E 02
0.16465E 00	0.63182E 02	0.58431E 02
0.16509E 00	0.64841E 02	0.58665E 02
0.16554E 00	0.64693E 02	0.58922E 02
0.16598E 00	0.62740E 02	0.59200E 02
0.16642E 00	0.59037E 02	0.59489E 02
0.16687E 00	0.58576E 02	0.59775E 02
0.16731E 00	0.62448E 02	0.60055E 02
0.16775E 00	0.64578E 02	0.60343E 02
0.16820E 00	0.64908E 02	0.60645E 02
0.16864E 00	0.63428E 02	0.60962E 02
0.16908E 00	0.60179E 02	0.61286E 02
0.16953E 00	0.55253E 02	0.61604E 02
0.16997E 00	0.48786E 02	0.61894E 02
0.17041E 00	0.40957E 02	0.62130E 02
0.17086E 00	0.31988E 02	0.62282E 02
0.17130E 00	0.22126E 02	0.62313E 02
0.17174E 00	0.11648E 02	0.62185E 02
0.17219E 00	0.84376E 00	0.61878E 02
0.17263E 00	0.0	0.61535E 02
0.17307E 00	0.0	0.61194E 02
0.17352E 00	0.0	0.60855E 02
0.17396E 00	0.0	0.60517E 02
0.17441E 00	0.0	0.60182E 02
0.17485E 00	0.58055E 02	0.59848E 02
0.17529E 00	0.59521E 02	0.59517E 02
0.17574E 00	0.63038E 02	0.59187E 02
0.17618E 00	0.64796E 02	0.58863E 02
0.17662E 00	0.64748E 02	0.58562E 02
0.17707E 00	0.62895E 02	0.58286E 02
0.17751E 00	0.59288E 02	0.58030E 02
0.17795E 00	0.58312E 02	0.57780E 02
0.17840E 00	0.62277E 02	0.57534E 02
0.17884E 00	0.64507E 02	0.57308E 02
0.17928E 00	0.64937E 02	0.57111E 02
0.17973E 00	0.63557E 02	0.56945E 02
0.18017E 00	0.60405E 02	0.56806E 02
0.18061E 00	0.56988E 02	0.56681E 02
0.18106E 00	0.61396E 02	0.56562E 02
0.18150E 00	0.64091E 02	0.56462E 02
0.18194E 00	0.65000E 02	0.56392E 02
0.18239E 00	0.64096E 02	0.56356E 02
0.18283E 00	0.61405E 02	0.56350E 02
0.18327E 00	0.57002E 02	0.56363E 02
0.18372E 00	0.60394E 02	0.56383E 02
0.18416E 00	0.63551E 02	0.56418E 02
0.18460E 00	0.64936E 02	0.56481E 02
0.18505E 00	0.64510E 02	0.56575E 02
0.18549E 00	0.62285E 02	0.56700E 02
0.18594E 00	0.58324E 02	0.56846E 02

HYDE,W.H. B3 R=0.8 OHMS, VREF=60.0

TIME	VIN	VOUT
C.18638E 00	0.59276E 02	0.56997E 02
0.18682E 00	0.62888E 02	0.57157E 02
0.18727E 00	0.64746E 02	0.57338E 02
0.18771E 00	0.64799E 02	0.57546E 02
0.18815E 00	0.63045E 02	0.57781E 02
0.18860E 00	0.59533E 02	0.58035E 02
0.18904E 00	0.58042E 02	0.58293E 02
0.18948E 00	0.62101E 02	0.58550E 02
0.18993E 00	0.64430E 02	0.58820E 02
0.19037E 00	0.64961E 02	0.59109E 02
0.19081E 00	0.63681E 02	0.59419E 02
0.19126E 00	0.60626E 02	0.59744E 02
0.19170E 00	0.55880E 02	0.60070E 02
0.19214E 00	0.49575E 02	0.60376E 02
0.19259E 00	0.41889E 02	0.60639E 02
0.19303E 00	0.33035E 02	0.60825E 02
0.19347E 00	0.23259E 02	0.60901E 02
0.19392E 00	0.12835E 02	0.60828E 02
0.19436E 00	0.20527E 01	0.60568E 02
0.19480E 00	0.0	0.60233E 02
0.19525E 00	0.63422E 02	0.59899E 02
0.19569E 00	0.64907E 02	0.59574E 02
0.19613E 00	0.64581E 02	0.59272E 02
0.19658E 00	0.62456E 02	0.58992E 02
0.19702E 00	0.58588E 02	0.58727E 02



# INITIAL DISTRIBUTION LIST

	No. Copies
1. Defense Documentation Center Cameron Station Alexandria, Virginia 22314	20
2. Library Naval Postgraduate School Monterey, California 93940	2
3. Commandant of the Marine Corps (Code A03G) Headquarters Marine Corps Washington, D. C. 22214	1
4. Breckinridge Library Marine Corps Educational Center M. C. Development and Education Command Quantico, Virginia 22134	1
5. Professor G. J. Thaler Department of Electrical Engineering Naval Postgraduate School Monterey, California 93940	15
6. Major Wilton H. Hyde, Jr., USMC 110 Ruland Street Hammond, Louisiana 70401	2

UNCLASSIFIED

Security Classification

## DOCUMENT CONTROL DATA - R &amp; D

(Security classification of title, body of abstract and indexing annotation must be entered when the overall report is classified)

ORIGINATING ACTIVITY (Corporate author)

Naval Postgraduate School  
Monterey, California 93940

2a. REPORT SECURITY CLASSIFICATION

UNCLASSIFIED

2b. GROUP

REPORT TITLE

INVESTIGATION OF SUBHARMONIC RIPPLE IN A FORCED LIMIT-CYCLING REGULATOR

DESCRIPTIVE NOTES (Type of report and, inclusive dates)

Thesis - December 1968

AUTHOR(S) (First name, middle initial, last name)

Wilton H. HYDE, Jr.

REPORT DATE

December 1968

7a. TOTAL NO. OF PAGES

100

7b. NO. OF REFS

12

8. CONTRACT OR GRANT NO.

9a. ORIGINATOR'S REPORT NUMBER(S)

9. PROJECT NO.

9b. OTHER REPORT NO(S) (Any other numbers that may be assigned this report)

10. DISTRIBUTION STATEMENT

Distribution of this document is unlimited.

11. SUPPLEMENTARY NOTES

12. SPONSORING MILITARY ACTIVITY

Naval Postgraduate School  
Monterey, California 93940

ABSTRACT

Some Nonlinear Feedback Control Systems under high gain conditions exhibit the phenomenon of subharmonic instability, or contain subharmonics of the fundamental output frequency. A general discussion of subharmonics in nonlinear systems is followed by an investigation of ripple instability in a forced limit-cycling voltage regulator containing a thyristor or SCR bridge utilizing an ON-OFF switching scheme.

A digital computer program is used to simulate the dynamic response of the system under different loading conditions and for different reference voltage levels.

### KEY WORDS

LINK A

LINK B

LINK C

ROLE

WT

NAME	ROLE
Mr. J. Edgar Hoover	Director
Mr. Clegg	Chief of Bureau
Mr. Glavin	Chief of Bureau
Mr. Ladd	Chief of Bureau
Mr. Nichols	Chief of Bureau
Mr. Rosen	Chief of Bureau
Mr. Tracy	Chief of Bureau
Mr. Carson	Chief of Bureau
Mr. Egan	Chief of Bureau
Mr. Gurnea	Chief of Bureau
Mr. Hendon	Chief of Bureau
Mr. Pennington	Chief of Bureau
Mr. Quinn	Chief of Bureau
Mr. Nease	Chief of Bureau
Mr. Gandy	Chief of Bureau

WT

NAME	ROLE
Mr. J. Edgar Hoover	Director
Mr. Clegg	Chief of Bureau
Mr. Glavin	Chief of Bureau
Mr. Ladd	Chief of Bureau
Mr. Nichols	Chief of Bureau
Mr. Rosen	Chief of Bureau
Mr. Tracy	Chief of Bureau
Mr. Carson	Chief of Bureau
Mr. Egan	Chief of Bureau
Mr. Gurnea	Chief of Bureau
Mr. Hendon	Chief of Bureau
Mr. Pennington	Chief of Bureau
Mr. Quinn	Chief of Bureau
Mr. Nease	Chief of Bureau
Mr. Gandy	Chief of Bureau

W

## Thyristor













thesH973

Investigation of subharmonic ripple in a



3 2768 001 03608 0  
DUDLEY KNOX LIBRARY